ABSTRACT

TEH, HAO WEI. Characterization of the Molecular Interactions between Maize Mosaic Virus and its Insect Vector, *Peregrinus maidis*. (Under the direction of Dr. Anna Whitfield).

Peregrinus maidis, the corn planthopper, is a tropical and subtropical hemipteran insect pest on maize and sorghum, and it is also the sole vector of maize mosaic virus (MMV), a plant- and insect-infecting rhabdovirus. MMV infection in plants causes symptoms like stunting and chlorosis, and the combination of viral infection and mechanical damage from insect feeding and oviposition activity results in significant crop yield losses in tropical maize-growing regions of the world. Insects acquire MMV by feeding on infected plant sap, after which the viral glycoprotein (G) attaches to currently unknown host receptors at the midgut epithelium for endocytosis. Viral replication then occurs, and the infection eventually disseminates throughout the insect via a neurotropic route. After a latent period of approximately five weeks post-acquisition, infected insects become viruliferous, transmitting MMV in a persistent-propagative manner. Studies on rhabdovirus biology show that proper interaction of the G protein with host proteins is crucial for viral infection to occur, and a membrane-based yeast-two-hybrid (MbY2H) library screen identified 107 insect proteins which interacted with the MMV-G protein. I hypothesize that some of those proteins play proviral or antiviral roles in the *P. maidis*-MMV interaction.

My dissertation presents data testing that hypothesis for three of those proteins, apolipophorin III (PmApo3), cyclophilin A (PmCypA), and lugensin (PmLgs) in Chapters 3 and 4. I also validated an insect cell culture-based protein-protein interaction assay which uses plasmid transfection to efficiently express proteins of interest fused to epitope tags and autofluorescent proteins in Sf9 cells, allowing for assays like cellular localization, bimolecular fluorescence complementation, and co-immunoprecipitation to be performed using insect and viral proteins (Chapter 2).

Interesting similarities were found between PmLgs and *Nilaparvata lugens* lugensin, an antimicrobial peptide (AMP). Classical sequence homology-based approaches and newer protein structure homology-based methods showed close resemblance between PmLgs and other delphacid AMPs. PmLgs transcript expression increased over insect development, and immunofluorescence staining showed PmLgs localization in fat bodies, gut tissue, salivary glands, and reproductive organs. Purified bacteria-expressed PmLgs inhibited *E. coli* and *Xanthomonas vasicola* (causal agent of bacterial leaf streak of corn) growth. These data suggest that PmLgs is a delphacid-specific AMP, and further work characterizing its effects on a wider range of organisms and environmental conditions could lead to the development of new biotechnology tools for plant pathogen control.

The interactions between PmApo3, PmCypA, PmLgs, and MMV-G, were re-validated using an MbY2H assay, and a strong interaction was observed for PmApo3 and PmLgs, and a weak interaction was observed for PmCypA. PmApo3 and PmLgs transcript expression increased over insect development, and there was no difference in PmCypA transcript expression across life stages. Transcript expression levels of the three proteins were compared between adult insects injected with MMV virions or buffer solution, and no differences were observed. Individual co-injections of MMV virions and dsRNA targeting the transcripts or targeting GFP showed successful dsRNA-mediated RNAi knockdown for the targeted transcripts, and no significant differences in viral accumulation between groups. These results provide insights guiding future studies of the *P. maidis*-MMV interaction, like the possibility that transcript abundance levels are uncoupled from protein abundance, or that the unnatural route of viral entry during hemocoel injections (bypassing the midgut barrier entirely) leads to a different response compared to natural viral acquisition.

My dissertation has contributed to advancing the field of protein research by providing new tools to study protein-protein interactions in insect cells. Additionally, I have further characterized and analyzed the role of three MMV-G interacting insect proteins within the vector during MMV infection, and functionally characterized PmLgs as an AMP, possibly leading to the discovery of new targets for vector, virus, or plant pathogen control.

Characterization of the Molecular Interactions between Maize Mosaic Virus and its Insect Vector, *Peregrinus maidis*

by
Hao Wei Teh

A dissertation submitted to the Graduate Faculty of
North Carolina State University
in partial fulfillment of the
requirements for the degree of
Doctor of Philosophy

Plant Pathology

Raleigh, North Carolina
2024

APPROVED BY:

_____	_____
Anna Whitfield Chair of Advisory Committee	Dorith Rotenberg
_____	_____
Timmy Sit	Marcé Lorenzen

_____
Aram Mikaelyan

DEDICATION

This dissertation is dedicated to my mother, father, and sister.

BIOGRAPHY

Hao Wei Teh was born in Malaysia and raised in Singapore. During his childhood, his parents gave him countless opportunities to develop and nurture his curiosity about the natural world around him, setting the stage for his career in life sciences. Growing up in Southeast Asia, a melting pot of people and cultures, exposed him to many perspectives and prepared him for his eventual move to pursue higher education alone in a foreign country.

He was admitted to Taylor's University in Malaysia in January 2015 before transferring to the University of Wisconsin-Madison in 2016, where he majored in Pharmacology and Toxicology. During his time there, he worked as an undergraduate research assistant in the lab of the late Dr. Thomas German, an exceptional scientist and mentor. It was through this experience that he learned more about plant virology and vector biology, culminating in his decision to pursue graduate studies in those fields.

After graduating with his bachelor's degree in 2019, he became a doctoral student under Dr. Anna Whitfield at North Carolina State University, Raleigh, NC, where he studied molecular insect vector-virus interactions. Over the course of his graduate career, he acquired a wealth of knowledge about virology, insect biology, and gained a deeper appreciation for the complexity and depth of the interactions between insect vectors and their associated viruses. He graduated in December 2024 with a Doctor of Philosophy, majoring in Plant Pathology and minoring in Entomology.

ACKNOWLEDGEMENTS

It would be difficult to look back upon my time in graduate school without mentioning those who have accompanied me through it. As such, I would like to acknowledge the people who have been beside me as I embarked on this journey: my coworkers, my friends, and my family.

I would first like to extend my gratitude to my advisory committee, who provided me with valuable guidance on my experiments and projects. I would like to thank my major advisor, Dr. Anna Whitfield, for giving me the opportunity to pursue graduate studies in her lab. Additionally, she has dedicated countless hours of support and mentorship to mold me into the scientist I am today, for which I will be forever grateful. I would also like to thank Dr. Marcé Lorenzen for providing genome data and resources for my dissertation, and Drs. Aram Mikaelyan, Dorith Rotenberg, and Tim Sit for passing along to me their passion for science, teaching, and mentoring.

I would also like to thank my current and former lab members, Camila Chabi de Jesus, Cesar Augusto Diniz Xavier, Deepjyoti Singh, Kirsten Lahre, Ordom Huot, Priya Rajarapu, Surapathrudu Kanakala, and Yuting Chen, who provided technical help for my experiments throughout the course of my graduate career, and who made me look forward to coming in to work every day.

To the current and former graduate students with whom I shared the highs and lows of graduate school, I would like to thank Anne Lindbergh, Emma Morris, Holly McInnes, Jake Seiter, Jinlong Han, Karolyn Agosto Shaw, Lucas de Oliveira, Marlonni Marastoni, Peyton Labonte, and Ryan Packer. I would also like to thank all our current and former undergraduate students, especially Clara Tyson and Leo Kerner, who have helped immensely with maintaining our insect colonies and keeping lab supplies stocked and ready.

Finally, I would like to extend my deepest gratitude to my family, my mother, father, and sister. This journey was made far more rewarding and fulfilling with them, and I would not be here today without the unconditional love, support, and encouragement given to me over these years.

TABLE OF CONTENTS

LIST OF TABLES

CHAPTER 2

CHAPTER 3

LIST OF FIGURES

CHAPTER 2

CHAPTER 3

CHAPTER 4

CHAPTER 1

Literature Review

Abstract

Insects serve as efficient vectors of plant viruses, and hemipteran insects such as aphids, whiteflies, and planthoppers are some of the most successful plant virus vectors due to their inherent biological characteristics. This review provides an overview of hemipterans as plant virus vectors, covering various facets of insect and virus biology such as modes of virus transmission and insect immunity. The focus of this review is the *Peregrinus maidis*-maize mosaic virus interaction, and the results of recent relevant studies are presented and discussed in the context of deepening our understanding of the unknown virus-vector molecular interactions which facilitate MMV acquisition by the insect host.

Introduction

Insects are ubiquitous in our environment and have served beneficial roles as sources of food, novel medical compounds, and even as cultural symbols. However, some insects have also exerted undesirable effects on humans when they act as disease vectors, decimating crop yields, and causing severe structural damage. These are just some examples of the many positive and negative influences that this diverse and successful group of organisms has on human society, and they are likely to continue playing these roles in the future. This review will focus on the role of hemipteran insects as vectors of plant pathogenic viruses, specifically on the transmission of plant rhabdoviruses by insects in the family Delphacidae.

Unlike their animal-infecting counterparts, plant-infecting viruses face different challenges when attempting to move between hosts. The sessile nature of plants places significant pressure on plant-infecting viruses to rely on vectors for efficient transmission, vectors such as arthropods, fungi, or nematodes. This interaction between plant viruses and their invertebrate vectors has evolved over

time to be highly specific and complex, with numerous examples of vector behavior being modified after viral infection (Mauck et al., 2012; Lu et al., 2017; Eigenbrode et al., 2018; Fiallo-Olivé et al., 2019; Cruzado-Gutiérrez et al., 2021; Tamborindeguy et al., 2023; Gao et al., 2023; Yu et al., 2024). Additionally, plant-infecting viruses have additional genes present in their genomes which encode for movement proteins which are required for intercellular movement in plants (Sanderfoot and Lazarowitz, 1996; Melcher, 2000; Morozov and Solovyev, 2003; Wu and Cheng, 2020; Kumar and Dasgupta, 2021). This broad repertoire of tools enables plant-infecting viruses to replicate and move efficiently within animal and plant hosts.

The most economically important plant virus vectors are found in the families Aphididae, Aleyrodidae, Cicadellidae, and Delphacidae within the order Hemiptera (Hogenhout et al., 2008). Aphids (Aphididae) are responsible for transmitting non-persistent viruses such as potyviruses and cucumoviruses, and persistent, non-propagative viruses like poleroviruses (Gray and Gildow, 2003; Hook and Fereres, 2006; Scholthof et al., 2011). Whiteflies (Aleyrodidae) transmit persistent, non-propagative viruses like begomoviruses, and semi-persistent viruses like criniviruses (Costa, 1976; Alegbejo, 2001; Rosen et al., 2015; Fiallo-Olivé et al., 2019; Wang and Blanc, 2021). Leafhoppers (Cicadellidae) transmit geminiviruses in a persistent, non-propagative, and circulative manner, and rhabdoviruses in a persistent-propagative manner (Arif et al., 2022; Horn et al., 1994). Delphacid insects are vectors of several important plant viruses from the families *Sedoreoviridae*, *Spinareoviridae*, *Phenuiviridae*, and *Rhabdoviridae* (Nault, 1997; Geijskes and Harding, 2008; Hogenhout et al., 2008; Zhang et al., 2021). These arthropod-transmitted plant viruses cause significant amounts of crop damage and yield losses, posing a major threat to food security.

Hemipterans as Plant Virus Vectors

The order Hemiptera contains insects which are highly efficient plant virus vectors for many of the plant viruses which have been characterized. Their feeding behavior and their ability to travel great distances allow them to transmit viruses across vast geographical areas (Hogenhout et al., 2008). Different modes of transmission are observed in different insect-virus systems, and the modes can be broadly categorized into non-persistent, semi-persistent, persistent circulative, and persistent propagative. The non-persistent and semi-persistent viruses generally have a short retention period in the vector which spans from a few minutes to hours, no latent period, and are localized to the insect mouthparts or foregut. The persistent viruses have a longer retention and latent period spanning hours to weeks and can be found within the hemolymph of the insect, and the propagative viruses are also capable of replicating within insect tissues. Transovarial transmission is also possible for some persistent propagative viruses (Hogenhout et al., 2008).

Delphacid-transmitted Plant Viruses

Planthoppers and leafhoppers, members of the families Delphacidae and Cicadellidae respectively, serve as vectors for several important plant viruses from the *Phenuiviridae*, *Reoviridae* and *Rhabdoviridae* families.

Tenuiviruses are plant viruses in the family *Phenuiviridae* of the order *Hareavirales* which have four to five negative-sense and ambisense genome segments contained within individual, non-enveloped virions (Ramírez and Haenni, 1994; Falk and Tsai, 1998). They have high vector specificity and are transmitted by delphacid planthoppers in a persistent-propagative manner, with their geographic incidence limited to the distribution of their insect vectors. The economic impact of tenuiviruses jeopardizes global food security as their host range spans vital crop plants such as

maize, rice, and sorghum. Rice stripe virus is a member of the genus *Tenuivirus*, transmitted by *Laodelphax striatellus* (Abo and Sy, 1998; Wang et al., 2008). Maize stripe virus is another tenuivirus, transmitted by *Peregrinus maidis*, the corn planthopper and occurs in tropical and subtropical regions of the world, following the distribution of *P. maidis* (Bolus et al., 2021). Tenuiviruses are transovarially transmitted from viruliferous females to progeny, with the sole exception of rice grassy stunt tenuivirus (Tsai and Zitter, 1982; Hibino et al., 1985; Zeigler and Morales, 1990; Falk and Tsai, 1998).

Delphacids are also vectors for plant reoviruses, which are found in the genera *Fijivirus, Phytoreovirus, and Oryzavirus* in the *Sedoreoviridae* and *Spinareoviridae* families within the order *Reovirales* (https://ictv.global/taxonomy, accessed September 2024). The fifteen other genera in those families contain animal-infecting reoviruses. Reoviruses have icosahedral virions that contain ten or twelve dsRNA segments within the core of the virion particle (Joklik, 1981). Fiji disease virus is a member of the genus *Fijivirus* and it is transmitted by delphacid planthoppers (Hatta and Franki, 1977). Rice dwarf virus is a member of the *Phytoreovirus* and infection in rice plants causes severe crop damage. Rice dwarf virus is transmitted by leafhoppers and is the most well-characterized virus in the *Phytoreovirus* genus, with numerous electron microscopy and crystallography studies performed on its virion structure (Nault and Ammar, 1989; Suzuki et al., 1994; Lu et al., 1998). Rice ragged stunt virus is a member of the *Oryzavirus,* and it is transmitted by the brown planthopper, *Nilaparvata lugens*. It causes rice ragged stunt disease and is one of the most economically important rice viruses in rice-growing regions like Southeast Asia (Ling et al., 1978; Hibino and Kimura, 1982; Hibino et al., 1986; Hibino, 1996). The plant reoviruses have plants from the family Gramineae being the most common host, though some also infect dicots. They can replicate in both their plant and insect hosts but are not pathogenic towards their insect

hosts, allowing for more efficient transmission by viruliferous insects, and some plant reoviruses are also capable of transovarial transmission (Chang, 1977; Geijskes and Harding, 2008; Jia et al., 2017).

The family *Rhabdoviridae* in the order Mononegavirales contains fifty-six genera, each containing viruses that infect an ecologically diverse range of hosts, including plants, vertebrates, and invertebrates (https://ictv.global/taxonomy, accessed August 2024). Animal-infecting rhabdoviruses such as rabies virus (RABV) and vesicular stomatitis virus (VSV) from the Lyssavirus and Vesiculovirus genera respectively pose a serious threat to human health. Plant viruses in the genera *Alphanucleorhabdovirus, Betanucleorhabdovirus, Gammanucleorhabdovirus, Cytorhabdovirus, Dichorhabdovirus,* and *Varicosavirus* are transmitted by various biological vectors and differ from those in the other genera within the family *Rhabdoviridae* as an additional movement protein enabling movement in plants is encoded within their genomes (Hogenhout et al., 2008; Whitfield et al., 2018). All rhabdoviruses share the same general defining characteristics in virion morphology and genome organization. Rhabdovirus virions have a bacilliform or bullet-like shape, with a single-stranded, negative sense RNA genome containing ORFs coding for five conserved structural proteins, the nucleoprotein (N), phosphoprotein (P), matrix protein (M), glycoprotein (G), and RNA-dependent-RNA-polymerase or the large protein (L). The N and P proteins encapsulate viral genome molecules and facilitate genome replication together with L. The matrix proteins are an integral part of the virion structure. The glycoproteins are embedded in the virion surface lipid membrane and are involved in viral attachment and entry to host cells. The viral polymerase L is involved in genome replication. Each individual gene sequence contains a conserved transcription start and stop signal and the genes are separated by short untranslated intergenic regions. The entire genome is flanked by leader and

trailer sequences at the 3’ and 5’ ends respectively and the terminal sequences exhibit some degree of complementarity like other negative sense RNA viruses.

Maize mosaic virus (MMV) is a nucleorhabdovirus in the species *Alphanucleorhabdovirus maydis* from the genus *Alphanucleorhabdovirus* which infects sorghum and maize and is transmitted solely by *P. maidis* in a persistent-propagative manner. MMV infection in plants causes stunting, chlorosis, and subsequent yield loss, while infection in insects does not appear to impose a fitness cost on the insects. Barley yellow striate mosaic virus is a cytorhabdovirus that is transmitted in a persistent-propagative manner by *L. striatellus*, infecting a wide variety of Gramineae, including species of notable economic importance such as sorghum and corn (Conti, 1940). The virus was shown to exhibit a different tropism from other persistent-propagative viruses, with the hindgut epithelium being the initial infection site instead of the midgut epithelium and anterior diverticulum (Cao et al., 2018).

Peregrinus maidis Vector Biology

P. maidis, the corn planthopper, is a hemipteran insect pest in the order Delphacidae which is distributed in tropical and subtropical regions. Their primary diet is comprised of sap from maize and sorghum, but the insect is oligophagous and can feed on various alternate host plant species (Namba and Higa, 1971). The complete life cycle of the insect consists of five instar stages followed by an adult stage, and it takes approximately thirty days to develop from egg to adult depending on the ambient temperature (Tsai and Wilson, 1986). Like other planthopper species, adult insects have a macropterous, flight-capable form and a brachypterous, flightless form, and the ratios within a population depend on the current environmental conditions. When food is abundant and population density is low, the proportion of shorter-winged and more fecund adults

in the population tends to increase, with the opposite being observed when food quantity and quality is limited and insect population density increases, resulting in efficient dispersal of insects to new areas for continued population growth (Denno and Roderick, 1990).

P. maidis is the only known vector of two maize viruses which are economically relevant, MMV and MSV (Tsai and Wilson, 1986). MMV is a plant and insect infecting rhabdovirus first described in Hawaii, and MSV is a plant and insect tenuivirus first described in southern Florida (Kunkel, 1927; Tsai 1975). Both viruses are part of a severe corn disease complex which occurred in south Florida from 1979 to 1980, consisting of at least five viral (MMV, MSV, maize dwarf mosaic potyvirus A and B, maize rayado fino marafivirus) and two mollicute (corn stunt spiroplasma, maize bushy stunt phytoplasma) plant pathogens (Bradfute et al., 1981). The combination of damage from insect feeding, oviposition activity, and viral infection results in significant crop losses, causing major economic problems in Hawaii and other tropical corn-growing regions outside of the United States.

MMV is acquired when healthy nymphs or adults ingest virions when feeding on infected plants, and transmission then occurs in a persistent-propagative manner. The ingested virions first travel to the midgut and associated tissues, where they attach to a currently unknown host receptor and are endocytosed. The virions then replicate and gradually infect more digestive tissues like the esophageal intestinal tract muscles, eventually disseminating throughout the insect via a neurotropic route to reach the salivary glands after a latent period of approximately five weeks post-acquisition. Transmission of MMV then occurs when viruliferous insects feed on and infect healthy host plants, restarting the entire infection cycle (Ammar and Hogenhout, 2008).

Natural acquisition rates of MMV from feeding on infected plants were reported to fall between 40% and 60% on average, tested using RT-PCR to generate an amplification product from the

MMV-M gene, with nymphs having a higher acquisition rate compared to adults (Barandoc-Alviar et al., 2016). This data is consistent with a previous study using enzyme-linked immunosorbent assays which showed a 58% acquisition rate for *P. maidis* feeding on infected plants, although that study did not specify whether adults or nymphs were used (Tsai and Falk, 1985). Microinjection of purified MMV virions directly into the insect hemocoel cavity was shown to be extremely efficient for MMV acquisition with MMV infection rates ranging from 85% to 100% in MMV-injected insects (Falk and Tsai, 1985; Yao et al., 2019). Higher MMV acquisition rates were observed when more virions were injected, supporting the hypothesis that a dose-response relationship is present between the amount of virus delivered to the insect and inoculation efficiency (Falk and Tsai, 1985; Yao et al., 2019). MMV could also be detected via qRT-PCR in MMV-microinjected planthoppers within 3 days post-injection and the latent period was shortened to about 6 days (Yao et al., 2019). Insects which were infected via plant feeding transmitted MMV at a rate of 42%, and insects which were infected via hemocoel injection of virions had a significantly increased transmission rate of 85% (Falk and Tsai, 1985). A more recent study showed that the quantity of virions injected into insects was correlated with virus transmission rates, from a peak of 93% transmission efficiency at the highest virion concentration injected to a lack of observable virus transmission at the lowest virion concentration. (Yao et al., 2019). An MMV infectious clone was developed recently, and the authors microinjected *P. maidis* nymphs with crude extract from infected maize plants to produce infected insects. The transmission rate of the transgenic MMV-GFP was reported to be 65%, compared to the transmission rate of wild-type MMV which was reported to be 90% efficient (Kanakala et al., 2023). MMV virions that were injected directly into insects had a similar tissue tropism as MMV virions that were naturally acquired during feeding, and acquisition efficiency was doubled or tripled in the case of acquisition

via injection compared to feeding on infected plants, suggesting that barriers to efficient viral infection and transmission exist at the insect gut and salivary glands (Yao et al., 2019). The basal lamina is a sheath of fibrous material which covers the *P. maidis* midgut and salivary glands, and this structure has been implicated as a barrier to transmission in aphids and mosquitoes for luteoviruses and arboviruses (Ammar, 1985; Gray and Gildow, 2003; Romoser et al., 2004; Ammar and Hogenhout, 2008).

Interestingly, MMV infection does not appear to impose detrimental fitness costs to persistently infected insects despite the presence of high viral titers within infected insects. This observation coupled with the fact that the infection is lifelong suggests that *P. maidis* may have developed mechanisms to modulate MMV infection and attain an equilibrium where insect health remains uncompromised by excessive viral replication, and viral titers are kept sufficiently high for efficient transmission. There are also no significant behavioral changes observed in MMV-infected insects, but this may be because characterizing specific behaviors and identifying behavioral anomalies is a challenging task for such small insects. Healthy *P. maidis* were also observed to prefer MMV infected plants over uninfected plants (Kerner, Xavier, Huot, and Whitfield, personal communication, 2019) The spatial dynamics of MMV infection in insect tissues over the course of infection is well understood, but the molecular mechanisms involved in infection initiation are not (Ammar and Hogenhout, 2008).

Insect Immunity

Exposure to pathogens like viruses is not a challenge unique to insects, but unlike vertebrates which have both an innate and acquired immune system, insects only possess innate immunity. Insect immunity is well studied with numerous published reviews covering that topic (Gillespie et

al., 1997; Strand, 2008; Zhang et al., 2021; Mahanta et al., 2023). This review will provide a brief overview of the humoral and cellular components of the insect immune system, followed by a more detailed discussion on antimicrobial peptides (AMPs).

The insect innate immune system is well adapted to effectively respond to immune challenges from a variety of pathogenic bacteria, fungi, and viruses. The humoral components of the insect immune system include effector molecules such as AMPs, complement-like proteins, and enzymes involved in the melanization signal cascade. The cellular components include phagocytosis and encapsulation of foreign bodies by insect hemocytes. The two components are highly interlinked with frequent regulation and crosstalk between them. Upon detection of pathogen associated molecular patterns (PAMPs) by pattern recognition receptors (PRRs), evolutionarily conserved immune signal transduction pathways like Imd, Toll, JAK/STAT are activated, triggering downstream host defense responses like hemocyte activation, cellular binding, encapsulation and melanization of foreign particles, and AMP production (Arbouzova and Zeidler, 2006 Eleftherianos et al., 2006; Valanne et al., 2011; Iatsenko et al., 2016).

Antimicrobial Peptides

AMPs are a class of short, cationic oligopeptides with a diverse range of structures and roles in immunity that have been identified in virtually all organisms (Ahmed et al., 2019). A vast majority of AMPs which have been discovered and characterized originated from insects. Since the first observation of antimicrobial activity in the hemolymph of silk moth pupa in 1974, and the purification of the first insect AMP (cecropin) in 1980, over 150 insect AMPs have been characterized (Yi et al., 2014). Insect-derived AMPs can be broadly classified into four families based on their structure or unique sequence identity: α-helical peptides like cecropin and moricin,

cysteine-rich peptides like defensin and drosomycin, proline-rich peptides like apidaecin and lebocin, and glycine-rich peptides like attacin and gloverin (Otvos, 2000; Bulet and Stocklin, 2005). Most insect AMPs have been found in more than two insect orders, but moricin and gloverin have only been found in *Lepidoptera*. They are mostly synthesized as inactive precursor proteins or pro-proteins, and partial proteolytic cleavage is required to activate them. Insects are extremely resistant to bacterial infections possibly because of the wide diversity of AMPs which they produce, and the mechanism of action of those AMPs are similarly varied and can involve induction of immune responses or direct targeting of biological processes used by those pathogens. AMPs are part of the innate immune system in prokaryotes and eukaryotes and typically act as the first line of defense against invading pathogens such as bacteria, fungi, or viruses. Antiviral peptides (AVP) have an overall positive charge and are generally cationic or amphipathic, enabling them to work as antimicrobials. A large-scale computational analysis studying the correlation between amphipathicity, charge and antimicrobial activity indicates that there are no significant physiochemical differences between AMPs and other AVPs (Wang et al. 2017). In another review, it was noted that all peptide entry inhibitors were hydrophobic or amphipathic, with a propensity to bind to bilayer membrane interfaces and other hydrophobic surfaces, suggesting that one mechanism of AVP antiviral activity against enveloped viruses was the physical interaction with hydrophobic surfaces exposed during viral-host membrane fusion events (Badani et al. 2014).

Defensins were first found to play a role in antiviral immunity in 1986 (Klotman and Chang, 2006), and they have since been demonstrated to have antiviral activity towards HIV, influenza A virus, human adenovirus, SARS, HPV, herpes simplex virus, and respiratory syncytial virus (Ahmed et al., 2019). Studies published so far suggest that the AMP could disrupt viral entry or viral trafficking within infected cells. Cecropin-A from *Hyalophora cecropia* was shown to inhibit HIV-

1, HSV-1 and 2, and Junin arenavirus (JV). Melittin, a bee venom-derived AVP, also inhibited viral replication of HIV-1, HSV, and JV, as well as the infectivity of a wide array of viruses like Coxsackie virus, IAV, VSV, and TMV (Memariani et al., 2020). Gloverins were shown to have antiviral properties against *Autographa californica* M nucleopolyhedrovirus in Sf9 cells (Moreno-Habel et al., 2012). Gloverin was shown to perforate vesicles and reduce baculovirus infectivity in vitro, suggesting that the AVP may be disrupting the viral membrane surrounding the nucleocapsid. In differential gene expression studies on *B. mori*, it was shown that gloverin-4 expression was upregulated in BmNPV-infection resistant silkworms, but no expression changes were observed in the infection-susceptible silkworms. Gloverin-2 and gloverin-3 were also shown to be upregulated in response to BMNPV infection in both resistant and susceptible silkworms. (Bao et al., 2009; Bao et al., 2010). There are also many other insect-derived AMPs besides these listed examples which have been tested against and shown to exhibit AVP activity against a wide variety of viruses (Feng et al., 2020).

Viral Glycoproteins

Viral glycoproteins serve important roles in receptor binding and virion entry, and these functions are conserved across multiple virus families (Choppin and Scheid, 1980; Sieczkarski and Whittaker, 2005; Bowden et al., 2011; Grove and Marsh, 2011; Albertini et al., 2012; Hulswit et al., 2021). Pseudotyping, which is the production of viruses with foreign viral surface glycoproteins, is a technique which was first described in a study involving the production of modified enterovirus virions containing an RNA genome of one enterovirus within the capsid of another heterologous enterovirus (Holland and Cords, 1964). More recent studies have expanded on this concept and designed viral vectors which express and incorporate heterologous

glycoproteins into their virion structure for functional studies (Burns et al., 1993; Akkina et al., 1996; Cronin et al., 2005; Salazar-García et al., 2021). Rabies virus and vesicular stomatitis virus (VSV) glycoproteins have been shown to be important for determining vector specificity, transmission competency, viral attachment, and membrane fusion processes in their animal hosts (Ci et al. 2018). However, unlike most other glycoproteins, the VSV glycoprotein does not bind to a specific set of cell surface receptors, instead it binds to a phospholipid component of the cell membrane to mediate viral attachment and entry, giving VSV a broad host range (Coil and Miller, 2004).

Like other viruses, the presence and proper function of rhabdovirus glycoproteins is required for entry into host cells (Coll, 1995; Walker and Kongsuwan, 1999; Dietzgen and Kuzmin, 2012). From previous studies on rhabdovirus glycoproteins, the MMV glycoprotein is also likely to play a key role in viral transmission. The identity of the *P. maidis* gut receptor, or receptors, which interact with the viral glycoprotein is currently unknown. A membrane-bound yeast-2-hybrid (MbY2H) assay was used to identify 107 *P. maidis* proteins which interacted with the MMV glycoprotein (Barandoc-Alviar et al., 2022). From that screen, three proteins were selected for further downstream analysis, apolipophorin III, cyclophilin A, and lugensin.

Apolipophorins

Apolipophorins are a complex of lipids and proteins that are involved in lipid transport in humans and insects. Insects have a single multifunctional lipoprotein termed lipophorin, composed of Apolipophorin-I and Apolipophorin-II which stem from a post-translationally processed precursor peptide (Weers et al., 1993). Certain insect orders such as Orthoptera and Lepidoptera possess a third distinct apolipoprotein, Apolipophorin-III (Apo3), which is involved in lipid transport

processes that fuel high energy activities like sustained flight muscle activity. Apo3 lacks cysteine residues and does not self-associate even at high protein concentrations in the absence of lipids, unlike other apolipoproteins (Cole et al., 1987; Kanost et al., 1988; Weise et al., 1998). Apo3 has segments of amphipathic α-helices which facilitate lipid binding and are well characterized in *Locusta migratoria* and *Manduca sexta* (Segrest et al., 1992).

The role of Apo3 in insect immunity has been characterized, and it is hypothesized that the lipid-bound form of Apo3 is a pattern recognition receptor (Dettloff et al., 2001; Niere et al., 2001; Whitten et al., 2004). Apo3 recognizes a variety of pathogen-associated molecular patterns from fungi and bacteria, like β-1,3-glucan, a fungal cell wall component, fungal conidia, lipoteichoic acids, and lipopolysaccharides, which are compounds present in Gram-positive and Gram-negative bacteria. In *Galleria mellonella*, Apo3 hemolymph transfer experiments elicited a dose-dependent immune response, and Apo3 was also found to act as a hemagglutinating agent in larval hemolymph (Wiesner et al., 1997; Iimura et al., 1998). In *Anopheles gambiae*, Apo3 was reported to have similar predicted tertiary structures as that of *M. sexta* Apo3. *A. gambiae* Apo3 is also potentially involved in the immune response to *Plasmodium berghei* as the number of parasite oocysts in insects significantly increased after Apo3 gene expression was silenced (Gupta et al., 2010). Apo3 is also involved in bacterial endotoxin detoxification (Dunphy and Halwani, 1999; Halwani et al., 2000; Whitten et al., 2004). In *Hyphantria cunea*, Apo3 induces AMP expression and binds to *E. coli* cell membranes (Kim et al., 2004). Silencing Apo3 expression in *Ae. aegypti* reduced Zika virus RNA copy numbers in the midgut (Chen et al., 2024).

Apo3 is abundant in the hemolymph and present in life stages of *G. mellonella and M. sexta* where the Apo3 lipid transport function is not needed, supporting the hypothesis that it is an immune surveillance molecule which can rapidly detect pathogens within the host (Wiesner et al., 1997).

In RABV-infected mice, the levels of serum apolipoprotein A1 could serve as a biomarker for preclinical diagnosis, with elevated apoLp-A1 in mice that had high levels of RABV replication (Yamada et al., 2021). Apolipoprotein D was also shown to interact with RABV-G and facilitated viral replication in mammalian cell culture (Zhang et al., 2024). The results from these studies along with the evidence that *P. maidis* Apo3 interacted with MMV-G in a co-immunoprecipitation assay suggest that Apo3 could be involved in the detection and recognition of MMV viral infection.

Cyclophilins

Cyclophilins belong to one of the three protein subfamilies of immunophilins, which possess peptidyl-prolyl *cis-trans* isomerase (PPI) activity, and they are found in virtually all organisms (Wang and Heitman, 2005). The identification of the first protein with PPIase activity in 1984 coincided with the independent identification of a protein with high binding affinity for the immunosuppressive drug Cyclosporine A (CsA) (Fischer et al., 1984; Handschumacher et al., 1984), and it was later discovered that they were the same protein (Fischer et al., 1989; Takahashi et al., 1989). All cyclophilins have PPIase activity and a conserved cyclophilin-like domain spanning approximately 109 amino acid resides, surrounded by various other domains related to their subcellular localization and function. They catalyze protein isomerization, a process which is integral for proper protein folding and assembly, especially for large multi-domain proteins.

In addition to their role as molecular chaperones, cyclophilins are also involved in cell signaling and immune responses of many organisms. In humans, CsA A binds to cyclophilin, producing an extremely stable complex which sequesters calcineurin and inhibits downstream phosphorylation of signaling molecules for immune cell activation (Huai et al., 2002; Hornbogen et al., 1992; Liu et al., 1991). Administering CsA to adult *Aedes aegypti* mosquitoes or mosquito larvae results in

mortality (Weiser and Matha, 1988; Matha et al., 1992; Dong et al., 2019). CsA has also been shown to suppress humoral immune responses in *G. mellonella* larvae, causing treated larvae to lose immunity to a bacterial pathogen (Fiolka, 2008).

Cyclophilins also play direct and indirect roles in the lifecycles of many different viruses (Peel and Scribner, 2013). HIV relies heavily upon Cyclophilin A (CypA) during its infection cycle within host cells. The HIV-1 Gag polyprotein binds and incorporates CypA into mature virions (Franke, 1994), and nuclear import of the virion occurs when the capsid protein binds to a cyclophilin protein (Schaller et al., 2011). Influenza A virus replication was found to be negatively affected by CypA during the early stages of infection, a yeast-two-hybrid screen revealed an interaction between the viral M1 protein and CypA, and incorporation of CypA into mature virions inhibited M1-M1 autointeraction and viral replication (Liu et al., 2009). Cyclophilins are also involved in the replication of insect viruses. Inhibiting CypA with CsA in Dengue virus-infected mosquito cell lines resulted in reduced secretion of the NS1 viral protein (Ramirez and Ludert, 2019). The transmission of tomato yellow leaf curl virus (TYLCV) by *Bemisia tabaci* is dependent on the expression of *B. tabaci* Cyclophilin B, with increased expression observed during TYLCV infection. Cyclophilin B also interacts and co-localizes with virions in host tissues (Kanakala and Ghanim, 2016). *B. tabaci* nymphs and adults which fed on plants expressing dsRNA targeting *B. tabaci* Cyclophilin B and HSP 70 genes resulted in high mortality rates among nymphs and adults and reduced TYLCV transmission rates by the adults (Kanakala et al., 2019). The results from these studies combined with data showing that *P. maidis* CypA co-immunoprecipitates with MMV-G suggests that CypA serves proviral functions for MMV, with one potential function being the transport of viral structures or complexes within host cells.

Lugensin

Lugensin is an AMP which was first identified in *N. lugens*, and it exhibits antibacterial activity towards a broad range of bacterial species (Zhou et al., 2019). Insect AMPs such as gloverins, cecropins, and defensins, as well as other classes of AMPs have been shown to possess both antiviral and antibacterial properties (Moreno-Habel et al., 2012; Bao et al., 2009; Bao et al., 2010; Memariani et al., 2019; Klotman and Chang, 2006; Ahmed et al., 2019). *P. maidis* lugensin was shown to interact with MMV-G in a membrane-based yeast-two-hybrid assay, and its function is currently unknown (Barandoc-Alviar et al., 2022). *P. maidis* lugensin could have similar immune functions to *N. lugens* lugensin and exert antibacterial activity on the bacterial species that *P. maidis* encounters, or it could be an antiviral AMP involved in the *P. maidis*-MMV interaction.

Conclusion

These three proteins, Apo3, CypA, and *P. maidis* lugensin, could perform important functions in the insect-virus interaction. The focus of my thesis will be characterizing the roles of those proteins in the context of viral infection, deepening our understanding of the molecular interactions between *P. maidis* and MMV, and providing valuable direction for future work focused on identifying the receptors used by MMV for cellular entry and infection.

References

Abo, M. E. & Sy, A. A. (1998). Rice Virus Diseases: Epidemiology and Management Strategies. *Journal of Sustainable Agriculture, 11*, 113-134.

Ahmed, A., Siman-Tov, G., Hall, G., Bhalla, N., & Narayanan, A. (2019). Human Antimicrobial Peptides as Therapeutics for Viral Infections. *Viruses*, *11*(8), 704.

Akkina, R. K., Walton, R. M., Chen, M. L., Li, Q. X., Planelles, V., & Chen, I. S. (1996). High-efficiency gene transfer into CD34+ cells with a human immunodeficiency virus type 1-based retroviral vector pseudotyped with vesicular stomatitis virus envelope glycoprotein G. *Journal of virology*, *70*(4), 2581–2585.

Albertini, A. A., Mérigoux, C., Libersou, S., Madiona, K., Bressanelli, S., Roche, S., Lepault, J., Melki, R., Vachette, P., & Gaudin, Y. (2012). Characterization of monomeric intermediates during VSV glycoprotein structural transition. *PLoS pathogens*, *8*(2), e1002556.

Alegbejo, M. D. (2001). Whitefly Transmitted Plant Viruses in Nigeria. *Journal of Sustainable Agriculture, 17*(2–3), 99–109.

Ammar, el-D., & Hogenhout, S. A. (2008). A neurotropic route for Maize mosaic virus (Rhabdoviridae) in its planthopper vector *Peregrinus maidis*. *Virus research*, *131*(1), 77–85.

Ammar, E. D., & Nault, L. R. (1985). Assembly and accumulation sites of maize mosaic virus in its planthopper vector. *Intervirology*, *24*(1), 33–41.

Arbouzova, N. I., & Zeidler, M. P. (2006). JAK/STAT signalling in *Drosophila*: insights into conserved regulatory and cellular functions. *Development (Cambridge, England)*, *133*(14), 2605–2616.

Arif, M., Farooq, S., Alasmari, A., Alshehri, M. A., Hashem, M., Alamri, S., Hemeg, H. A., & Alabdallah, N. M. (2022). Molecular study of geminiviruses: Complex biology, host-vector interactions, and increasing diversity. *Journal of King Saud University - Science*, *34*(4), 102051.

Badani, H., Garry, R. F., & Wimley, W. C. (2014). Peptide entry inhibitors of enveloped viruses: the importance of interfacial hydrophobicity. *Biochimica et biophysica acta*, *1838*(9), 2180–2197.

Bao, Y.-Y., Tang, X.-D., Lv, Z.-Y., Wang, X.-Y., Tian, C.-H., Xu, Y. P., & Zhang, C.-X. (2009). Gene expression profiling of resistant and susceptible *Bombyx mori* strains reveals nucleopolyhedrovirus-associated variations in host gene transcript levels. *Genomics*, *94*(2), 138–145.

Bao, Y.-Y., Lv, Z.-Y., Liu, Z.-B., Xue, J., Xu, Y.-P., & Zhang, C.-X. (2010). Comparative analysis of *Bombyx mori* nucleopolyhedrovirus responsive genes in fat body and haemocyte of *B. mori* resistant and susceptible strains. *Insect Molecular Biology*, *19*(3), 347–358.

Barandoc-Alviar, K., Ramirez, G. M., Rotenberg, D., & Whitfield, A. E. (2016). Analysis of Acquisition and Titer of Maize Mosaic Rhabdovirus in Its Vector, *Peregrinus maidis* (Hemiptera: Delphacidae). *Journal of insect science (Online)*, *16*(1), 14.

Barandoc-Alviar, K., Rotenberg, D., Martin, K. M., & Whitfield, A. E. (2022). The physical interactome between *Peregrinus maidis* proteins and the maize mosaic virus glycoprotein provides insights into the cellular biology of a rhabdovirus in the insect vector. *Virology*, *577*, 163–173.

Bolus, S., Braithwaite, K. S., Grinstead, S. C., Fuentes-Bueno, I., Beiriger, R., Falk, B. W., & Mollov, D. (2021). Completion of Maize Stripe Virus Genome Sequence and Analysis of Diverse Isolates. *Frontiers in microbiology*, *12*, 684599.

Bowden, T. A., Jones, E. Y., & Stuart, D. I. (2011). Cells under siege: viral glycoprotein interactions at the cell surface. *Journal of structural biology*, *175*(2), 120–126.

Bradfute, O. E. (1981). Corn stunt spiroplasma and viruses associated with a maize disease epidemic in Southern Florida. *Plant Disease 65*: 837–841.

Bulet, P., & Stöcklin, R. (2005). Insect antimicrobial peptides: structures, properties and gene regulation. *Protein and peptide letters*, *12*(1), 3–11.

Burns, J. C., Friedmann, T., Driever, W., Burrascano, M., & Yee, J. K. (1993). Vesicular stomatitis virus G glycoprotein pseudotyped retroviral vectors: concentration to very high titer and efficient gene transfer into mammalian and nonmammalian cells. *Proceedings of the National Academy of Sciences of the United States of America*, *90*(17), 8033–8037.

Cao, Q., Xu, W. Y., Gao, Q., Jiang, Z. H., Liu, S. Y., Fang, X. D., Gao, D. M., Wang, Y., & Wang, X. B. (2018). Transmission Characteristics of Barley Yellow Striate Mosaic Virus in Its Planthopper Vector *Laodelphax striatellus*. *Frontiers in microbiology*, *9*, 1419.

Chang, V.C.S. (1977) Transovarial transmission of the Fiji disease virus in *Perkinsiella saccharicida* Kirk. *Sugarcane Pathologists' Newsletter*, *18*, 22-23

Chen, T.-Y., Raduwan, H., Marín-López, A., Cui, Y., & Fikrig, E. (2024). Zika virus exists in enterocytes and enteroendocrine cells of the *Aedes aegypti* midgut. *IScience*, *27*(7).

Choppin, P. W., & Scheid, A. (1980). The Role of Viral Glycoproteins in Adsorption, Penetration, and Pathogenicity of Viruses. *Reviews of Infectious Diseases*, *2*(1), 40–61.

Ci, Y., Yang, Y., Xu, C., & Shi, L. (2018). Vesicular stomatitis virus G protein transmembrane region is crucial for the hemi-fusion to full fusion transition. *Scientific Reports*, *8*(1), 10669.

Coil, D. A., & Miller, A. D. (2004). Phosphatidylserine is not the cell surface receptor for vesicular stomatitis virus. *Journal of virology*, *78*(20), 10920–10926.

Cole, K. D., Fernando-Warnakulasuriya, G. P., Boguski, M. S., Freeman, M., Gordon, J. I., Clark, W. A., Law, J. H., & Wells, M. A. (1987). Primary structure and comparative sequence analysis of an insect apolipoprotein. Apolipophorin-III from *Manduca sexta*. *Journal of Biological Chemistry*, *262*(24), 11794–11800.

Coll, J. M. (1995). The glycoprotein G of rhabdoviruses. *Archives of Virology*, *140*(5), 827–851.

Conti, M. (1980). Vector relationships and other characteristics of barley yellow striate mosaic virus (BYSMV). *Annals of Applied Biology*, *95*(1), 83–92.

Costa, A. S. (1976). Whitefly-Transmitted Plant Diseases. *Annual Review of Phytopathology*, *14*(Volume 14,), 429–449.

Cronin, J., Zhang, X. Y., & Reiser, J. (2005). Altering the tropism of lentiviral vectors through pseudotyping. *Current gene therapy*, *5*(4), 387–398.

Cruzado-Gutiérrez, R. K., Sadeghi, R., Prager, S. M., Casteel, C. L., Parker, J., Wenninger, E. J., Price, W. J., Bosque-Pérez, N. A., Karasev, A. V, & Rashed, A. (2021). Interspecific interactions within a vector-borne complex are influenced by a co-occurring pathosystem. *Scientific Reports*, *11*(1), 2242.

Denno, R. F., & Roderick, G. K. (1990). Population Biology of Planthoppers. *Annual Review of Entomology*, *35*(1), 489–520.

Dettloff, M., Kaiser, B., & Wiesner, A. (2001). Localization of injected apolipophorin III in vivo — new insights into the immune activation process directed by this protein. *Journal of Insect Physiology*, *47*(7), 789–797.

Dietzgen, R. G., Kondo, H., Goodin, M. M., Kurath, G., & Vasilakis, N. (2017). The family Rhabdoviridae: mono- and bipartite negative-sense RNA viruses with diverse genome organization and common evolutionary origins. *Virus research*, *227*, 158–170.

Dong S, Dimopoulos G. Antiviral Compounds for Blocking Arboviral Transmission in Mosquitoes. *Viruses*. 2021; 13(1):108.

Halwani, A. E., & Dunphy, G. B. (1999). Apolipophorin-III in *Galleria mellonella* potentiates hemolymph lytic activity. *Developmental and comparative immunology*, *23*(7-8), 563–570.

Eigenbrode, S. D., Bosque-Pérez, N. A., & Davis, T. S. (2018). Insect-Borne Plant Pathogens and Their Vectors: Ecology, Evolution, and Complex Interactions. *Annual review of entomology*, *63*, 169–191.

Eleftherianos, I., Marokhazi, J., Millichap, P. J., Hodgkinson, A. J., Sriboonlert, A., ffrench-Constant, R. H., & Reynolds, S. E. (2006). Prior infection of Manduca sexta with non-pathogenic Escherichia coli elicits immunity to pathogenic *Photorhabdus luminescens*: Roles of immune-related proteins shown by RNA interference. *Insect Biochemistry and Molecular Biology*, *36*(6), 517–525.

Falk B. W., Tsai J. H. 1985. Serological detection and evidence for multiplication of Maize mosaic virus in the planthopper vector, *Peregrinus maidis*. Phytopathology 75: 852–855.

Falk, B. W., & Tsai, J. H. (1998). Biology and molecular biology of viruses in the genus Tenuivirus. *Annual review of phytopathology*, *36*, 139–163.

Feng, M., Fei, S., Xia, J., Labropoulou, V., Swevers, L., & Sun, J. (2020). Antimicrobial Peptides as Potential Antiviral Factors in Insect Antiviral Immune Response. *Frontiers in Immunology*, *11*.

Fiallo-Olivé, E., & Navas-Castillo, J. (2019). Tomato chlorosis virus, an emergent plant virus still expanding its geographical and host ranges. *Molecular plant pathology*, *20*(9), 1307–1320.

Fiolka M. J. (2008). Immunosuppressive effect of cyclosporin A on insect humoral immune response. *Journal of invertebrate pathology*, *98*(3), 287–292.

Fischer, G., Bang, H., & Mech, C. (1984). [Determination of enzymatic catalysis for the cis-trans-isomerization of peptide binding in proline-containing peptides]. *Biomedica biochimica acta*, *43*(10), 1101–1111.

Fischer, G., Wittmann-Liebold, B., Lang, K., Kiefhaber, T., & Schmid, F. X. (1989). Cyclophilin and peptidyl-prolyl cis-trans isomerase are probably identical proteins. *Nature*, *337*(6206), 476–478.

Franke, E. K., Yuan, H. E., & Luban, J. (1994). Specific incorporation of cyclophilin A into HIV-1 virions. *Nature*, *372*(6504), 359–362.

Gao, D.-M., Qiao, J.-H., Gao, Q., Zhang, J., Zang, Y., Xie, L., Zhang, Y., Wang, Y., Fu, J., Zhang, H., Han, C., & Wang, X.-B. (2023). A plant cytorhabdovirus modulates locomotor activity of insect vectors to enhance virus transmission. *Nature Communications*, *14*(1), 5754.

Geijskes, R. J., & Harding, R. M. (2008). Plant Reoviruses. In *Encyclopedia of Virology* (pp. 149–155). Elsevier Ltd.

Gillespie, J. P., Kanost, M. R., & Trenczek, T. (1997). Biological mediators of insect immunity. *Annual review of entomology*, *42*, 611–643.

Gray, S., & Gildow, F. E. (2003). Luteovirus-aphid interactions. *Annual review of phytopathology*, *41*, 539–566.

Grove, J., & Marsh, M. (2011). The cell biology of receptor-mediated virus entry. *The Journal of cell biology*, *195*(7), 1071–1082.

Gupta, L., Noh, J. Y., Jo, Y. H., Oh, S. H., Kumar, S., Noh, M. Y., Lee, Y. S., Cha, S. J., Seo, S. J., Kim, I., Han, Y. S., & Barillas-Mury, C. (2010). Apolipophorin-III mediates antiplasmodial epithelial responses in *Anopheles gambiae* (G3) mosquitoes. *PloS one*, *5*(11), e15410.

Halwani, A. E., Niven, D. F., & Dunphy, G. B. (2001). Apolipophorin-III in the greater wax moth, Galleria mellonella (Lepidoptera: Pyralidae). *Archives of Insect Biochemistry and Physiology*, *48*(3), 135–143.

Handschumacher, R. E., Harding, M. W., Rice, J., Drugge, R. J., & Speicher, D. W. (1984). Cyclophilin: A Specific Cytosolic Binding Protein for Cyclosporin A. *Science*, *226*(4674), 544–547.

Hatta, T., & Francki, R. I. B. (1977). Morphology of Fiji disease virus. *Virology*, *76*(2), 797-807.

Hibino, H., & Kimura, I. (1982). Detection of Rice ragged stunt virus in insect vectors by enzyme-linked immunosorbent assay. *Phytopathology*, *72*(6), 656-659.

Hibino, H., Usugi, T., Omura, T., Tsuchizaki, T., Shohara, K., & Iwasaki, M. (1985). Rice grassy stunt virus: a planthopper-borne circular filament. *Phytopathology*, *75*(8), 894-899.

Hibino, H. (1986). Rice grassy stunt virus. *Tropical Agriculture Research Series*, *19*, 165-172.

Hibino, H. (1996). Biology and epidemiology of rice viruses. *Annual Review of Phytopathology*, *34*(1), 249-274.

Hogenhout, S. A., Ammar, E.-D., Whitfield, A. E., & Redinbaugh, M. G. (2008). Insect Vector Interactions with Persistently Transmitted Viruses. *Annual Review of Phytopathology*, *46*(Volume 46, 2008), 327–359.

Holland, J. J., & Cords, C. E. (1964). Maturation of Poliovirus RNA with Capsid Protein Coded By Heterologous Enteroviruses. *Proceedings of the National Academy of Sciences of the United States of America*, *51*(6), 1082–1085.

Hooks, C. R., & Fereres, A. (2006). Protecting crops from non-persistently aphid-transmitted viruses: a review on the use of barrier plants as a management tool. *Virus research*, *120*(1-2), 1–16.

Horn, N.M., Reddy, S.V., & Reddy, D.V. (1994). Virus-vector relationships of chickpea chlorotic dwarf geminivirus and the leafhopper *Orosius orientalis* (Hemiptera: Cicadellidae). *Annals of Applied Biology*, *124*, 441-450.

Hornbogen, T., Pieper, R., Hoffmann, K., Kleinkauf, H., & Zocher, R. (1992). Two new cyclophilins from *Fusarium sambucinum* and *Aspergillus niger*: resistance of cyclophilin/cyclosporin A complexes against proteolysis. *Biochemical and biophysical research communications*, *187*(2), 791–796.

Huai, Q., Kim, H.-Y., Liu, Y., Zhao, Y., Mondragon, A., Liu, J. O., & Ke, H. (2002). Crystal structure of calcineurin–cyclophilin–cyclosporin shows common but distinct recognition of immunophilin–drug complexes. *Proceedings of the National Academy of Sciences*, *99*(19), 12037–12042.

Hulswit R.J.G., Paesen G.C., Bowden T.A., Shi X. Recent Advances in Bunyavirus Glycoprotein Research: Precursor Processing, Receptor Binding and Structure. *Viruses*. 2021; 13(2):353.

Iatsenko, I., Kondo, S., Mengin-Lecreulx, D., & Lemaitre, B. (2016). PGRP-SD, an Extracellular Pattern-Recognition Receptor, Enhances Peptidoglycan-Mediated Activation of the Drosophila Imd Pathway. *Immunity*, *45*(5), 1013–1023.

Iimura, Y., Ishikawa, H., Yamamoto, K., & Sehnal, F. (1998). Hemagglutinating properties of apolipophorin III from the hemolymph of *Galleria mellonella* larvae. *Archives of insect biochemistry and physiology*, *38*(3), 119–125.

Jia, D., Mao, Q., Chen, Y., Liu, Y., Chen, Q., Wu, W., Zhang, X., Chen, H., Li, Y., & Wei, T. (2017). Insect symbiotic bacteria harbour viral pathogens for transovarial transmission. *Nature Microbiology*, *2*(5), 17025.

Joklik W. K. (1981). Structure and function of the reovirus genome. *Microbiological reviews*, *45*(4), 483–501.

Kanakala, S., & Ghanim, M. (2016). RNA Interference in Insect Vectors for Plant Viruses. *Viruses*, *8*(12), 329.

Kanakala, S., Kontsedalov, S., Lebedev, G., & Ghanim, M. (2019). Plant-Mediated Silencing of the Whitefly *Bemisia tabaci* Cyclophilin B and Heat Shock Protein 70 Impairs Insect Development and Virus Transmission. *Frontiers in Physiology*, *10*, 557.

Kanakala, S., Xavier, C. A. D., Martin, K. M., Tran, H. H., Redinbaugh, M. G., & Whitfield, A. E. (2023). Rescue of the first alphanucleorhabdovirus entirely from cloned complementary DNA: An efficient vector for systemic expression of foreign genes in maize and insect vectors. *Molecular plant pathology*, *24*(7), 788–800.

Kanost, M., Boguski, M., Freeman, M., Gordon, J., Wyatt, G., & Wells, M. (1988). Primary structure of apolipophorin-III from the migratory locust, *Locusta migratoria*. Potential

amphipathic structures and molecular evolution of an insect apolipoprotein. *The Journal of Biological Chemistry*, *263*, 10568–10573.

Kim, H. J., Je, H. J., Park, S. Y., Lee, I. H., Jin, B. R., Yun, H. K., Yun, C. Y., Han, Y. S., Kang, Y. J., & Seo, S. J. (2004). Immune activation of apolipophorin-III and its distribution in hemocyte from *Hyphantria cunea*. *Insect biochemistry and molecular biology*, *34*(10), 1011–1023.

Klotman, M. E., & Chang, T. L. (2006). Defensins in innate antiviral immunity. *Nature reviews. Immunology*, *6*(6), 447–456.

Kumar, G., & Dasgupta, I. (2021). Variability, Functions and Interactions of Plant Virus Movement Proteins: What Do We Know So Far?. *Microorganisms*, *9*(4), 695.

Kunkel, L.O. (1927). The corn mosaic of Hawaii distinct from sugar cane mosaic. *Phytopathology*. 17:41. (Abstract).

Ling, K. C., Tiongco, E. R., & Aguiero, V. M. (1978). Rice ragged stunt, a new virus disease. *Plant Disease Reporter 62*(70), 5.

Liu, J., Farmer, J. D., Jr, Lane, W. S., Friedman, J., Weissman, I., & Schreiber, S. L. (1991). Calcineurin is a common target of cyclophilin-cyclosporin A and FKBP-FK506 complexes. *Cell*, *66*(4), 807–815.

Liu, X., Sun, L., Yu, M., Wang, Z., Xu, C., Xue, Q., Zhang, K., Ye, X., Kitamura, Y., & Liu, W. (2009). Cyclophilin A interacts with influenza A virus M1 protein and impairs the early stage of the viral replication. *Cellular microbiology*, *11*(5), 730–741.

Lu, G., Zhou, Z. H., Baker, M. L., Jakana, J., Cai, D., Wei, X., & Chiu, W. (1998). Structure of double-shelled rice dwarf virus. *Journal of Virology*, *72*(11), 8541-8549.

Lu, S., Li, J., Wang, X., Song, D., Bai, R., Shi, Y., Gu, Q., Kuo, Y. W., Falk, B. W., & Yan, F. (2017). A Semipersistent Plant Virus Differentially Manipulates Feeding Behaviors of Different Sexes and Biotypes of Its Whitefly Vector. *Viruses*, *9*(1), 4.

Mahanta, D. K., Bhoi, T. K., Komal, J., Samal, I., Nikhil, R. M., Paschapur, A. U., Singh, G., Kumar, P. V. D., Desai, H. R., Ahmad, M. A., Singh, P. P., Majhi, P. K., Mukherjee, U., Singh, P., Saini, V., Shahanaz, Srinivasa, N., & Yele, Y. (2023). Insect-pathogen crosstalk and the cellular-molecular mechanisms of insect immunity: uncovering the underlying signaling pathways and immune regulatory function of non-coding RNAs. *Frontiers in Immunology*, *14*.

Matha, V., Jegorov, A., Weiser, J., & Pillai, J. S. (1992). The mosquitocidal activity of conidia of *Tolypocladium tundrense* and *Tolypocladium terricola*. *Cytobios*, *69*(278-279), 163-170.

Mauck, K., Bosque-Pérez, N. A., Eigenbrode, S. D., De Moraes, C. M., & Mescher, M. C. (2012). Transmission mechanisms shape pathogen effects on host–vector interactions: evidence from plant viruses. *Functional Ecology*, *26*(5), 1162-1175.

Melcher, U. (2000). The '30K'superfamily of viral movement proteins. *Journal of General Virology*, *81*(1), 257-266.

Memariani, H., Memariani, M., Moravvej, H., & Shahidi-Dadras, M. (2020). Melittin: a venom-derived peptide with promising anti-viral properties. *European Journal of Clinical Microbiology & Infectious Diseases*, *39*(1), 5-17.

Moreno-Habel, D. A., Biglang-awa, I. M., Dulce, A., Luu, D. D., Garcia, P., Weers, P. M., & Haas-Stapleton, E. J. (2012). Inactivation of the budded virus of Autographa californica M nucleopolyhedrovirus by gloverin. *Journal of invertebrate pathology*, *110*(1), 92-101.

Morozov, S. Y., & Solovyev, A. G. (2003). Triple gene block: modular design of a multifunctional machine for plant virus movement. *Journal of General Virology*, *84*(6), 1351-1366.

Namba, R. & Higa, S. (1971). Host plant studies of the corn planthopper, *Peregrinus maidis* (Ashmead), in Hawaii. *Hawaiian Entomological Society*, *21*, 105–108.

Nault, L. R., & Ammar, E. D. (1989). Leafhopper and Planthopper Transmission of Plant Viruses. *Annual Review of Entomology*, *34*(Volume 34, 1989), 503–529.

Nault, L. R. (1997). Arthropod Transmission of Plant Viruses: a New Synthesis. *Annals of the Entomological Society of America*, *90*(5), 521–541.

Niere, M., Dettloff, M., Maier, T., Ziegler, M., & Wiesner, A. (2001). Insect immune activation by apolipophorin III is correlated with the lipid-binding properties of this protein. *Biochemistry*, *40*(38), 11502–11508.

Otvos L., Jr (2000). Antibacterial peptides isolated from insects. *Journal of peptide science: an official publication of the European Peptide Society*, *6*(10), 497–511.

Peel, M., & Scribner, A. (2013). Cyclophilin inhibitors as antiviral agents. *Bioorganic & medicinal chemistry letters*, *23*(16), 4485–4492.

Ramírez, B. C., & Haenni, A. L. (1994). Molecular biology of tenuiviruses, a remarkable group of plant viruses. *The Journal of general virology*, *75 (Pt 3)*, 467–475.

Rosales Ramirez, R., & Ludert, J. E. (2019). The Dengue Virus Nonstructural Protein 1 (NS1) Is Secreted from Mosquito Cells in Association with the Intracellular Cholesterol Transporter Chaperone Caveolin Complex. *Journal of virology*, *93*(4), e01985-18.

Romoser, W. S., Wasieloski, L. P., Jr, Pushko, P., Kondig, J. P., Lerdthusnee, K., Neira, M., & Ludwig, G. V. (2004). Evidence for arbovirus dissemination conduits from the mosquito (Diptera: Culicidae) midgut. *Journal of medical entomology*, *41*(3), 467–475.

Rosen, R., Kanakala, S., Kliot, A., Cathrin Pakkianathan, B., Farich, B. A., Santana-Magal, N., Elimelech, M., Kontsedalov, S., Lebedev, G., Cilia, M., & Ghanim, M. (2015). Persistent, circulative transmission of begomoviruses by whitefly vectors. *Current opinion in virology*, *15*, 1–8.

Salazar-García, M., Acosta-Contreras, S., Rodríguez-Martínez, G., Cruz-Rangel, A., Flores-Alanis, A., Patiño-López, G., & Luna-Pineda, V. M. (2022). Pseudotyped Vesicular Stomatitis Virus-Severe Acute Respiratory Syndrome-Coronavirus-2 Spike for the Study of Variants, Vaccines, and Therapeutics Against Coronavirus Disease 2019. *Frontiers in Microbiology*, *12*.

Sanderfoot, A. A., & Lazarowitz, S. G. (1996). Getting it together in plant virus movement: cooperative interactions between bipartite geminivirus movement proteins. *Trends in cell biology*, *6*(9), 353–358.

Schaller, T., Ocwieja, K. E., Rasaiyaah, J., Price, A. J., Brady, T. L., Roth, S. L., Hué, S., Fletcher, A. J., Lee, K., KewalRamani, V. N., Noursadeghi, M., Jenner, R. G., James, L. C., Bushman, F. D., & Towers, G. J. (2011). HIV-1 capsid-cyclophilin interactions determine nuclear import pathway, integration targeting and replication efficiency. *PLoS pathogens*, *7*(12), e1002439.

Scholthof, K. B., Adkins, S., Czosnek, H., Palukaitis, P., Jacquot, E., Hohn, T., Hohn, B., Saunders, K., Candresse, T., Ahlquist, P., Hemenway, C., & Foster, G. D. (2011). Top 10 plant viruses in molecular plant pathology. *Molecular plant pathology*, *12*(9), 938–954.

Segrest, J. P., Jones, M. K., De Loof, H., Brouillette, C. G., Venkatachalapathi, Y. V., & Anantharamaiah, G. M. (1992). The amphipathic helix in the exchangeable

apolipoproteins: a review of secondary structure and function. *Journal of lipid research*, *33*(2), 141–166.

Sieczkarski, S. B., & Whittaker, G. R. (2005). Viral entry. *Current topics in microbiology and immunology*, *285*, 1–23.

Strand, M. R. (2008). The insect cellular immune response. *Insect Science*, *15*(1), 1–14.

Suzuki, N., Sugawara, M., Kusano, T., Mori, H., & Matsuura, Y. (1994). Immunodetection of Rice Dwarf Phytoreoviral Proteins in Both Insect and Plant Hosts. *Virology*, *202*(1), 41–48.

Takahashi, N., Hayano, T., & Suzuki, M. (1989). Peptidyl-prolyl cis-trans isomerase is the cyclosporin A-binding protein cyclophilin. *Nature*, *337*(6206), 473–475.

Tamborindeguy, C., Hata, F. T., Molina, R. de O., & Nunes, W. M. de C. (2023). A New Perspective on the Co-Transmission of Plant Pathogens by Hemipterans. *Microorganisms*, *11*(1).

Tsai, J.H. (1975). Occurrence of a corn disease in Florida transmitted by *Peregrinus maidis*. *Plant Disease Reporter 59*:830-833.

Tsai, J. H., & Wilson, S. W. (1986). Biology of *Peregrinus maidis* with Descriptions of Immature Stages (Homoptera: Delphacidae). *Annals of the Entomological Society of America*, *79*(3), 395–401.

Tsai, J. H., & Zitter, T. A. (1982). Characteristics of Maize Stripe Virus Transmission by the Corn Delphacid. *Journal of Economic Entomology*, *75*(3), 397–400.

Valanne, S., Wang, J. H., & Rämet, M. (2011). The Drosophila Toll signaling pathway. *Journal of immunology (Baltimore, Md. : 1950)*, *186*(2), 649–656.

Walker, P. J., & Kongsuwan, K. (1999). Deduced structural model for animal rhabdovirus glycoproteins. *The Journal of general virology*, *80 (Pt 5)*, 1211–1220.

Wang, X. W., & Blanc, S. (2021). Insect Transmission of Plant Single-Stranded DNA Viruses. *Annual review of entomology*, *66*, 389–405.

Wang, P., & Heitman, J. (2005). The cyclophilins. *Genome biology*, *6*(7), 226.

Wang, H. D., Chen, J. P., Zhang, H. M., Sun, X. L., Zhu, J. L., Wang, A. G., Sheng, W. X., & Adams, M. J. (2008). Recent Rice stripe virus Epidemics in Zhejiang Province, China, and Experiments on Sowing Date, Disease-Yield Loss Relationships, and Seedling Susceptibility. *Plant disease*, *92*(8), 1190–1196.

Wang, C. K., Shih, L. Y., & Chang, K. Y. (2017). Large-Scale Analysis of Antimicrobial Activities in Relation to Amphipathicity and Charge Reveals Novel Characterization of Antimicrobial Peptides. *Molecules (Basel, Switzerland)*, *22*(11), 2037.

Weers, P. M., Van Marrewijk, W. J., Beenakkers, A. M., & Van der Horst, D. J. (1993). Biosynthesis of locust lipophorin. Apolipophorins I and II originate from a common precursor. *Journal of Biological Chemistry*, *268*(6), 4300–4303.

Weise, C., Franke, P., Kopácek, P., & Wiesner, A. (1998). Primary structure of apolipophorin-III from the greater wax moth, Galleria mellonella. *Journal of protein chemistry*, *17*(7), 633–641.

Weiser, J., & Matha, V. (1988). The insecticidal activity of cyclosporines on mosquito larvae. *Journal of invertebrate pathology*, *51*(1), 92–93.

Whitfield, A. E., Huot, O. B., Martin, K. M., Kondo, H., & Dietzgen, R. G. (2018). Plant rhabdoviruses-their origins and vector interactions. *Current opinion in virology*, *33*, 198–207.

Whitten, M. M., Tew, I. F., Lee, B. L., & Ratcliffe, N. A. (2004). A novel role for an insect apolipoprotein (apolipophorin III) in beta-1,3-glucan pattern recognition and cellular

encapsulation reactions. *Journal of immunology (Baltimore, Md.: 1950)*, *172*(4), 2177–2185.

Wiesner, A., Losen, S., Kopáček, P., Weise, C., & Götz, P. (1997). Isolated Apolipophorin III from *Galleria mellonella* Stimulates the Immune Reactions of This Insect. *Journal of Insect Physiology*, *43*(4), 383–391.

Wu, X., & Cheng, X. (2020). Intercellular movement of plant RNA viruses: Targeting replication complexes to the plasmodesma for both accuracy and efficiency. *Traffic*, *21*(12), 725–736.

Yamada, K., Kuribayashi, K., Inomata, N., Noguchi, K., Kimitsuki, K., Demetria, C. S., Saito, N., Inoue, S., Park, C. H., Kaimori, R., Suzuki, M., Saito-Obata, M., Kamiya, Y., Manalo, D. L., Quiambao, B. P., & Nishizono, A. (2021). Validation of serum apolipoprotein A1 in rabies virus-infected mice as a biomarker for the preclinical diagnosis of rabies. *Microbiology and immunology*, *65*(10), 438–448.

Yao, J., Rotenberg, D., & Whitfield, A. E. (2019). Delivery of maize mosaic virus to planthopper vectors by microinjection increases infection efficiency and facilitates functional genomics experiments in the vector. *Journal of Virological Methods*, *270*, 153–162.

Yi, H. Y., Chowdhury, M., Huang, Y. D., & Yu, X. Q. (2014). Insect antimicrobial peptides and their applications. *Applied microbiology and biotechnology*, *98*(13), 5807–5822.

Yu, J., Zhao, W., Chen, X., Lu, H., Xiao, Y., Li, Q., Luo, L., Kang, L., & Cui, F. (2024). A plant virus manipulates the long-winged morph of insect vectors. *Proceedings of the National Academy of Sciences*, *121*(3), e2315341121.

Zeigler, R. S., & Morales, F. J. (1990). Genetic determination of replication of rice hoja blanca virus within its planthopper vector, *Sogatodes oryzicola*. *Phytopathology*, *80*(6), 559-566.

Zhang, L., Wu, N., Ren, Y., & Wang, X. (2021). Insights Into Insect Vector Transmission and Epidemiology of Plant-Infecting Fijiviruses. *Frontiers in microbiology*, *12*, 628262.

Zhang, W., Tettamanti, G., Bassal, T., Heryanto, C., Eleftherianos, I., & Mohamed, A. (2021). Regulators and signalling in insect antimicrobial innate immunity: Functional molecules and cellular pathways. *Cellular signalling*, *83*, 110003.

Zhang, H., Liang, X., Li, D., Zhang, C., Wang, W., Tang, R., Zhang, H., Kiflu, A. B., Liu, C., Liang, J., Li, X., & Luo, T. R. (2024). Apolipoprotein D facilitates rabies virus propagation by interacting with G protein and upregulating cholesterol. *Frontiers in immunology*, *15*, 1392804.

Zhou, X., Peng, L. Y., Wang, Z. C., Wang, W., Zhu, Z., Huang, X. H., Chen, L. B., Song, Q. S., & Bao, Y. Y. (2019). Identification of novel antimicrobial peptides from rice planthopper, Nilaparvata lugens. *Insect biochemistry and molecular biology*, *113*, 103215.

CHAPTER 2

Design and Validation of Plasmid Vectors for Characterizing Protein–Protein Interactions in *Spodoptera frugiperda* Insect Cells*

This chapter was published in PhytoFrontiers™: Teh, H. W., Martin, K., & Whitfield, A. E. (2021). Design and validation of plasmid vectors for characterizing protein-protein interactions in Spodoptera frugiperda insect cells. *PhytoFrontiers™*. https://doi.org/10.1094/PHYTOFR-09-21-0059-TA

Abstract

There are limited molecular biology resources for interrogating protein–protein interactions (PPIs) in insect cells. To address this deficiency, we developed plasmid vectors for localization, bimolecular fluorescence complementation (BiFC), and co-immunoprecipitation (co-IP) assays in Sf9 insect cells. Plasmids were designed to express a protein of interest as a fusion with epitope tags and autofluorescent proteins using the Gateway cloning system. Two robust interactors were utilized to validate this system: the nucleoprotein (N) and the phosphoprotein (P) of maize mosaic virus. The viral N was fused with the carboxy-terminal portion of eYFP and a FLAG epitope tag, and P was fused with the amino-terminal portion of eYFP and a myc epitope tag. The two expression plasmids were cotransfected into Sf9 cells, fluorescence microscopy was used to visualize BiFC, and co-IP was performed to confirm that this system was sensitive enough to detect PPI between the two proteins. BiFC was seen in cells cotransfected with N and P, and co-IP validated the interaction. This plasmid-based system can be used to investigate a variety of PPIs that occur in insects. We validated viral protein interactions that occur in the insect vector, which provides further insights into the biology of rhabdoviruses that are transmitted by insects. The ability to express viral and insect proteins in insect cells for studying PPIs with this streamlined system represents an advancement for protein research in insects. Future work will focus on identifying interacting viral and host proteins and discovery of targets for control of viruses and insect vectors.

Introduction

Protein–protein interaction (PPI) assays are important tools for investigating the relationship between viruses and their host organisms. Investigating PPIs between viral and host proteins

enables identification and validation of novel interactions and functions and is important for understanding the virus infection cycle in insects. Molecular assays such as co-immunoprecipitation (co-IP) or yeast two-hybrid assays have been used extensively in the past to study PPIs, and as new technologies continue to be developed and refined, more sophisticated assays such as bimolecular fluorescence complementation (BiFC) or fluorescence resonance energy transfer have become commonplace in the molecular biology toolbox (Bailer and Haas 2009; Kerppola 2008; Kodama and Hu 2012).

Studying PPIs in live insect cells can help to elucidate the function and localization of proteins within them, but the lack of insect cell culture lines for numerous insect species, especially vectors of plant pathogens, has hindered this work. Researchers are hence reliant on commercially available S2 (*Drosophila melanogaster*) and Sf9 and Sf21 (*Spodoptera frugiperda*) insect cell lines to answer research questions in similar but divergent systems. Although there are tools currently available for use in insect cell culture research, many of them rely on baculovirus expression vector systems, which introduce additional variables into the system because of the effect of the virus on the cell, thus complicating interpretation of the study.

Maize mosaic alphanucleorhabdovirus is a member of the family *Rhabdoviridae*, which contains viruses that infect animals, plants, and insects (Whitfield et al. 2018). Maize mosaic virus (MMV) is transmitted by the corn planthopper *Peregrinus maidis* in a persistent, propagative manner. The biology of MMV transmission by *P. maidis* is well characterized, making it a model system for plant rhabdovirus-vector interactions (Barandoc-Alviar et al. 2016; Klobasa et al. 2021; Martin et al. 2017; Whitfield et al. 2011; Yao et al. 2013, 2019). Understanding the interactions between viral and host proteins in plant and insect cells will yield valuable information about how MMV functions in vivo, providing a more complete understanding of the viral life cycle and thus paving

the way for implementation of unique management options for MMV. Methods for studying PPIs in plant cells are well established, but the ability to make direct comparisons to the insect phase of the infection cycle has been hampered by a lack of molecular biology tools in insects.

In this study, we have developed and validated a novel set of plasmids to investigate PPIs in Sf9 insect cells. This system utilizes Gateway technology, which enables the use of a single entry clone that can be moved into multiple destination vectors within the same system, as well as other Gateway-compatible systems, allowing for efficient screening of many virus–virus or virus–host protein interactions within insect cells using localization, co-IP, and BiFC. Two expression plasmids encoding proteins of interest fused to either the N- or C-terminal half of enhanced yellow fluorescent protein (YFP) and an epitope tag are cotransfected into Sf9 cells, then co-IP and BiFC experiments are performed to confirm the presence or absence of an interaction between the two proteins. Separate expression plasmids encoding proteins of interest fused to either enhanced green fluorescent protein (GFP) or monomeric red fluorescent protein (RFP) were also used to corroborate the localization patterns observed with the proteins fused to split YFP halves. We chose to use the nucleoprotein (N) and the phosphoprotein (P) of MMV as our test proteins because the interaction between N and P is robust and highly conserved among all rhabdoviruses (Goodin et al. 2001; Gupta et al. 2003; Tsai et al. 2005). Previous studies have also shown that the N and P proteins colocalize in *Nicotiana benthamiana* and *Drosophila melanogaster* S2 cells (Martin and Whitfield 2018).

Materials and Methods

Construction of the GFP and RFP Vectors

To add autofluorescent proteins to the original plasmid, pIB/V5-His-DEST (Thermo Fisher Scientific, Waltham, MA, U.S.A.), we used a combination of gene synthesis and standard restriction enzyme cloning to generate C-terminal tag constructs. GFP was modified to be placed before the Gateway cassette in pIB/V5-His-DEST by the addition of sequences to the 5' and 3' ends and synthesis by GenScript (Piscataway, NJ, U.S.A.). The 5' end of GFP was modified to contain KasI and NdeI restriction sites, and sequences from pIB including the 3' end of the pOpIE2 promoter were added to the KasI restriction site. The NdeI contains the ATG site used to initiate translation at the beginning of GFP and sets the frame for other insertions. The 3' end of GFP was modified to remove the stop codon and to add a HindIII restriction site, and this synthesized intermediate construct was renamed GFP-N1. Subsequent digestion with KasI and HindIII was performed to ligate it into the pIB/V5-His-DEST vector. This vector was renamed pIGW. A full description of the plasmid naming scheme is provided in Table 1.1. RFP was added to pIGW with PCR amplification using Phusion polymerase (Thermo Fisher Scientific) with each of the fragments with NdeI and HindIII restriction sites added to the 5' and 3' ends, respectively. The insect vector pHRW (emb.carnegiescience.edu/drosophilagateway-vector-collection, Murphy, unpublished; Drosophila Resource Center, Indiana State University, Bloomington, IN) was used as the template for RFP amplification, and the amino-terminal YFP half (nYFP) and carboxy-terminal YFP half (cYFP) were amplified from the pSITE-BiFC vectors, a collection of plasmids used for expression in plants (Martin et al. 2009). All primer sequences are provided in Table 1.2. The RFP-N1, nYFPN1, and cYFP-N1 fragments were all amplified with their respective primer

pairs. Digestion of the fragments and ligation into a similarly digested pIGW resulted in the construction of pIRW, pInYW, and pIcYW.

To generate the vectors for C-terminal autofluorescent protein fusions, the fluorescent proteins were added with a combination of synthesis, PCR amplification, and restriction digestion. The GFP fragment was synthesized by GenScript with flanking SalI and AgeI sites, with a small fragment of the Gateway cassette added after the native SalI site to complete the attR2 site for Gateway recombination. The 3' end of GFP was modified to remove the stop codon and add an XbaI site. To preserve the reading frame with an added AscI site at the 5' end, an extra nucleotide was added to the sequence. The fragment described above was subsequently digested with SalI and AgeI before ligation into a similarly digested pIB/V5-His-DEST, resulting in the construction of pIWG. The RFP-C1, nYFP-C1, and cYFP-C1 intermediate pieces were amplified from the vectors stated above using Phusion polymerase (Thermo Fisher Scientific). The fragments were digested with AscI and XbaI and ligated into a similarly digested pIWG vector to construct the pIWR, pIWnY, and pIWcY vectors, respectively.

Table 1.1: Names and features of the newly constructed pI vectors. GW = Gateway cassette; GOI = gene of interest; GFP = green fluorescent protein; RFP = red fluorescent protein; and n/cYFP = amino or carboxy terminal half of yellow fluorescent protein, respectively.

Vector	Orientation	Features
pIWG	GW-GOI	Gateway cassette, EGFP, V5, 6xHis
pIWR	GW-GOI	Gateway cassette, mRFP, V5, 6xHis
pIWnY	GW-GOI	Gateway cassette, nEYFP, V5, 6xHis
pIWcY	GW-GOI	Gateway cassette, cEYFP, V5, 6xHis
pIWnYM	GW-GOI	Gateway cassette, nEYFP, 6x c-myc, 6xHis
pIWcYF	GW-GOI	Gateway cassette, cEYFP, 6x FLAG, 6xHis

Table 1.1 (continued).

pIGW	GOI-GW	EGFP, Gateway cassette, V5, 6xHis
pIRW	GOI-GW	mRFP, Gateway cassette, V5, 6xHis
pInYW	GOI-GW	nEYFP, Gateway cassette, V5, 6xHis
pIcYW	GOI-GW	cEYFP, Gateway cassette, V5, 6xHis
pInYWM	GOI-GW	nEYFP, cassette, 6x c-myc, 6xHis
pIcYWF	GOI-GW	cEYFP, Gateway cassette, 6x FLAG, 6xHis

Table 1.2: List of primer sequences used for cloning pI vectors.

Primer Name	Primer sequence (5' - 3')	Purpose
mRFP-N1_F	CGAATTTACATATGGCCTCCTCCGAG GACGTCATCAAGGAG	Movement of mRFP into vector-marked NdeI site
mRFP-N1_R	CGATATCAAGCTTGGCGCCGGTGGA GTGGCGGCCCTCGGCGC	Movement of mRFP into vector-marked HindIII site
nEYFP-N1_F	CGAATTTACATATGGTGAGCAAGGG CGAGGAGCTGTTC	Initial cloning for V5 site-marked NdeI site
nEYFP-N1_R	CGATATCAAGCTTCTTGTACAGCTCG TCCATGCCGTGAGTGATCCC	Initial cloning for V5 site-marked HindIII site
cEYFP-N1_F	GTTCGAATTTACATATGGGCGGCAG CGTGCAGCTCGCCGACCA	Initial cloning for V5 site-marked NdeI site
cEYFP-N1_R	AATTCGATATCAAGCTTCTTGTACAG CTCGTCCATGCCGAGAGTGATC	Initial cloning for V5 site-marked HindIII site
mRFP-C1_F	CGGGAGGGCGCGCCATGGCCTCCTC CGAGGACGTCATCAAGGAG	Initial cloning for V5 site-marked AscI site
mRFP-C1_R	CGGGCCCTTTCTAGAGGCGCCGGTG GAGTGGCGGCCCTCGGCGCGC	Initial cloning for V5 site-marked XbaI site
nEYFP-C1_F	CCCGGGAGGGCGCGCCATGGTGAGC AAGGGCGAGGAGCTGTTCACCGGG	Initial cloning for V5 site-marked AscI site
nEYFP-C1_R	CCGCGGGCCCTTTCTAGAGTCCTCGA TGTTGTGGCGGATCTTGAAG	Initial cloning for V5 site-marked XbaI site
cEYFP-C1_F	CCCGGGAGGGCGCGCCGGCAGCGTG CAGCTCGCCGACCACTACCAGC	Initial cloning for V5 site-marked AscI site
cEYFP-C1_R	ACCGCGGGCCCTTTCTAGACTTGTAC AGCTCGTCCATG	Initial cloning for V5 site-marked XbaI site

Table 1.2 (continued).

MBP_F	CACCATGAAAATCGAAGAAGGTAAACTG	Cloning of MBP into pENTR d-Topo
MBP_R	AGTCTGCGCGTCTTTCAGGGC	Cloning of MBP into pENTR d-Topo

Modification of the Epitopes in the BiFC Vectors for Pull-down Studies

Epitope tags 6x myc or 6x FLAG were added to the pInYW, pIcYW, pIWnY, and pIWcY vectors by synthesizing the entire nYFP and cYFP sequence (GenScript) in frame with either the 6x myc epitope or the 6x FLAG epitope. Addition of nYFP and cYFP was done with restriction cloning. The AscI and AgeI sites were used for cloning the amino terminal fusions to the Gateway cassette, and the SalI and AgeI sites were used for the carboxy terminal fusions to the Gateway cassette. The addition of epitope tags allowed for pull-down assays to be conducted with the different fusion proteins after BiFC imaging to confirm the expression of the proteins if no interaction was observed and to show a secondary method of interaction. There are two sets of BiFC vectors: those containing the 6x myc (nYFP) and 6x FLAG tags (cYFP) and the versions containing the original V5 epitope. This was done to ensure that each YFP half was associated with only one epitope tag, as multiple orientations of the fluorescent protein halves may be required to detect an interaction. A 6x myc or 6x FLAG sequence flanked by XbaI and AgeI restriction sites was synthesized and then digested with XbaI and AgeI before being ligated with the similarly digested pInYW and pIcYW vectors to produce pInYWM and pIcYWF. The same cloning steps and restriction digests used to make the plasmids above were also used to generate pIWnYM or pIWcYF.

Construction of MMV N and P Expression Clones

For validation of the functionality of the pIB vectors, we used the MMV Nand P genes. In previous work, pENTR_MMV-N and pENTR_MMV-P entry vectors were constructed and used to test

expression, BiFC in plants, and localization in insect cells (Martin and Whitfield 2018). The negative control protein used in these PPI assays was the maltose-binding protein (MBP) from *E. coli*, and MBP was amplified from pMAL-c2x. The MBP forward and reverse primers in Table 2 were used to clone MBP into pENTR. Gateway recombination using LR Clonase II (Thermo Fisher Scientific) was then performed with various combinations of entry and destination vectors. The final expression clones used for cell transfections are as follows: pING (N-GFP), pIPR (P-RFP), pIcYNF (cYFP-N), pIPnYM (P-nYFP), pIMnYM (MBP-nYFP), and pIcYMF (cYFP-MBP).

Plasmid DNA Transfection into Sf9 Cells

To prepare the transfection reagent, 3 μg of plasmid DNA for each construct and 8 μl of Cellfectin II Reagent (Thermo Fisher Scientific) were added to 200 μl of supplemented Grace's Insect Medium (Thermo Fisher Scientific) and incubated at room temperature for at least 30 min. An additional 800 μl of supplemented Grace's Insect Medium (Thermo Fisher Scientific) was added to the solution afterward. Sf9 cells were diluted in fresh Sf900-III serum-free medium (Thermo Fisher Scientific) to a final concentration of 4×10^5 cells/ml, and 2 ml of cell solution was seeded in each well of a 35-mm six-well plate (Thermo Fisher Scientific) before being incubated for 1 h at 27°C for cell reattachment. The medium in the six-well plates was then replaced with 1 ml of transfection reagent and incubated at 27°C for at least 3 h, after which the transfection reagent was replaced with 2.5 ml of fresh Sf900-III medium. After a 72-h incubation at 27°C, the cells either had total protein extracted from them or were used for fluorescence imaging.

Co-IP of N and P Fusion Proteins

Total protein was extracted from transfected Sf9 cells by first resuspending the cells in 1 ml of fresh Sf900-III serum-free medium, centrifuging them at 2,000×*g* for 1 min, and then washing the pellet with an ice-cold solution of phosphate-buffered saline (PBS; pH 7.4). The cells were then centrifuged again at 2,000 × *g* for 1 min, and the PBS was replaced with Pierce IP Lysis Buffer with Halt Protease Inhibitor (Thermo Fisher Scientific) before being incubated on ice for 5 min. The cell lysate was then centrifuged at 2,000 × *g* for 1 min, and the supernatant was transferred to a separate 1.7-ml microcentrifuge tube containing anti-FLAG affinity gel (Bimake, Houston, TX, U.S.A.) that had been washed with a mixture of Tris-buffered saline with 1% Tween-20 (TBST). An aliquot of the supernatant was saved for direct western blot analysis to confirm successful protein expression. The cell supernatant was incubated with the washed anti-FLAG affinity gel for at least 3 h at room temperature on a Mini LabRoller Rotator (Labnet, Edison, NJ, U.S.A.), then centrifuged at 5,000 × *g* for 5 min at 4°C. The affinity gel was washed once with Pierce IP Lysis Buffer before direct addition of Laemmli buffer to the tube containing the gel. The sample was then heated at 95°C for 10 min before being loaded into a 10% SDS-PAGE protein gel for downstream western blot analysis.

Western Blot Analysis of Proteins

For analysis of proteins, 10% SDS-PAGE gels were cast with the TGX FastCast acrylamide kit (Bio-Rad, Hercules, CA, U.S.A.) following the manufacturer's protocol. The Mini- PROTEAN Tetra Cell (Bio-Rad) was used to run the gel at 150 V for approximately 30 to 45 min, and the Trans-Blot Turbo Transfer System (Bio-Rad) was used to transfer the proteins in the gel onto a PVDF membrane. The membrane was blocked with 5% dry milk in TBST before probing with anti-myc (1:5,000 dilution) (Thermo Fisher Scientific) or anti-FLAG (1:5,000 dilution) (Thermo

Fisher Scientific) antibodies. The membrane was then washed with TBST and incubated with horseradish peroxidase (HRP)-conjugated secondary antibodies (Bio-Rad) against the corresponding primary antibodies. In the case of the membrane containing protein samples from co-IP experiments with contamination from the mouse anti-FLAG antibodies from the affinity gel, mouse TrueBlot HRP-conjugated secondary antibodies (Rockland Immunochemicals, Pottstown, PA, U.S.A.) were used for staining. Another TBST wash was performed on the membrane after secondary antibody incubation, and Clarity Western ECL Substrate (Bio-Rad) was used to visualize the bands on the membrane using the iBright Western Blot Imaging System (Thermo Fisher Scientific).

Fluorescence Imaging of Sf9 Cells

Each well of plasmid-transfected Sf9 cells was diluted fourfold with Sf900-III SFM in a new six-well plate after the initial 72-h incubation period. The cells were incubated at 27°C for 1 h for reattachment, and then the medium was replaced with PBS 7.4 and 105 ng/μl of 4’,6-diamidino-2-phenylindole, dihydrochloride (Thermo Fisher Scientific) to stain the cell nuclei. After 10 min, the PBS medium was removed, and the cells were washed with fresh PBS. The Cytation 5 Cell Imaging Multi-Mode Reader (BioTek) was then used to assay for fluorescent protein expression in the cells.

Results

Vectors for Expression of Fusion Proteins in Insect Cells

A collection of plasmid vectors for expressing proteins and studying PPIs in insect cells was created. All plasmids use the baculovirus immediate early promoter (OpIE2) from *Orgyia pseudotsugata* multiple nucleopolyhedrovirus (OpMNPV) for expression, which has been shown to function in diverse insect cell lines (Theilmann and Stewart 1992). Insect expression plasmids were constructed for expression of fusions with autofluorescent (RFP and GFP) proteins at the N- or C- terminus. These plasmids also contain the V5 and 6x His tags for detection and purification. Plasmids were also designed for BiFC experiments in insect cells, and the split YFP halves were inserted into the vectors for in-frame expression as N- or C-terminal fusions. In these vectors, we replaced the V5 tag with myc or FLAG tags for co-IP experiments to validate BiFC assays and to confirm protein expression using western blots. The MMV N and P and the negative control MBP proteins were transferred from entry clones into expression vectors for validation of the system using standard Gateway recombination reactions. The resulting plasmid vectors are shown in Figure 1.1.

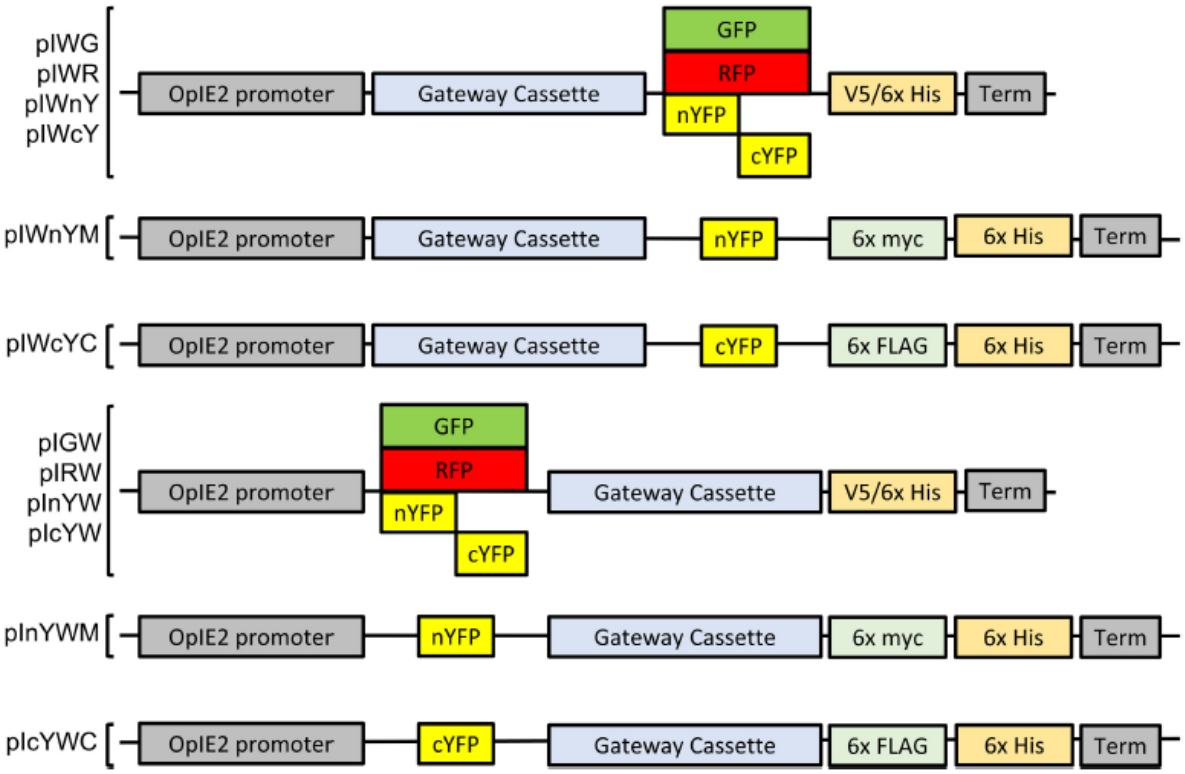

Figure 1.1: Schematic of the pI plasmid vector system showing the orientation of constructs within each plasmid. The plasmid naming scheme is as follows: W refers to the Gateway cassette, G refers to green fluorescent protein, R refers to red fluorescent protein, and nY and cY refer to the amino-terminal or the carboxy-terminal portion of yellow fluorescent protein. OpIE2 is the immediate early promoter of the *Orgyia pseudotsugata* multiple nucleopolyhedrovirus. The Gateway cassette is located either before or after the autofluorescent proteins, depending on the construct, to enable creation of N- or C-terminal fusion proteins. The original plasmid backbone contains V5 and 6x His epitope tags on the C-terminus region just before the OpIE2 polyadenylation signal/terminator (Term). Additional vectors were constructed for dual bimolecular fluorescence complementation and co-immunoprecipitation by replacing the V5 tag with either a 6x myc or a 6x FLAG epitope tag.

Imaging of Autofluorescent Fusion Proteins

Strong fluorescence signals were observed in insect cells transfected with plasmid constructs of MMVN-GFP and P-RFP. GFP fluorescence was seen in the nuclear region of N-GFP-transfected cells, with weak fluorescence seen in the cytoplasm. RFP fluorescence was strictly nuclear-localized in P-RFP-transfected cells (Fig. 2.1B). To determine if the N and P fusion proteins would influence the localization of the other, as seen previously (Martin and Whitfield 2018), the two expression plasmids were cotransfected into Sf9 cells. Small, punctate green and yellow foci, as well as red fluorescence, were seen in the nuclear region of the cells, with green fluorescence seen in the cytoplasm as well (Fig. 2.1C). These results suggest that the interaction between the viral proteins was not disrupted by the presence of the fused fluorescent proteins. The colocalization of the N and P fusion proteins in the nucleus Sf9 cells is consistent with that in S2 insect cells and plant cells (Martin and Whitfield 2018).

BiFC imaging was performed on Sf9 cells co-expressing cYFP-N and P-nYFP, and yellow fluorescence was observed in the nuclear region (Fig. 2.2B). No yellow fluorescence was observed in the negative controls where MBP was expressed in place of N or P protein. Even in cases of low transfection efficiency, imaging of fluorescently tagged proteins using epifluorescence microscopy is possible because a single 9.6-cm^2 well of a six-well plate contains thousands of cells. The BiFC assay with N and P validates that the pI vectors function in insect cells.

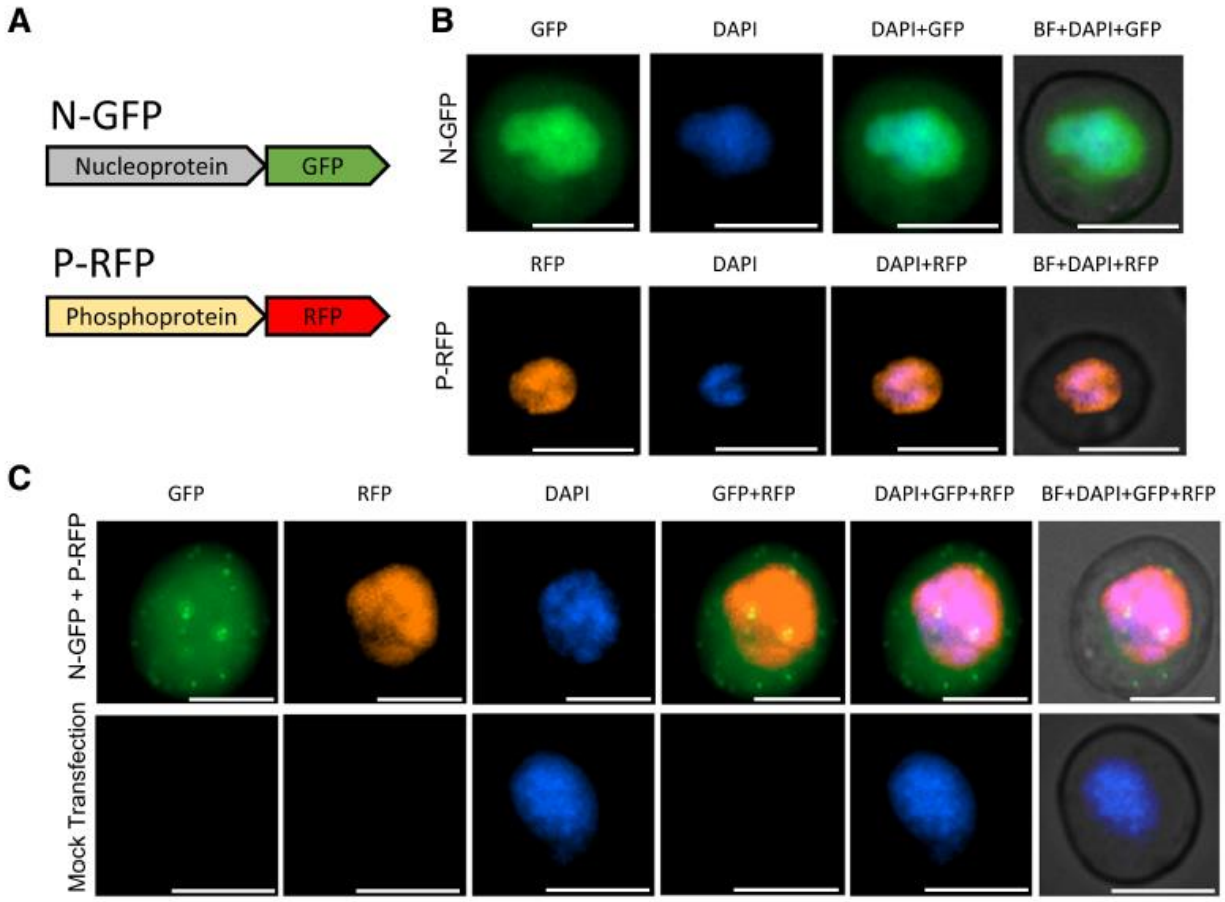

Figure 2.1: A: Pictorial representation of the fusion proteins encoded by the respective plasmids. B: Fluorescence microscopy imaging of Sf9 insect cells transfected with pING. Strong green fluorescent protein (GFP) fluorescence is observed in the nucleus, and faint GFP signals can be seen in the cytoplasm, N appears to be primarily nuclear-localized. Red fluorescent protein fluorescence is seen only in the nucleus of Sf9 cells transfected with pIPR, the localization of P appears to be strictly nuclear. C: Cotransfection of N and P fusion proteins into Sf9 cells appears to have no effect on the original localization of the N or P proteins. Small punctate green foci are also observed in the cell nucleus. DAPI = 4',6-diamidino-2-phenylindole; BF = Brightfield; and scale bars represent 15 μM.

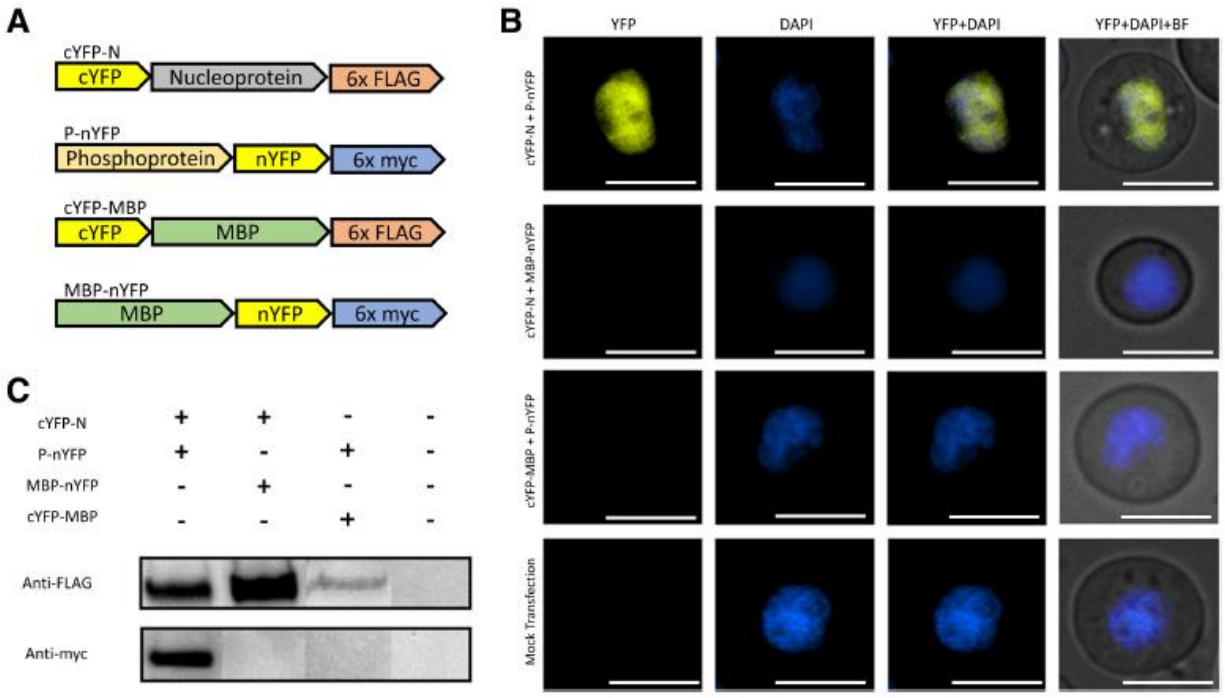

Figure 2.2: A: Pictorial representation of the different fusion protein constructs. B: Bimolecular fluorescence complementation (BiFC) imaging of Sf9 insect cells cotransfected with the listed combination of plasmids. Yellow fluorescence is observed in the nuclear region of cells co-expressing cYFP-N and P-nYFP fusion proteins but not in any of the negative controls expressing maltose-binding protein (MBP) in place of either N or P protein. Scale bars represent 15 μM. C: Western blotting results after co-immunoprecipitation of raw cell lysate from cotransfected Sf9 cells was performed with anti-FLAG affinity gel. P was able to be coprecipitated with N, but MBP was not able to be precipitated by N, and MBP was not able to precipitate P.

Western Blotting and Co-IP Analysis of N and P Fusion Proteins

Western blots of cell lysate from cells expressing cYFP-N and P-nYFP, stained with anti-FLAG and anti-myc primary antibodies, respectively, showed the presence of bands corresponding to the predicted molecular weights of the fusion proteins, confirming stable expression of the constructs

in Sf9 cells (Supplementary Fig. 1). The control fusion, cYFP-MBP and MBP-nYFP, proteins could also be detected via western blotting when total protein from transfected Sf9 cells was loaded onto SDS-PAGE gels and stained with the appropriate anti-myc or FLAG primary antibodies. Co-immunoprecipitation of N and P was performed with anti-FLAG affinity gel (Rockland), and the N-FLAG fusion protein successfully precipitated the P-myc fusion protein. The MBP-FLAG negative control did not precipitate P-myc (Fig. 2.2C). These results confirm that the system is sensitive enough to detect the strong, conserved PPI between the two viral proteins without detecting a signal between the control treatment of MBP and the viral P protein.

Discussion

We have developed a plasmid-based system to enable medium-throughput screening of protein interactions via BiFC and co-IP and to conduct experiments without the use of another virus that could have confounding effects on cell physiology, increasing the repertoire of tools available for use in similar types of studies. The Sf9 insect cell line is a useful analogous system for studying PPIs of vector-borne plant viruses and their vectors, such as *P. maidis* and other insects that lack cell culture lines. These PPI tools for examining viral protein and virus–host interactions will further advance our understanding of viruses that replicate in their insect vectors, an area of study with a rapidly expanding array of technological resources (reviewed in German et al. 2020). There are limited tools available for use in insect systems to study PPIs compared with methods used in plant systems. Protein localization and BiFC studies are often used in planta to assay PPIs because plant cells are easy to modify via agrobacterium-mediated delivery of plasmids and high levels of protein expression are routinely achieved. Conversely, insect cell lines can be difficult to develop and maintain, and there are numerous challenges to overcome when attempting to overexpress

foreign proteins in insect cells. The shortage of non-baculovirus expression vector system-based tools for standard insect cell lines stalls functional analysis studies. Past studies have identified promoters for use in insect cells, but without a complete set of fluorescent proteins in a user-friendly and versatile system, individual design and validation of a variety of tools to study specific proteins of interest was required for each system. In addition, some PPI tools developed are highly specific to insect cell types. For example, BiFC tools have been developed to study PPI in *Bombyx mori*, but the specific promoter that the system relies on limits its use to only *B. mori* (Bao et al. 2013). To circumvent the issue of host specificity, the plasmids developed herein rely on the second immediate early regulatory gene of the baculovirus OpMNPV (Theilmann and Stewart 1992). The immediate early promoters of baculoviruses have been shown to function effectively in diverse host cells, indicating that they might be useful in other insect cells systems as they are developed (Pfeifer et al. 1997). In experiments with a cell line of *Graminella nigrifrons*, the hemipteran vector of maize fine streak virus and maize rayado fino virus, we observed expression of GFP from the OpIE2 promoter (Martin, Wayadande, and Whitfield, unpublished).

Another advantage of this system is that the plasmids are generated via the Gateway system, resulting in a more streamlined and higher-throughput cloning process compared with other conventional cloning methods. Plasmid transfection to express foreign proteins in insect cells is also less time- and labor-intensive than using baculovirus expression vector systems, at the cost of comparatively lower foreign protein expression levels. For complex systems such as those involving a virus, a plant, and an insect host, investigating the biological functions of each component often requires extensive familiarity and expertise with DNA manipulation, plasmid design, and other molecular biology techniques. Our system uses the same entry clones for both plant and insect cells, improving workflow efficiency and ease of implementation. The same entry

clones developed can be used in experiments with the insect system described here or in the pSITE-BiFC and pSITE-II series of plasmids for testing in plants (Martin et al. 2009). This system is useful for viruses that replicate in insects and plants for comparative analysis of viral protein interactions and can be applied to the study of virus–host interactions as well. We also expect that researchers focused on insect-specific viruses and the function of insect proteins will find these plasmid vectors useful.

A key step in the optimization of BiFC for insect cells was the selection of a negative-control protein to demonstrate the specificity of protein interactions. We generated constructs with Glutathione S-transferase (GST), a portion of Lac-Z, and MBP and tested three of them in our experiments (data not shown). We found that the Lac-Z construct was not expressed efficiently in insect cells and could not be detected in western blots. The GST protein that is commonly used as a nonbinding control in experiments in plants resulted in nonspecific interactions in insect cells. MBP was selected as the best control because it was expressed as a full-length fusion protein and did not show nonspecific interactions when tested against N and P in BiFC and co-IP assays.

Based on our results with the pI vectors described here and comparison to previous experiments with various viral and insect proteins, we propose an optimized PPI discovery and validation workflow (Badillo-Vargas et al. 2019; Martin and Whitfield 2018; Martin et al. 2009). First, we recommend that proteins be expressed as N- or C-terminal fusions with autofluorescent proteins for observing localization patterns and validation of full-length protein using western blots. It is often helpful to express target proteins as N- and C-terminal autofluorescent protein fusions to determine the optimal site for tag location. If the target protein has been studied in other systems, preliminary insect cell expression enables comparisons of localization patterns. In our validation system, MMV-N and P, we found that protein localization in Sf9 cells followed a similar pattern

as observed in plant and *Drosophila* cells (Martin and Whitfield 2018). The second step for exploring PPIs in insect cells would be BiFC experiments to determine if proteins interact and the subcellular localization of the protein interactions. Transfection conditions may need to be optimized for each protein target. In some cases, the transfection efficiency and inability to deliver sufficient plasmid quantities of plasmids can result in few cells expressing high levels of fluorescent fusion proteins. For this reason, we recommend secondary validation of interactions by co-IP, and the design of these plasmid vectors enables the same constructs to be used in these two PPI assays. The epitope tags present in all vectors also enable purification of proteins for other downstream applications.

Acknowledgments

We dedicate this paper to Dr. Michael Goodin, a pioneer in the field of rhabdovirus PPI and a dear friend and colleague.

References

Badillo-Vargas, I. E., Chen, Y., Martin, K. M., Rotenberg, D., and Whitfield, A. E. 2019. Discovery of novel thrips vector proteins that bind to the viral attachment protein of the plant bunyavirus tomato spotted wilt virus. J. Virol. 93:e00699-19.

Bailer, S.M., and Haas, J. 2009. Connecting viral with cellular interactomes. Curr. Opin. Microbiol. 12:453-459.

Bao, Y. Y., Chen, L. B., Wu, W. J., Zhao, D., Wang, Y., Qin, X., and Zhang, C. X. 2013. Direct interactions between bidensovirus BmDNV-Z proteins and midgut proteins from the virus target *Bombyx mori*. FEBS J. 280: 939-949.

Barandoc-Alviar, K., Ramirez, G. M., Rotenberg, D., and Whitfield, A. E. 2016. Analysis of acquisition and titer of maize mosaic rhabdovirus in its vector, *Peregrinus maidis* (Hemiptera: Delphacidae). J. Insect Sci. 16:14.

German, T. L., Lorenzen, M. D., Grubbs, N., and Whitfield, A. E. 2020. New technologies for studying negative-strand RNA viruses in plant and arthropod hosts. Mol. Plant-Microbe Interact. 33:382-393.

Goodin, M. M.,Austin, J., Tobias, R., Fujita, M.,Morales, C., and Jackson, A. O. 2001. Interactions and nuclear import of the N and P proteins of sonchus yellow net virus, a plant nucleorhabdovirus. J. Virol. 75:9393-9406.

Gupta, A. K., Shaji, D., and Banerjee, A. K. 2003. Identification of a novel tripartite complex involved in replication of vesicular stomatitis virus genome RNA. J. Virol. 77:732-738.

Kerppola T. K. 2008. Bimolecular fluorescence complementation (BiFC) analysis as a probe of protein interactions in living cells. Annu. Rev. Biophys. 37:465-487.

Klobasa, W., Chu, F. C., Huot, O., Grubbs, N., Rotenberg, D., Whitfield, A. E., and Lorenzen, M. D. 2021. Microinjection of corn planthopper, *Peregrinus maidis*, embryos for CRISPR/Cas9 genome editing. J. Vis. Exp. 169:e62417.

Kodama, Y., and Hu, C.-D. 2012. Bimolecular fluorescence complementation (BiFC): A 5-year update and future perspectives. BioTechniques 53: 285-298.

Martin, K., Kopperud, K., Chakrabarty, R., Banerjee, R., Brooks, R., and Goodin, M.M. 2009. Transient expression in *Nicotiana benthamiana* fluorescent marker lines provides enhanced definition of protein localization, movement and interactions in planta. Plant J. 59:150-162.

Martin, K. M., Barandoc-Alviar, K., Schneweis, D. J., Stewart, C. L., Rotenberg, D., and Whitfield, A. E. 2017. Transcriptomic response of the insect vector, *Peregrinus maidis*, to maize mosaic rhabdovirus and identification of conserved responses to propagative viruses in hopper vectors. Virology 509:71-81.

Martin, K. M., and Whitfield, A. E. 2018. Cellular localization and interactions of nucleorhabdovirus proteins are conserved between insect and plant cells. Virology 523:6-14.

Pfeifer, T. A., Hegedus, D. D., Grigliatti, T. A., and Theilmann, D. A. 1997. Baculovirus immediate-early promoter-mediated expression of the Zeocin resistance gene for use as a dominant selectable marker in dipteran and lepidopteran insect cell lines. Gene 188:183-190.

Theilmann, D. A., and Stewart, S. 1992. Molecular analysis of the transactivating IE-2 gene of *Orgyia pseudotsugata* multicapsid nuclear polyhedrosis virus. Virology 187:84-96.

Tsai, C. W., Redinbaugh, M. G., Willie, K. J., Reed, S., Goodin, M., and Hogenhout, S. A. 2005. Complete genome sequence and in planta subcellular localization of maize fine streak virus proteins. J. Virol. 79: 5304-5314.

Whitfield, A. E., Huot, O. B., Martin, K. M., Kondo, H., and Dietzgen, R. G. 2018. Plant rhabdoviruses-their origins and vector interactions. Curr. Opin. Virol. 33:198-207.

Whitfield, A. E., Rotenberg, D., Aritua, V., and Hogenhout, S. A. 2011. Analysis of expressed sequence tags from maize mosaic rhabdovirus-infected gut tissues of *Peregrinus maidis* reveals the presence of key components of insect innate immunity. Insect Mol. Biol. 20:225-242.

Yao, J., Rotenberg, D., Afsharifar, A., Barandoc-Alviar, K., and Whitfield, A. E. 2013. Development of RNAi methods for *Peregrinus maidis*, the corn planthopper. PLoS One 8:e70243. doi: 10.1371/journal.pone. 0070243.

Yao, J., Rotenberg, D., and Whitfield, A. E. 2019. Delivery of maize mosaic virus to planthopper vectors by microinjection increases infection efficiency and facilitates functional genomics experiments in the vector. J. Virol. Methods 270:153-162.

Supplementary Information

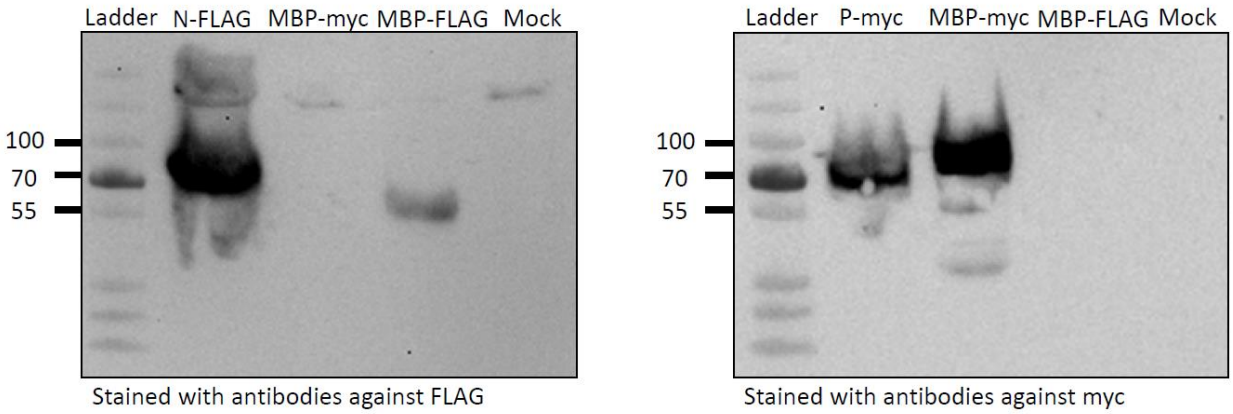

Supplementary Figure 1: Western blots of protein extracts from Sf9 cells transfected with plasmids expressing N-FLAG, P-myc, MBP-FLAG, and MBP-myc fusion proteins. Mock-transfected cells were used as a negative control for non-specific antibody binding.

CHAPTER 3

Characterization of *Peregrinus maidis* Lugensin

Abstract

Peregrinus maidis is a tropical and subtropical hemipteran insect pest on maize, causing significant crop damage during feeding and oviposition. It is also the sole vector for maize mosaic virus (MMV), a plant- and insect-infecting rhabdovirus in the species *Alphanucleorhabdovirus maydis*. MMV infection in plants causes striping and stunting, compounding the damage caused by the insect. When insects encounter pathogens, the insect innate immune response is induced and leads to the downstream production of antimicrobial peptides (AMPs), which are small peptides with varying structures and mechanisms of action. The specific AMPs produced by *P. maidis* are currently unknown, and in this study, we have identified a putative *P. maidis* AMP, *P. maidis* lugensin, and further characterized its structure and function. Classical sequence homology-based bioinformatic techniques and newer protein structure homology-based approaches were used to investigate similarities between *P. maidis* lugensin and other related insect proteins. In vivo experiments characterizing *lugensin* transcript expression levels in different *P. maidis* life stages and lugensin tissue localization in adult insects, and in vitro experiments involving heterologous expression and purification of *P. maidis* lugensin for bacterial growth inhibition assays were also performed. I found that lugensin expression increased over insect development, and it was localized to the fat bodies, gut tissue, salivary glands, and reproductive organs. Purified lugensin protein inhibited the growth of *E. coli* and *Xanthomonas vasicola* (the causal agent of bacterial leaf streak of corn). My bioinformatics analysis results also indicate that *P. maidis* lugensin was very similar in sequence and structure to AMPs from other delphacids, suggesting that it could be a delphacid-specific AMP. Additional experiments investigating the other roles of lugensin in the interactions between bacterial and fungal communities within the insect will provide a more

complete picture of its function, and testing its effects on a greater range of organisms and conditions could lead to the development of a new biotechnology tool for plant pathogen control.

Introduction

The insect order Hemiptera contains families of economically relevant insect pests that cause extensive crop damage through a combination of feeding activity and plant virus transmission. These families are the Aphididae (aphids), Aleyrodidae (whiteflies), Cicadellidae (leafhoppers), and Delphacidae (delphacid planthoppers). Most described plant viruses are transmitted by hemipteran insects (Nault, 1997; Hogenhout et al., 2008). The delphacid planthoppers are part of this group of pests and a serious threat to grain production worldwide, with *Nilaparvata lugens* (brown planthopper), *Laodelphax striatellus* (small brown planthopper), and *Sogatella furcifera* (white-backed planthopper) being some of the most notable pests on rice. Those insects and other related delphacids transmit plant viruses from a diverse set of genera, e.g. rice ragged stunt virus (*Oryzavirus*), rice stripe virus (*Tenuivirus*), and Southern rice black-streaked dwarf (*Fijivirus*) (Hogenhout et al., 2008; Heong and Hardy, 2009; Gurr et al., 2010; Cho et al., 2013; Zhou et al., 2013). The corn planthopper, *Peregrinus maidis*, is an insect pest that causes similarly devastating effects on maize and sorghum, and it is also the sole vector of maize mosaic virus (MMV), a plant and insect-infecting rhabdovirus (Autrey, 1983; Falk and Tsai, 1985; Ammar and Nault, 2002). *P. maidis* is an important economic pest as plant damage from insect feeding and oviposition, combined with symptoms of plant viral infection like stunting cause significant yield losses in tropical corn-growing regions of the world (Brewbaker, 2003; Singh and Seetharama, 2008). The molecular mechanism of MMV acquisition by the insect vector is currently unknown, and performing basic research to elucidate the host factors involved will lead to a better understanding

of this virus-vector interaction and possibly inform the development of future integrated pest management strategies.

Detection of pathogen infection induces an immune response in a healthy organism, triggering a series of defense mechanisms to suppress pathogen replication such as the induction of antimicrobial peptide (AMP) production. AMPs are a class of small peptides found in virtually all organisms which perform a variety of immune-related functions like pathogen detection or elimination, and most AMPs which have been characterized to date have been isolated from insects (Bulet et al., 1999; Ganz 2003; Yi et al., 2014; Ahmed et al., 2019). Some AMPs may also function in roles beyond that of immune pathways, performing regulatory roles in neuronal function and aging (Dissel et al., 2015; Stuart et al., 2022). Though the interaction between viruses and their insect hosts is complex and likely involves one or more immune pathways, AMP production in response to viral infection generally involves the Toll, Immune deficiency (IMD), and JAK/STAT pathways (Engström 1999; Tauszig 2000; Liu et al., 2015; Manniello et al., 2021; Stączek et al., 2023). Previous studies on the *P. maidis* transcriptome reveal the presence of the Immune deficiency pathway in the insect (Whitfield et al., 2011).

A membrane-based yeast-two-hybrid screen previously identified a set of *P. maidis* proteins which interact with the MMV glycoprotein, an important protein involved in viral infection initiation in the planthopper vector (Alviar et al., 2022). One of those insect protein interactors was *P. maidis* lugensin (PmLgs), an ortholog of a putative AMP first identified in another hemipteran insect, *Nilaparvata lugens* (Zhou et al., 2019). In that study, the authors characterized two novel *N. lugens* AMPs, lugensin A and lugensin B, showing that insect expression of both proteins were induced by bacterial challenge and that the proteins exerted antibacterial effects against Gram-negative and Gram-positive bacteria by disrupting their cellular membranes. I performed a series of

bioinformatic analyses on PmLgs using classical sequence homology-based approaches, and relatively newer protein structure homology-based methods using AlphaFold2 software. *PmLgs* shares sequence similarities with *N. lugens* lugensin B and several uncharacterized *L. striatellus* proteins. PmLgs also shares significant structural homology with *N. lugens* lugensin A and B, and a lower degree of homology with some other insect AMPs such as gloverins. We successfully expressed and purified PmLgs from *E. coli* for use in antibacterial growth assays and found that it was able to inhibit bacterial growth. These data suggest that PmLgs is a delphacid-specific AMP with antibacterial activity.

Materials and Methods

Gene Annotation and Phylogenetic Analysis

The full cDNA sequences, open reading frames, and translated peptide sequences of the five *P. maidis lugensin* (PmLgs1 through 5) models were analyzed using NCBI BLAST, WebApollo (*P. maidis* genome assembly provided by Lorenzen, M.), and Clustal Omega (Madeira et al., 2024). MEGA 11 was used to generate a phylogenetic tree by aligning the PmLgs ORF amino acid sequence with other insect proteins using the MUSCLE algorithm, then using that alignment to construct a maximum-likelihood tree with 1000 bootstrap replications. The tree was visualized using the Interactive Tree of Life v5 (Letunic and Bork, 2021).

Protein Domain, Structure, and Homology Prediction

The amino acid sequence of PmLgs was analyzed using SignalP 6.0 to identify signal peptide motifs and DeepLoc 2.0 to predict cellular localization. Protein structure predictions of various peptides were generated by analyzing their amino acid sequences using AlphaFold (Jumper et al.,

2021) in the Google collaborative notebook ColabFold v1.5.3, accessed in March 2023. All parameters were kept at their default values, except for "number of models generated" which was set to 3, and "recycling count" which was set to 48. The structural models with the highest confidence values were used as queries against structurally resolved proteins in the Protein Data Bank using the Dali server. Superimposition of predicted protein structures were performed and visualized using UCSF Chimera and FirstGlance in Jmol. The nucleotide sequences of disordered protein structure regions were aligned using Clustal Omega and analyzed further using Blastp.

RNA Extraction, cDNA Synthesis, and RT-qPCR

Varying numbers of *Peregrinus maidis* insects were pooled to form individual biological replicates for different life stages; first instar (40), second instar (20), third instar (4), fourth instar (3), fifth instar (3), and adult (3). The insects were homogenized in TRIzol reagent (Thermo Fisher Scientific) using micropestles in 1.7mL microcentrifuge tubes, and RNA was extracted following the manufacturer's protocols. The RNA samples were then treated with DNase I using the TURBO DNA-free kit (Thermo Fisher Scientific) to remove residual contaminating DNA before RNA quantification was performed with the NanoDrop One spectrophotometer. The Verso cDNA Synthesis kit (Thermo Fisher Scientific) was used to synthesize cDNA using 500ng of total RNA, then the synthesized cDNA was diluted 5-fold using nuclease-free water for use as template material in subsequent RT-qPCR analysis assays to quantify gene expression in various *P. maidis* life stages. The RT-qPCR reaction mixes were set up using iTaq Universal SYBR Green Supermix (Bio-Rad) and run on a CFX Connect Real-Time System (Bio-Rad) and the cycling conditions are as follows: an initial denaturation step at 95°C for 1 min, then 40 cycles of amplification involving a step at 95°C for 15s followed by a step at 60°C for 1 min. Melt curve analyses showed that

amplicons produced a single peak and all wells were run in duplicate to serve as technical replicates. The comparative cycle threshold method ($2^{-\Delta\Delta Ct}$) was used to quantify gene expression levels. Following previous publications investigating *P. maidis* target gene expression, the internal reference gene chosen for these RT-qPCR experiments was *RPL10* (Barandoc-Alviar et al., 2016; Xavier et al., 2024). All primers used for RT-qPCR had efficiencies between 90% to 110% and primer sequences are available in Supplementary Table 1. Statistical analysis of the life stage gene expression analysis of *PmLgs* was performed using the Kruskal-Wallis test with post-hoc Dunn's and Bonferroni correction.

RNA Extraction and 5' Rapid Amplification of cDNA Ends

Groups of three *P. maidis* adults separated by sex were pooled and homogenized using micropestles in 1.7mL microcentrifuge tubes. RNA was then extracted using TRIzol reagent (Thermo Fisher Scientific), and RNA quality and quantity were verified using gel electrophoresis and spectrophotometer analysis using the NanoDrop One spectrophotometer (Thermo Fisher Scientific). 5' RACE was performed using the SMARTer® RACE 5'/3' Kit (Takara Bio USA) following the manufacturer's protocols. Insufficient quantities of cDNA were produced using oligo dT primers, so random primers were used instead for cDNA synthesis. The RACE products were analyzed using gel electrophoresis and cloned into pRACE plasmids using the InFusion Snap Assembly system (Takara Bio USA). The pRACE plasmids were then heat-shocked transformed into DH5α cells, and multiple colonies which grew on LB carbenicillin agar plates were selected and screened using PCR with M13F and InFusion GSP1R primers (Supplementary Table 1). Colonies containing RACE inserts were then propagated in liquid LB carbenicillin media for plasmid purification using the High-Speed Mini Plasmid Kit (IBI Scientific). The plasmids were

then Sanger sequenced using M13F primers to obtain RACE product sequence data, which was further processed by trimming regions outside of the 5'UTR area from the raw sequence reads.

Antibody Production and Validation

Two rabbits, R10240 and R10152, were immunized with bacteria-expressed PmLgs peptide to generate polyclonal antibodies (GenScript). The PmLgs antibodies were validated using western blots with protein extracts from *P. maidis* insects and PmLgs-expressing *E. coli*.

Insect Protein Extraction, Quantification, and Immunoblot Analysis

Peregrinus maidis insects from different life stages were pooled in the following quantities: first instar (40), second instar (25), third instar (12), fourth instar (8), fifth instar (8), male macropter (4), male brachypter (5), female macropter (4), female brachypter (4). The insects were homogenized in 200µL of 1x Laemmli Buffer (diluted using TBS pH 7.4 buffer) using micropestles in 1.7mL microcentrifuge tubes. The crude protein extracts were heated at 100°C for 10 minutes for protein denaturation, then centrifuged at 16000 x *g* for two minutes to pellet insoluble debris. The soluble fraction proteins were quantified using the Pierce 660nm Protein Assay kit (Thermo Fisher Scientific) following the manufacturer's instructions.

Protein samples were boiled in Laemmli buffer at 100°C for ten minutes and 20µL of each sample was loaded on to 10% polyacrylamide gels cast using the TGX Fast Cast Acrylamide kit (Bio-Rad), and the gels were run for one hour at 150 volts. Coomassie blue staining of polyacrylamide gels was done using GelCode Blue Stain Reagent (Thermo Fisher Scientific) following the manufacturer's protocols. The proteins were transferred to a PVDF membrane using the Trans-Blot Turbo RTA Transfer Kit (Bio-Rad) following the manufacturer's protocols, then blocked

using 5% non-fat dry milk in Tris-buffered saline with 0.1% Tween-20 added (TBS-T) for thirty minutes at 25°C with gentle agitation. Antibodies against *P. maidis* lugensin (GenScript) were added to a final dilution of 1:5000 and incubated overnight at 4°C. The membranes were washed three times using TBS-T for five minutes per wash, then incubated with HRP-conjugated anti-rabbit secondary antibodies (Genesee Scientific) at a dilution of 1:5000 for one hour at 25°C. The membranes were washed again with TBS-T three times, five minutes per wash, then chemiluminescent detection was performed using ProSignal Pico ECL reagent (Genesee Scientific) following the manufacturer's protocols. All imaging steps were performed using the iBright CL1000 Imaging system (Thermo Fisher Scientific).

Immunofluorescence Staining

Adult *Peregrinus maidis* insects were anesthetized on ice before being dissected in 70% ethanol. Dissected organs were separated into individual watch glasses and incubated overnight at 4°C in 4% paraformaldehyde in PBS 7.4 and 0.1% Triton X-100 (PBS-T) for tissue fixation and permeabilization. The organs were then blocked in PBS-T containing 10% normal goat serum (NGS) for 1 hour at room temperature, then incubated with PBS-T and 1% NGS with lugensin primary antibodies (GenScript) at a dilution of 1:20 for three hours at room temperature. Negative control tissue samples were incubated in PBS-T without lugensin primary antibodies. The organs were washed in PBS-T 3 times, 5 minutes per wash, then incubated with PBS-T and AlexaFluor 488-conjugated secondary rabbit antibodies (Thermo Fisher Scientific) at a dilution of 1:200 for 2 hours at room temperature. The organs were then washed again following the steps above and incubated with AlexaFluor 594-conjugated phalloidin (Thermo Fisher Scientific) for 1 hour at room temperature. After another washing step with PBS-T, the organs were mounted on glass

slides using one to two drops of SlowFade™ Diamond Antifade Mountant (Thermo Fisher Scientific), and the edges were sealed with transparent nail polish. All images were acquired using the MICA imager (Leica Microsystems) and processed using large volume computational clearing.

Cloning PmLgs into pET_SUMO

All primer sequences are provided in Supplementary Table 1. Primers 1 through 4 were designed to amplify the *PmLgs* ORF without the N-terminal signal peptide sequence for cloning into a modified pET_SUMO vector containing an mCherry ORF to produce pET_SUMO_Lgs:mCherry, which expresses truncated PmLgs with a C-terminal mCherry fusion. The cloning steps were performed using the NEBuilder HiFi DNA Assembly kit (New England Biolabs). Primers 5 and 6 were designed to amplify pET_SUMO_Lgs:mCherry without the mCherry sequence. Phusion high-fidelity polymerase (ThermoFisher) was used to perform the PCR amplification, and the PCR products were purified using the Monarch PCR and DNA Cleanup kit (New England Biolabs), then treated with KLD enzyme mix (New England Biolabs) to ligate PCR products and remove parental plasmids to produce pET_SUMO_Lgs. The plasmid was then transformed into DH5α competent cells and sequence-verified using Sanger sequencing. The SUMO sequence was then removed from pET_SUMO_Lgs using the same method using primers 7 and 8 to produce the pET_Lgs vector which expresses a truncated version of PmLgs with an N-terminal 6x His tag fusion.

Induction of Protein Expression

The pET_Lgs vector was heat-shock transformed into BL21 (DE3) competent cells for protein expression. Transformed BL21 (DE3) cells were grown in Luria Broth (LB) with kanamycin (50mg/mL) and 1% glucose at 37°C, 225 RPM until the log growth phase. Isopropyl β-d-1-thiogalactopyranoside (IPTG) was then added to a final concentration of 1mM for protein expression induction, and bacteria were harvested at time points of zero-, one-, two-, and four-hours post-induction for protein expression analysis. Harvested bacteria were normalized using their OD_{600} measurements, then the samples were boiled in 1x Laemmli buffer and loaded into 10% polyacrylamide gels for Coomassie blue staining and western blotting using anti-His antibodies. The soluble and insoluble fractions of the bacterial lysates were also analyzed separately to determine the solubility of the expressed PmLgs protein.

Protein Purification and Quantification

Protein purification under native conditions was performed by inducing protein expression in 100mL of BL21 (DE3) *E. coli* culture with IPTG following previous protocols. The cells were then lysed in Xtractor extraction buffer (Takara Bio), and the soluble fraction was incubated with Ni-NTA resin in a 1.7mL microcentrifuge tube to bind His-tagged proteins. The resin-protein complex was washed using Wash Buffer (50mM NaH_2PO_4, 300mM NaCl, 20mM imidazole) three times, then the bound proteins were eluted using Elution Buffer (50mM NaH_2PO_4, 300mM NaCl, 250mM imidazole) in three separate elution steps. Each fraction was boiled in 1x Laemmli buffer for protein denaturation and western blotting. Coomassie blue staining and western blotting with lugensin antibodies was then performed to evaluate the purity of the eluted protein. The various

His:PmLgs protein fractions were also quantified using a Bradford assay to determine the amount of protein lost in each purification step.

Slide-A-Lyzer dialysis cassettes (Thermo Fisher Scientific) were used to dialyze Ni-NTA-purified His:PmLgs protein. One hundred microliters of protein in Elution Buffer were added to each cassette, before being loaded onto a floating tube holder in a 1L beaker containing 500mL of 1x TBS (pH 7.4). A magnetic stir bar was used to gently stir the solution at 200RPM for four hours at room temperature. UV-Vis spectroscopy was used to analyze the dialyzed sample for the presence of imidazole.

Antibacterial Liquid Growth Assays

Liquid cultures of *E. coli* DH5α cells were grown in Luria Broth (LB) at 37°C, *Serratia marcescens* was grown in LB at 30°C, and *Xanthomonas vasicola* was grown in nutrient broth at 30°C. The bacterial cultures were diluted to a final concentration of 0.2 OD_{600} units, then 100µL of each culture was added to a well of a 96-well plate. Varying quantities of dialyzed PmLgs were added to different wells to achieve final protein concentrations ranging from 50 to 200 µg/mL in a final volume of 200µL per well. Wells containing 100µL of TBS 7.4, kanamycin (50 µg/mL), or no bacteria at all were used as positive, negative, and sterility controls respectively. The 96-well plate was then incubated with agitation (425 cpm) for 24 hours in a Biotek plate reader (Agilent) at 37°C for *E. coli*, and 30°C for *X. vasicola* and *S. marcescens*, with OD_{600} readings taken at 30-minute intervals. All experiments were repeated at least three times.

Results

Gene Annotation

The open reading frame (ORF) of the PmLgs protein identified in the MbY2H assay was used as a BLAT query in WebApollo and matching regions were identified only on Scaffold 5 of the *P. maidis* genome in WebApollo. Five gene models were then manually annotated and validated: 8AU, AUC, ACG, C1N, and 543 (Figure 1.1). The gene models were renamed to PmLgs1, PmLgs2, PmLgs3, PmLgs4, and PmLgs5 respectively.

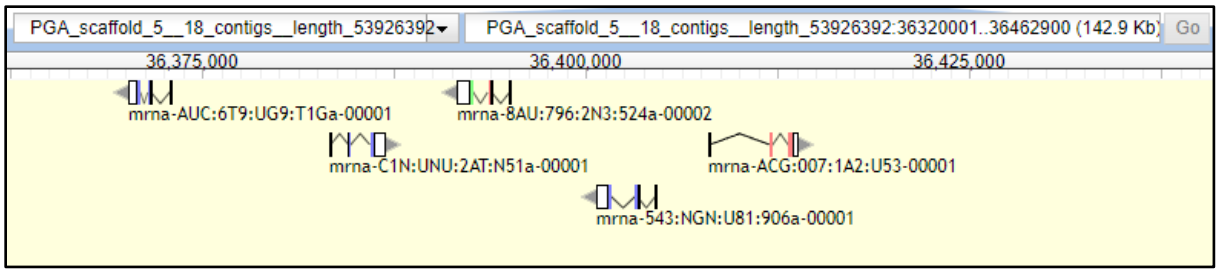

Figure 1.1: Annotated PmLgs gene models visualized in WebApollo. The five annotated *lugensin* models are located closely together on scaffold five. The gray arrow at the end of each model shows the orientation of the transcript relative to the genome, 5' on the left and 3' on the right.

Nucleotide and amino acid sequence alignments performed using NCBI BLAST showed that PmLgs3 had lower percent identities compared to the other sequences (Table 1.1, 1.2, and 1.3). Since PmLgs3 did not align well with the other four models, it was omitted from the Clustal Omega alignment. Almost all amino acid sequence mismatches between the four remaining models were synonymous amino acid substitutions (Figure 1.2). These data suggest that the four gene models are highly similar to each other at the nucleotide and protein level. In the absence of further lines of evidence, together with low percent identities (<97%), it is not possible to conclusively state if

they are duplication artefacts within the genome data or if they are separate genes. The protein encoded by each of the four gene models is similar enough that they probably have the same function. PmLgs3 could be describing a separate lugensin gene as it has lower percent identities at the nucleotide and amino acid level compared to the other gene models.

Table 1.1: BLASTn alignment of the cDNA sequence data of the five PmLgs gene models obtained using sequence PmLgs1 as the query.

Description	Max Score	Total Score	Query Cover	E value	Per. Ident	Acc. Len
PmLgs5	1147	1728	93%	0	95.21	1310
PmLgs4	948	1848	89%	0	95.09	1342
PmLgs2	900	1328	76%	0	94.99	1278
PmLgs3	165	165	11%	1.00E-43	85.19	1037

Table 1.2: BLASTn alignment of the CDS sequence data of the five PmLgs gene models obtained using sequence PmLgs1 as the query.

Description	Max Score	Total Score	Query Cover	E value	Per. ident	Acc. Len
PmLgs5	721	721	100%	0	97.62	420
PmLgs4	721	721	100%	0	97.62	420
PmLgs2	710	710	100%	0	97.14	420
PmLgs3	165	165	38%	1.00E-44	85.19	426

Table 1.3: BLASTp alignment of the CDS sequence data of the five PmLgs gene models obtained using sequence PmLgs1 as the query.

Description	Max Score	Total Score	Query Cover	E value	Per. ident	Acc. Len
PmLgs4	275	275	100%	2.00E-101	97.12	139
PmLgs5	275	275	100%	3.00E-101	97.12	139
PmLgs2	274	274	100%	3.00E-101	96.4	139
PmLgs3	136	136	100%	2.00E-46	56.76	141

```
CLUSTAL O(1.2.4) MULTIPLE SEQUENCE ALIGNMENT


PMLGS1      MDVRVLVVLLVVAVVSSLAKRYDHPPPGYDKKLINRPPPPKTFVDRTRMYRSAPDETMHE       60
PMLGS4      MDVRVLVVLLVVAVVSSLAKRYDPPPPGYDRKLINRPPPPKTFVDRTRMYRSAPDESMHE       60
PMLGS5      MDVRVLVVLLVVAVVSSLAKRYDSPPPGYDKKLINRPPPPKTFVDRPRMYRSAPDESMHE       60
PMLGS2      MDVRVLVVLLVVAVVSSLAKRYDSPPPGYDNKLINRPPPPKTFADRTRMYRSAPDETMHE       60
            ********************** ******.************.** *********:***

PMLGS1      RLRRSPEEKRGSVVLSGSRTEQRGGPPQQSVRGEYNHNLWRGKNGASIDANTYYQRNWGG       120
PMLGS4      RLRRSPEEKRGSVVLSGTRTEQRGGPPQQSVRGEYNHNLWRGKNGASIDANTYYQRNWGG       120
PMLGS5      RLRRSPEEKRGSVVLSGTRTEQRGGPPQQSVRGEYNHNLWRGKNGASIDANTYYQRNWGG       120
PMLGS2      RLRRSPEEKRGSVVLSGTRTEQRGGPPQQSVRGEYNHNLWRGKNGATIDANTYYQRNWGG       120
            ****************:****************************:*************

PMLGS1      GPKQDYGGGIRGSIPFGRR 139
PMLGS4      GPKQDYGGGIRGSIPFGRR 139
PMLGS5      GPKQDYGGGIRGSIPFGRR 139
PMLGS2      GPKQDYGGGIRGSIPFGRR 139
            ******************
```

Figure 1.2: Clustal Omega alignment of the amino acid sequence of the PmLgs gene models. An extremely high degree of conservation is present between the four models, with synonymous amino acid mutations accounting for almost all amino acid mismatches.

Sequence Comparison with Experimentally Obtained Transcripts

RNA was extracted from three pooled adult *P. maidis* insects using TRIzol reagent, then cDNA was synthesized, and primers 11 and 12 were used to clone the ORF of *PmLgs* into a pENTR vector for sequencing and further downstream work (Supplementary Table 1). The nucleic acid and amino acid sequences of the ORFs in the five gene models and the experimentally cloned ORF (Lgs_exp) were compared with that of the transcript obtained from the MbY2H assay (seq182), and a high level of similarity between the ORFs was observed (Tables 2.1 and 2.2).

Table 2.1: Nucleic acid sequence alignment of the ORFs of PmLgs gene models and an experimentally obtained *PmLgs* sequence with the ORF of the *PmLgs* sequence identified from an MbY2H screen.

Description	Max Score	Total Score	Query Cover	E value	Per. ident	Acc. Len
PmLgs2	758	758	100%	0	99.06	420
Lgs_exp	752	752	100%	0	98.82	420
PmLgs5	702	702	100%	0	96.7	420
PmLgs4	691	691	100%	0	96.23	420
PmLgs1	691	691	100%	0	96.23	420
PmLgs3	165	165	37%	2.00E-44	85.19	426

Table 2.2: Amino acid sequence alignment of the ORFs of PmLgs gene models and an experimentally obtained *PmLgs* sequence with the ORF of the *PmLgs* sequence identified from an MbY2H screen.

Description	Max Score	Total Score	Query Cover	E value	Per. ident	Acc. Len
PmLgs1	283	283	100%	3.00E-104	100	139
PmLgs4	275	275	100%	3.00E-101	97.12	139
PmLgs5	275	275	100%	4.00E-101	97.12	139
PmLgs2	274	274	100%	4.00E-101	96.4	139
Lgs_exp	242	242	100%	4.00E-88	95.68	140
PmLgs3	136	136	100%	2.00E-46	56.76	141

5' RACE Sequence Analysis

Very few colonies grew on LB carbenicillin plates containing bacteria transformed with pRACE vectors. Two colonies were selected from the plate containing RACE inserts from female *P. maidis* and six colonies were selected from the plate with RACE inserts from male *P. maidis* for colony PCR screening using M13F and InFusion GSP1R primers, and various amplification bands were seen on the gel (Figure 2.1). Colonies F1, F2, M1, M3, M5, and M6 were selected for plasmid purification and Sanger sequencing. F2, M1, and M6 were identical and contained complete

adapter sequences, indicating that their sequences were likely complete, while F1, M3, and M5 contained missing or incomplete adapter sequences, suggesting that they were likely to be off-target amplification products.

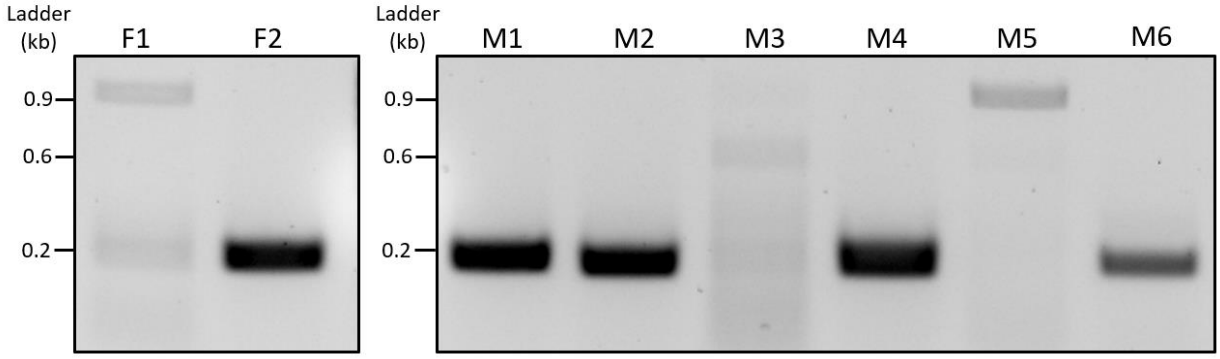

Figure 2.1: Colony PCR screening results for DH5α transformed using pRACE plasmids. A variety of inserts with different lengths are present in the plasmids. Lanes labelled 'F' contain a pRACE plasmid with inserts from female insects, and lanes labelled 'M' contain a pRACE plasmid with inserts from male insects.

The 5' UTR sequence (F2, M1, and M6) obtained from the 5' RACE experiment was compared with that of the other *PmLgs* transcripts, and there was significantly less homology between them, with only 5' UTRs of PmLgs2, 5, and 1 aligning with that of the transcript obtained from the MbY2H assay (Table 2.3). The experimentally sequenced 5' UTR is almost identical to the 5' UTR of the transcript identified in the MbY2H screen and PmLgs2.

Table 2.3: Nucleotide sequence alignment of the 5' UTR of PmLgs gene models and an experimentally determined 5' UTR with the 5' UTR of the *PmLgs* sequence identified from an MbY2H screen.

Description	Max Score	Total Score	Query Cover	E value	Per. ident	Acc. Len
5' RACE_exp	237	237	99%	4.00E-67	99.24	184
PmLgs2	230	230	96%	6.00E-65	99.21	295
PmLgs5	152	152	83%	1.00E-41	91.82	110
PmLgs1	135	135	88%	1.00E-36	88.89	107

Phylogenetic Analysis

From the sequence comparisons of the nucleic acid, amino acid, and 5' UTR of the different *PmLgs* transcripts, we hypothesize that there are three *lugensin* genes in the *P. maidis* genome, represented by PmLgs1, PmLgs4, and PmLgs5 (gene 1), PmLgs2 (gene 2), and PmLgs3 (gene 3). PmLgs4 and PmLgs5 were omitted from the phylogenetic analysis as they were likely to be identical copies. The *PmLgs* sequence obtained from the MbY2H assay (seq182) and the lugensin transcript experimentally cloned from *P. maidis* cDNA (Lgs_exp) are most likely represented by PmLgs2 as their ORF nucleic acid sequence and 5' UTR sequence are most similar to each other. *N. lugens* lugensin A and B, and uncharacterized *N. lugens* and *L. striatellus* proteins which were identified in an NCBI BLAST search using PmLgs1 as a query were also included in this phylogenetic analysis, and a probable antibacterial peptide from *Halyomorpha halys* was designated as the outgroup (Figure 3.1).

The *PmLgs* gene models clustered together with the exception of PmLgs3, which clustered with uncharacterized proteins from *N. lugens* and *L. striatellus* suggesting that PmLgs3 encodes for a separate *P. maidis* protein that is more closely related to other planthopper proteins. PmLgs1 clustered with seq182 and PmLgs2 clustered separately with Lgs_exp (Lgs Experimental). These

results support our hypothesis that PmLgs1, PmLgs2, and PmLgs3 are distinct. The experimentally cloned ORF obtained from *P. maidis* cDNA (Lgs_exp) is the sequence used for further downstream experiments, and will be referred to as *Peregrinus maidis* lugensin, or PmLgs hereafter.

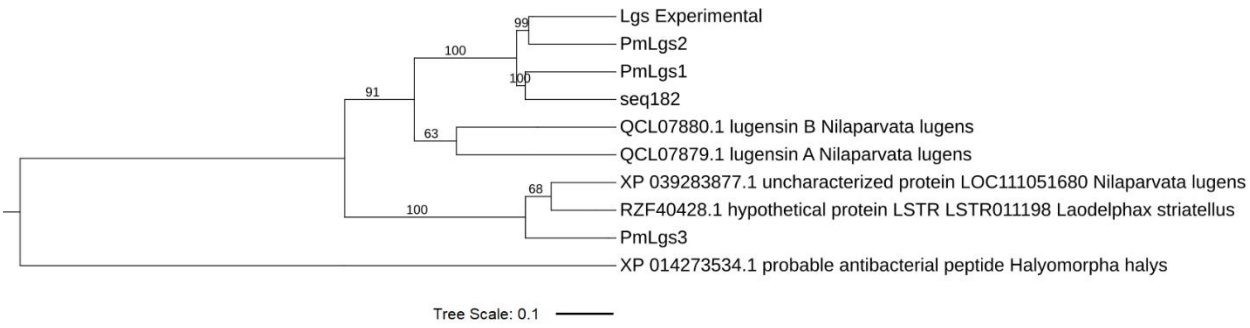

Figure 3.1: *P. maidis* lugensin phylogenetic tree generated using MEGA 11 and visualized using the Interactive Tree of Life v5. MEGA 11 was used to generate a phylogenetic tree by aligning the PmLgs amino acid sequence of with other insect proteins using the MUSCLE algorithm, then that alignment was used to construct a maximum-likelihood tree with 1000 bootstrap replications. Bootstrap values are shown as percentages.

Peregrinus maidis **Lugensin Protein Structure and Domain Prediction**

The amino acid sequence of PmLgs (Supplementary Table 2) was analyzed using AlphaFold and SignalP 6.0. The predicted protein structure contains an N-terminal signal peptide (aa1-21), followed by a disordered region (aa22-56), and a C-terminal beta-sheet (aa57-139) (Figure 4.1). However, SignalP 6.0 predicted the N-terminal signal peptide to span from aa1-19, with a high probability (0.981833) of a cleavage site between aa19 and aa20 (Figure 4.2). The SignalP prediction for the signal peptide sequence is more reliable as there is a reduction in pLDDT values near the end of the signal peptide region in the model generated using AlphaFold. PmLgs is

predicted to localize extracellularly when analyzed using DeepLoc 2.0 (Table 3.1), providing more evidence that it could be an AMP as some AMPs are secreted out of the cell.

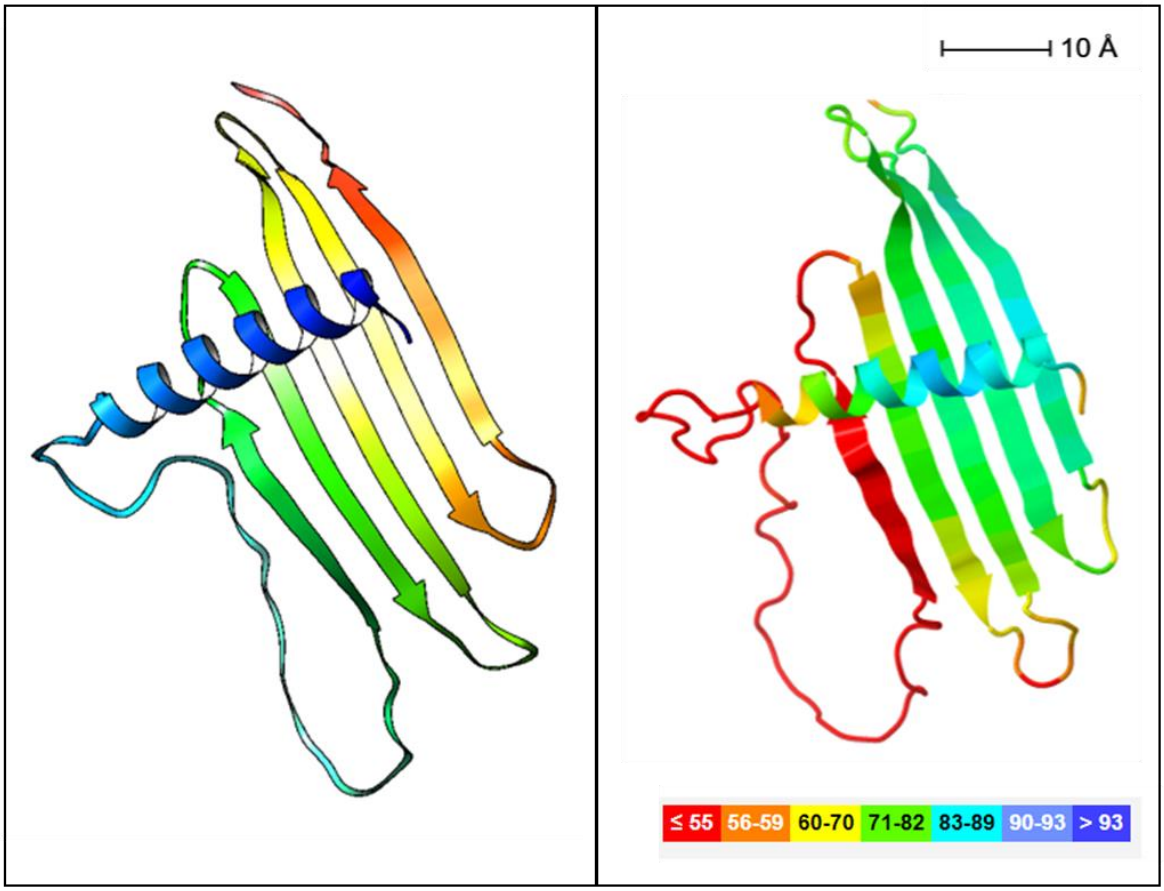

Figure 4.1: Predicted protein structure of *Peregrinus maidis* lugensin with pLDDT values. The model of *P. maidis* lugensin on the left was visualized using Chimera, showing predicted structural features with the N-terminal region shaded in blue. The model on the right was visualized using FirstGlance, showing the pLDDT value associated with each amino acid residue, with higher values representing higher confidence in the reliability of the model prediction.

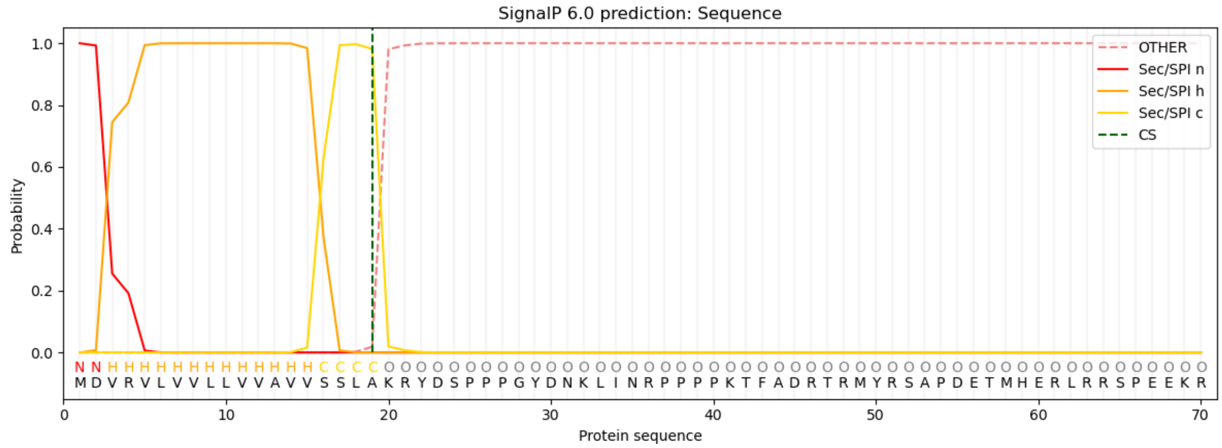

Figure 4.2: SignalP 6.0 prediction of the signal peptide sequence in *Peregrinus maidis* lugensin. A cleavage site between amino acid 19 and 20 is predicted with a probability of 0.981833.

Table 3.1: Predicted subcellular localizations of *Peregrinus maidis* lugensin.

Localization	Probability
Extracellular	0.9651
Cell membrane	0.1356
Endoplasmic reticulum	0.1000
Cytoplasm	0.0978
Mitochondrion	0.0868
Lysosome/Vacuole	0.0814
Nucleus	0.0791
Golgi apparatus	0.0489
Plastid	0.0411
Peroxisome	0.0031

***Peregrinus maidis* Lugensin Protein Homology Prediction**

The PmLgs AlphaFold structural model was used as a query for protein structure comparisons against proteins in the Protein Data Bank using the Dali server. The top result was a porin protein, and many of the other proteins identified as matches were also membrane-associated proteins. The predicted structure of PmLgs was superimposed over a section of a bacterial porin protein (PDB

ID: 5ldt). Structurally conserved regions shown in blue suggest that PmLgs may multimerize to form a beta-barrel pore structure (Figure 4.3).

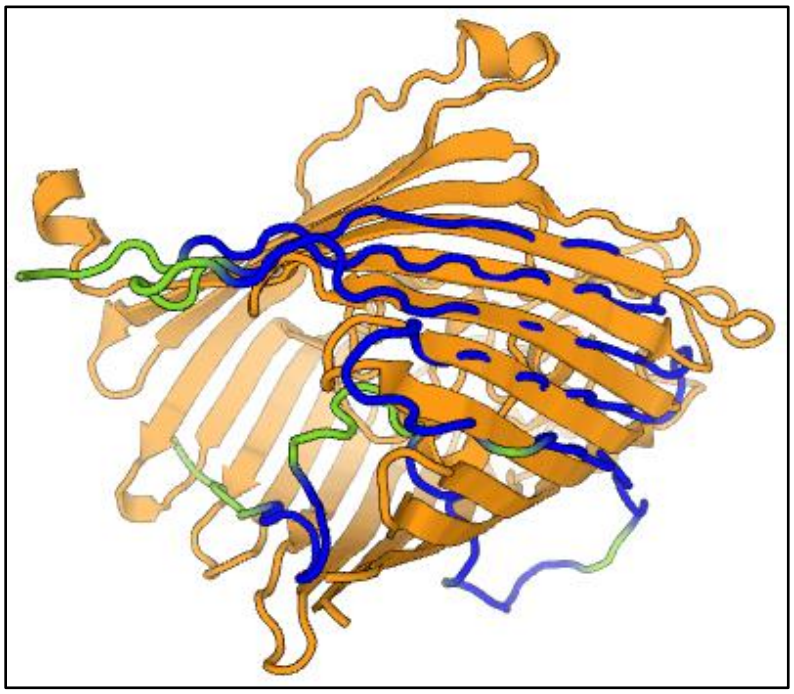

Figure 4.3: Superimposition of *Peregrinus maidis* lugensin with a bacterial porin protein (PDB ID: 5ldt). The overlapping, structurally conserved regions between the two proteins are shown as blue lines.

Structural Homology Comparison with *Nilaparvata lugens* Lugensins

Protein structure models were also generated for *Nilaparvata lugens* lugensin A and B using AlphaFold for comparison with PmLgs. All three proteins had disordered regions flanked by N-terminal signal peptide regions and C-terminal beta-sheet regions (Figure 4.4). *N. lugens* lugensin A is predicted to have an N-terminal signal peptide (aa1-20), followed by a disordered region (aa21-58), and a beta-sheet region (aa59-139). *N. lugens* lugensin B is predicted to have an N-terminal signal peptide (aa1-18), followed by a disordered region (aa19-59) and a beta-sheet region

(aa60-142). These results show that there is a high level of structural similarity between the three proteins, suggesting that they could also perform similar functions.

Structural Homology Comparisons with other Insect AMPs

Protein structure predictions for gloverin proteins from *Galleria mellonella* and *Trichoplusia ni* were generated using AlphaFold for structural comparison with PmLgs. All proteins shared highly conserved C-terminal beta-sheets, the with un-conserved disordered regions that followed their N-terminal signal peptide sequences (Figure 4.5). The *G. mellonella* gloverin protein is predicted to have an N-terminal signal peptide (aa1-16), followed by a disordered region (aa17-47) and a beta-sheet region (aa48-183). The *T. ni* gloverin protein is predicted to have an N-terminal signal peptide (aa1-18), followed by a disordered region (aa19-30) and a beta-sheet region (aa31-163). This high level of structural homology, like that observed in *N. lugens* lugensin A and B, suggests that PmLgs and gloverin could perform similar functions. The protein structures of other classes of insect AMPs were also investigated, but no structural or sequence similarity to PmLgs was observed so they were not analyzed further.

Figure 4.4: Protein structure predictions and structural superimpositions of *Nilaparvata lugens* lugensin A and B with *Peregrinus maidis* lugensin. A: The model of *N. lugens* lugensin A on the left and of *N. lugens* lugensin B on the right was generated using AlphaFold and visualized using FirstGlance. The numbers shown represent the pLDDT values, which represent the estimated level of confidence for the predicted structure. B: A superimposition of the predicted structures of *P. maidis* lugensin (blue) and of *N. lugens* lugensin A (brown) generated using Chimera is shown on the left, and a superimposition of the predicted structures of *P. maidis* lugensin (blue) and of *N. lugens* lugensin B (brown) is shown on the right. Removal of the signal peptide region from *P. maidis* lugensin was required for an optimal view of the beta sheet region alignment of *N. lugens* lugensin B with *P. maidis* lugensin.

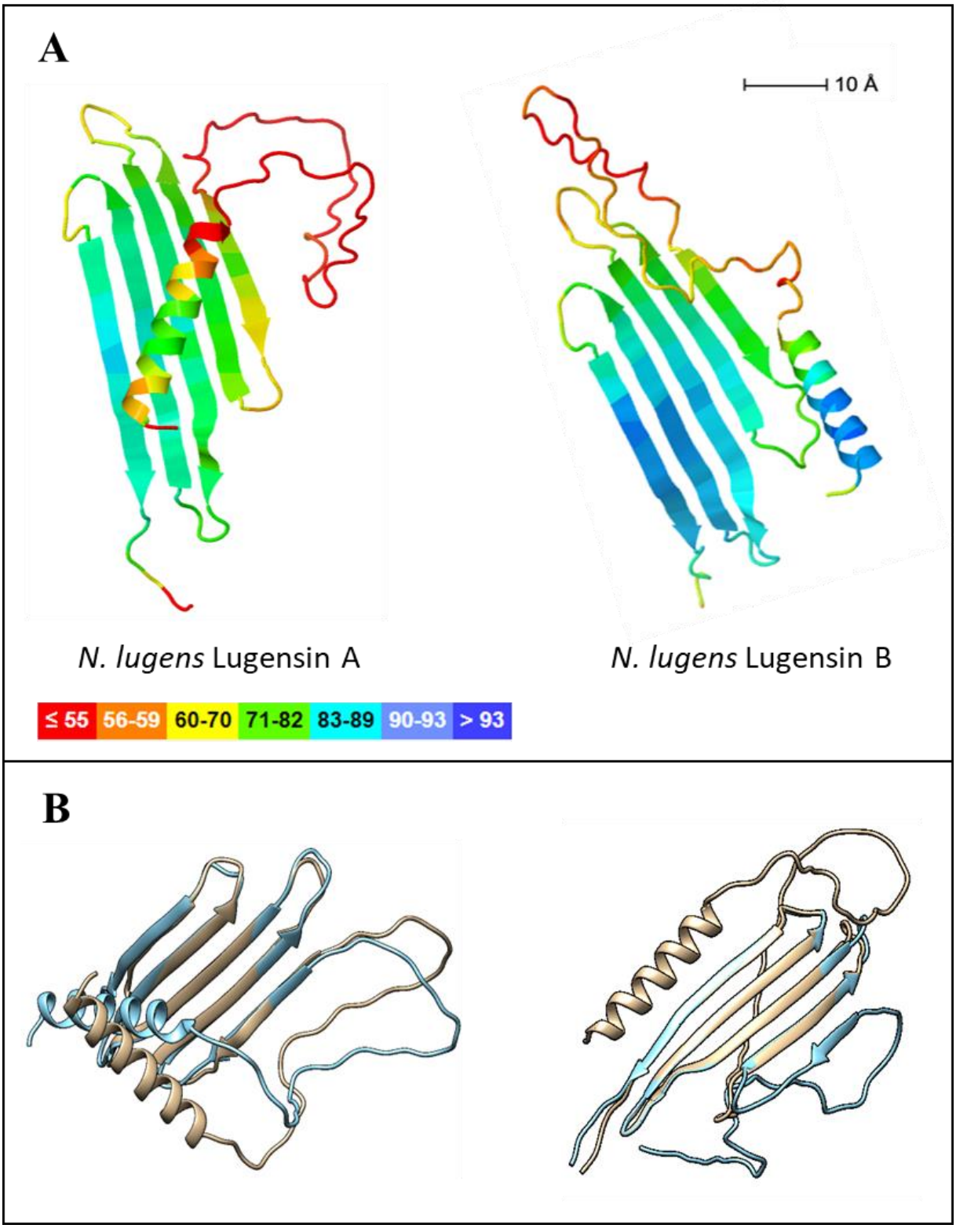
A
10 Å
N. lugens Lugensin A
N. lugens Lugensin B
≤ 55
56-59
60-70
71-82
83-89
90-93
> 93
B

Figure 4.5: Protein structure predictions and structural superimpositions of *Galleria mellonella* and *Trichoplusia ni* gloverins with *Peregrinus maidis* lugensin. A: The model of *G. mellonella* gloverin on the left and *T. ni* gloverin on the right was generated using AlphaFold and visualized using FirstGlance. The numbers shown represent the pLDDT values, which represent the estimated level of confidence for the predicted structure. B: A superimposition of the predicted structures of *P. maidis* lugensin (blue) and *G. mellonella* gloverin (brown) generated using Chimera is shown on the left, and a superimposition of the predicted structures of *P. maidis* lugensin (blue) and *T. ni* gloverin (brown) is shown on the right.

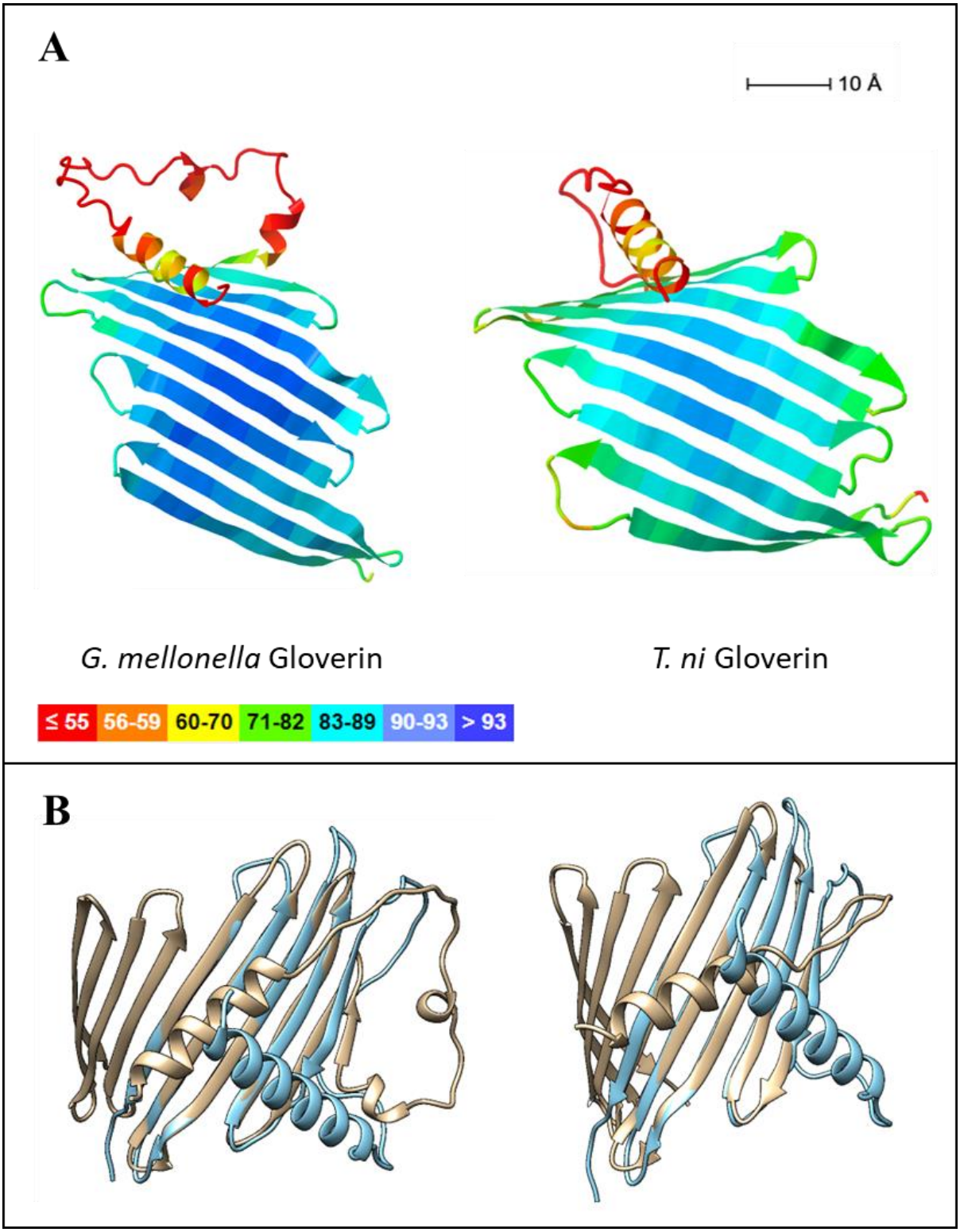
A
10 Å
G. mellonella Gloverin
T. ni Gloverin
≤ 55
56-59
60-70
71-82
83-89
90-93
> 93
B

Structural Comparison of Disordered Regions

The disordered region between the signal peptide and beta sheet region of each protein was delineated using SignalP 6.0 to map the signal peptide region and Chimera to map the start of the beta sheet region. Multiple sequence alignments on the disordered regions were then performed using Clustal Omega (Figure 4.6). The disordered regions of gloverins from *T. ni* and *G. mellonella* had low amino acid sequence conservation with the hemipteran lugensin proteins, so they were omitted from downstream analyses. The disordered regions of *N. lugens* lugensin A, B, and PmLgs were highly conserved, with 78% amino acid sequence similarity between lugensin A and PmLgs, and 74% amino acid sequence similarity between lugensin B and PmLgs. The disordered region of PmLgs was then queried against the Blastp nr protein database, and two highly conserved proteins were identified; an unannotated *Laodelphax striatellus* protein (72% similarity) and an unannotated *N. lugens* protein (78% similarity). These results suggest that PmLgs could belong to an uncharacterized class of delphacid-specific AMPs.

Figure 4.6: Multiple sequence alignment of disordered regions from various insect AMPs performed using Clustal Omega. A high degree of conservation is present between the disordered region amino acid sequences of *Nilaparvata lugens* lugensin A, B, and *Peregrinus maidis* lugensin (78%), but not with that of *Trichoplusia ni* and *Galleria mellonella* gloverin.

Transcript Expression Analysis

PmLgs transcript expression levels were normalized to *RPL10* transcript expression levels and found to be significantly lower in early instars compared to later instars and adults (Figure 5.1).

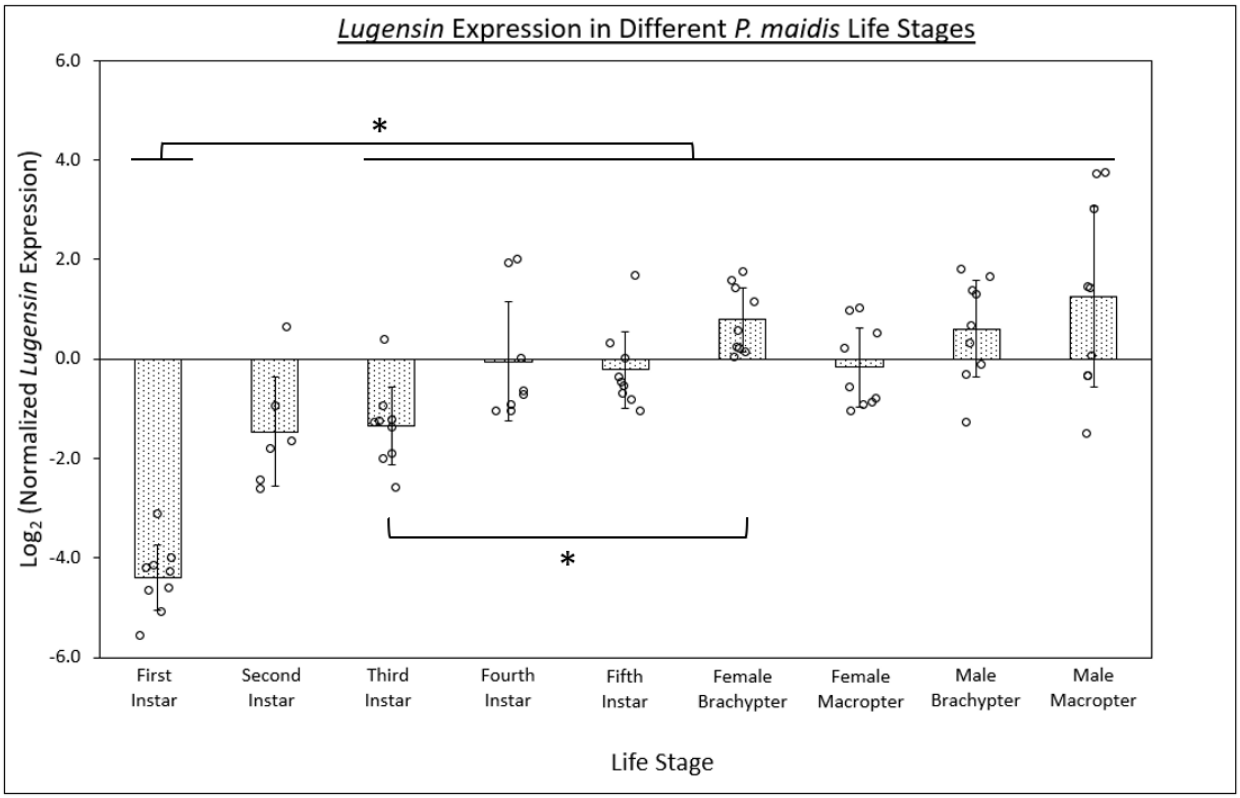

Figure 5.1: *Peregrinus maidis lugensin* transcript expression levels in different insect life stages. Each life stage is represented by at least nine biological replicates, with each biological replicate consisting of at least three insects. Error bars represent standard deviation. Significant differences in *lugensin* expression were observed between first instars and other developmental stages. An asterisk denotes $p < 0.001389$ (after Bonferroni correction with an initial $p < 0.05$).

Antibody Production and Validation

The antibodies from rabbit R10240 were able to detect both bacteria-expressed and insect-expressed PmLgs, while the antibodies from rabbit R10152 were only able to detect bacteria-expressed lugensin protein (Figure 5.2).

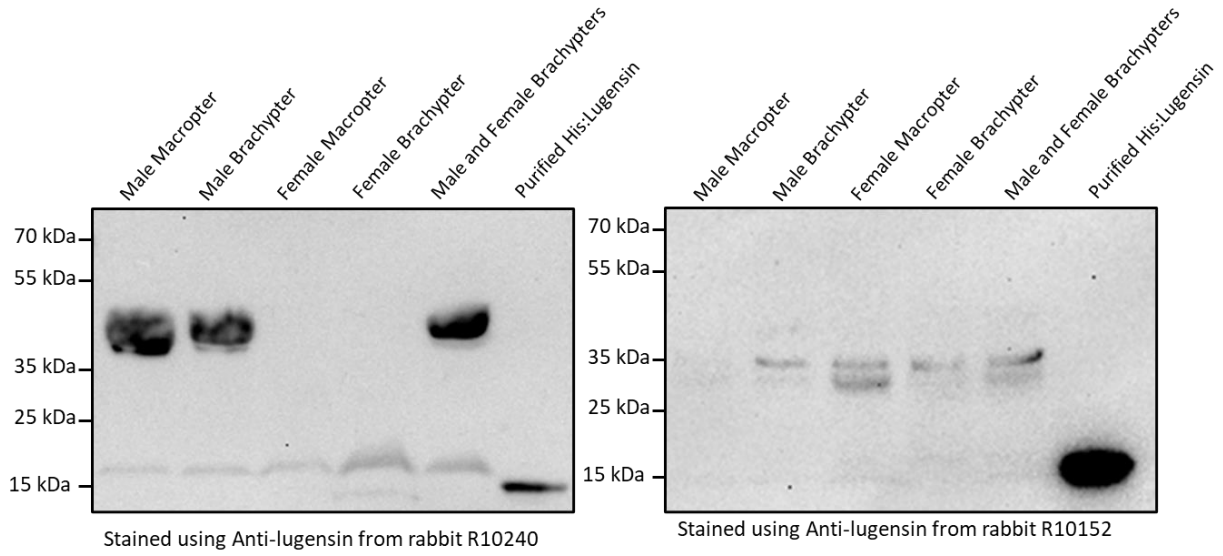

Figure 5.2: Western blots of various protein samples stained using different antibodies against *Peregrinus maidis* lugensin. Antibodies from R10240 successfully detect *P. maidis* lugensin and bacteria-expressed lugensin, and antibodies from R10152 could only detect bacteria-expressed lugensin.

Protein Expression Analysis

The total protein collected from homogenized *P. maidis* insects of different life stages were quantified using the Pierce 660nm protein quantification assay (Table 4.1). The protein quantities were normalized and loaded into a 10% polyacrylamide gel for Coomassie Blue staining and western blotting using PmLgs antibodies. The Coomassie Blue-stained gel showed that approximately equal quantities of protein were loaded into each well (Supplementary Figure 1).

The western blotting data shows that a band approximately 15 kDa in size is detected in every lane, corresponding to the predicted size of PmLgs. PmLgs expression is lowest in the early instar stages, and gradually increases as the insects age (Figure 5.3). Additionally, two bands at approximately 45 kDa are only seen in the lanes containing protein from adult male insects.

Table 4.1: Protein quantification data obtained using the Pierce 660nm Protein Quantification Assay.

Life Stage	No. of insects	Protein quantity (µg/mL)
First instar	40	2050
Second instar	25	1744
Third instar	12	1495
Fourth instar	8	2694
Fifth Instar	8	2885
Male Macropter	4	2358
Male Brachypter	4	1790
Female Macropter	4	2386
Female Brachypter	4	2755

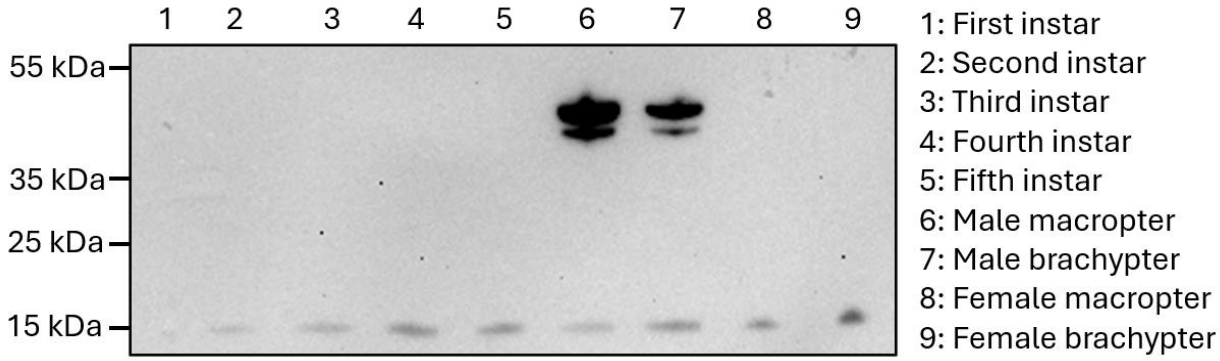

Figure 5.3: Western blotting results show that lugensin protein expression increases as insects develop over time. The band detected at around 14 kDa is the expected size according to amino acid sequence molecular weight predictions. Two bands were seen at approximately 45 kDa in the lanes containing protein from male macropters and brachypters which were not present in any other lane.

Immunofluorescence Staining and Protein Localization

Immunofluorescence staining of dissected *P. maidis* tissues was performed to evaluate tissue localization patterns of *P. maidis* lugensin. The salivary glands, guts, reproductive organs, and fat bodies were fixed and stained with lugensin antibodies and Alexa Fluor 488-conjugated secondary antibodies. The tissues were then incubated with phalloidin and DAPI to stain actin and cell nuclei. The fluorescence microscopy results show that lugensin is distributed throughout the gut tissues, salivary glands, male and female reproductive organs, and fat bodies (Figures 5.4, 5.5, and 5.6). No signals from AF 488 were detected in tissues which had been stained with only secondary antibodies, confirming that the secondary antibodies did not bind nonspecifically (data shown in Supplementary Figures 2, 3, and 4). All dissected tissues were obtained from male or female adult *P. maidis*, and Supplementary Table 3 summarizes the total number of tissues imaged.

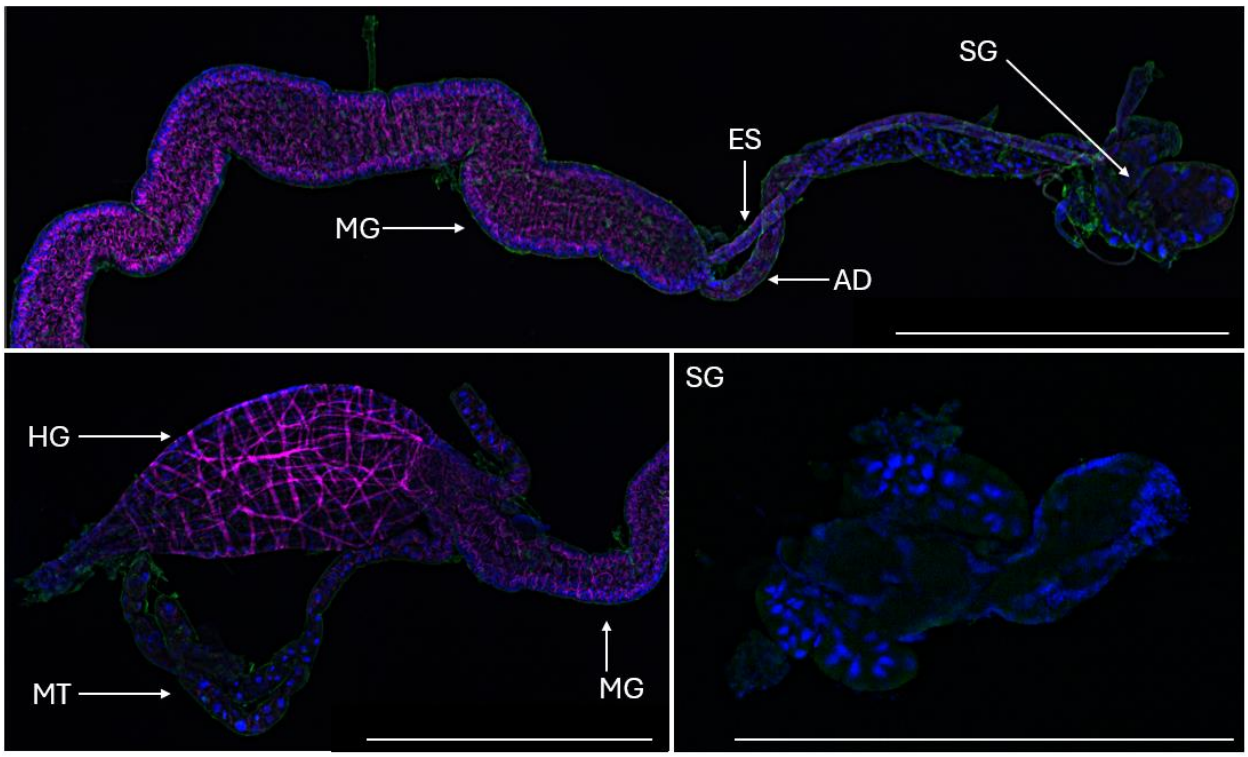

Figure 5.4: PmLgs is present in *Peregrinus maidis* guts and salivary glands. Actin fibers were stained using AF 594-conjugated phalloidin (magenta), cell nuclei were stained using DAPI (blue), and PmLgs was stained using anti-PmLgs and AF 488-conjugated rabbit antibodies (green). MG: midgut; ES: esophagus; AD: anterior diverticulum; SG: salivary glands; HG: hindgut; MT: Malpighian tubule. These images are representative of multiple imaged tissues from adult male and female *P. maidis* insects. The scale bar represents 1 mm.

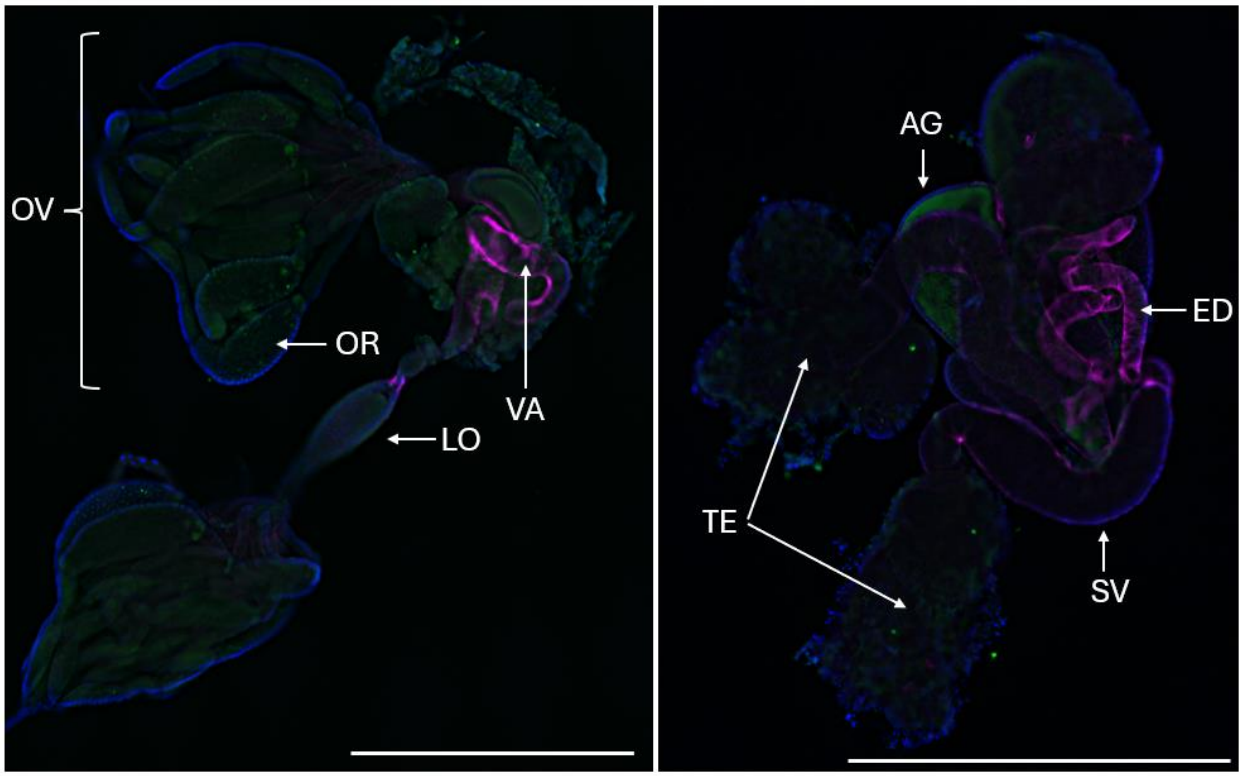

Figure 5.5: PmLgs is present in *Peregrinus maidis* male and female reproductive organs. The female reproductive organs are shown on the left and the male reproductive organs are shown on the right. Actin fibers were stained using AF 594-conjugated phalloidin (magenta), cell nuclei were stained using DAPI (blue), and PmLgs was stained using anti-PmLgs and AF 488-conjugated rabbit antibodies (green). OV: ovary; OR: ovarioles; LO: lateral oviduct; VA: vagina; TE: testes; AG: accessory gland; SV: seminal vesicle; ED: ejaculatory duct. These images are representative of multiple imaged tissues from adult male and female *P. maidis* insects. The scale bar represents 1 mm.

Figure 5.6: PmLgs is present in *Peregrinus maidis* fat bodies. The images in the left column show the AF488 signals detected from fat bodies on the inner surface of *P. maidis* abdomens, and the images in the right column show an overlay of the brightfield channel on the fluorescence microscopy images for clearer visualization of the dissected insect abdomens. Actin fibers were stained using AF 594-conjugated phalloidin (magenta), cell nuclei were stained using DAPI (blue), and PmLgs was stained using anti-PmLgs and AF 488-conjugated rabbit antibodies (green). These images are representative of multiple imaged tissues from adult male and female P. maidis insects. The scale bar represents 1 mm.

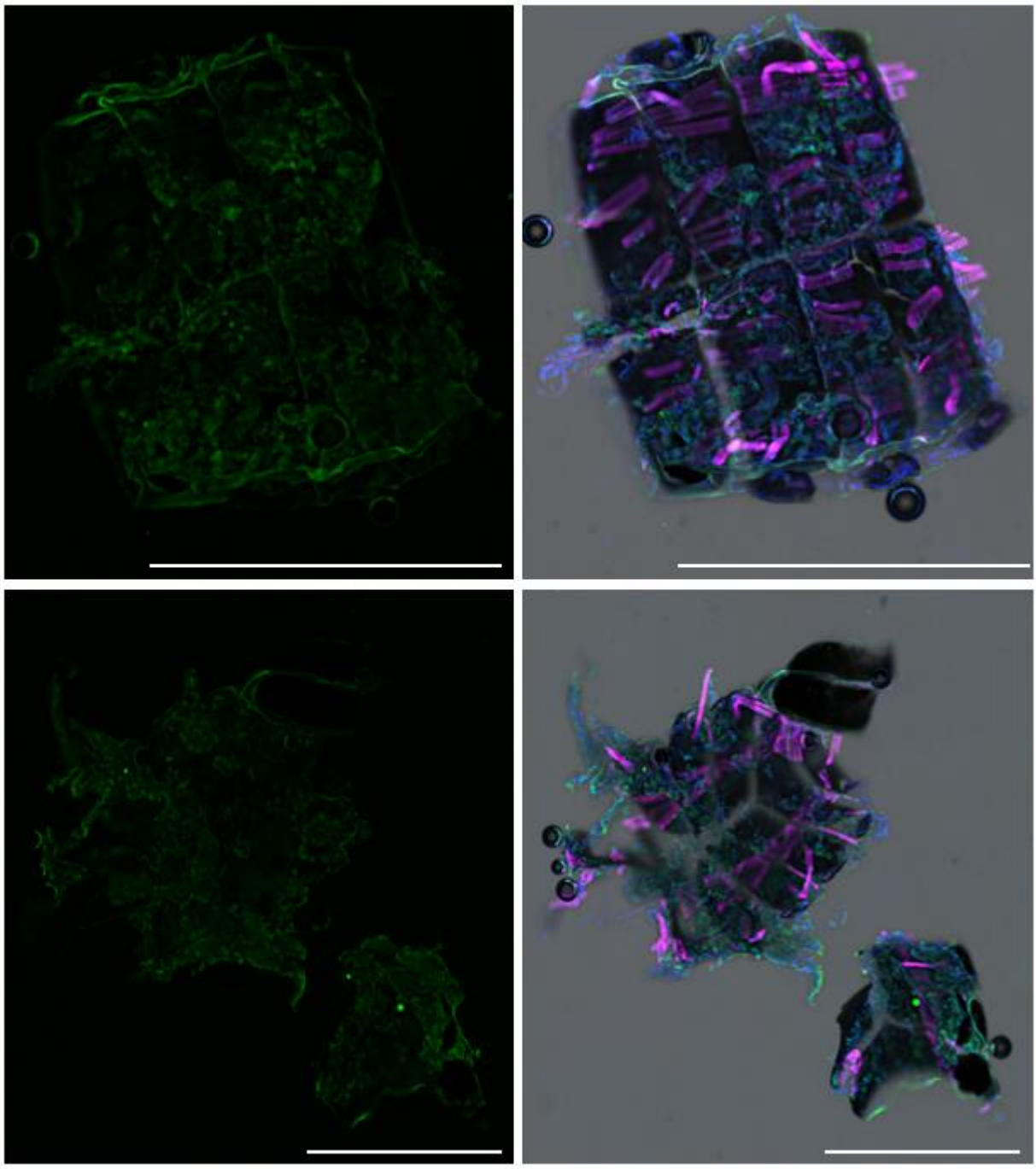

Lugensin Protein Expression, Purification, and Quantification

BL21 (DE3) *E. coli* culture was induced to express *P. maidis* lugensin for purification. Coomassie blue staining and western blotting results indicate that Ni-NTA-purified His:Lugensin is partially soluble and of the expected size (Figure 7.1). The purified lugensin was then dialyzed using TBS pH 7.4 to remove contaminating salts from the elution buffer. The volume recovered after dialysis was slightly greater than 100µL, and there was precipitation observed in the dialyzed samples. UV-Vis spectroscopy showed that the un-dialyzed samples and the protein elution buffer had 209nm absorbance values exceeding 20 units, while those of the dialyzed samples were less than 5 units, indicating that a large portion of contaminating salts in the sample were effectively removed after dialysis as imidazole is the main contaminant and it has an absorption peak near 209nm. The dialyzed lugensin protein preparations were then used for bacterial inhibition assays.

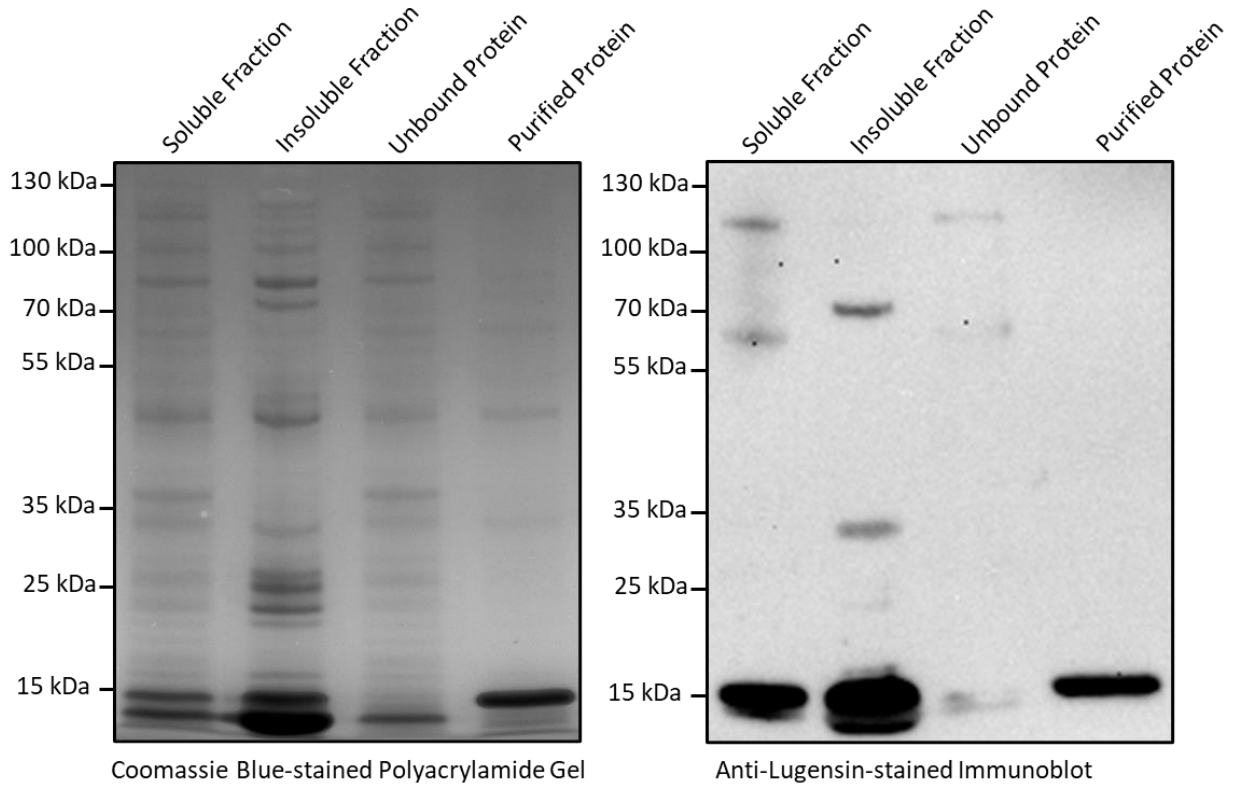

Figure 6.1: Coomassie Blue and western blot analysis of bacteria-expressed His:Lgs. 12.5µg of purified protein was added into the lane for the Coomassie Blue-stained gel, and 25µg of purified protein was added into the lane for the anti-lugensin-stained gel.

Bacterial Growth Inhibition Assays

PmLgs inhibited the growth of *E. coli* and *X. vasicola* but had no inhibitory effect on the growth of *S. marcescens* (Figures 6.1, 6.2, and 6.3). No growth was observed in wells containing no bacteria or wells containing kanamycin, except for the wells containing *S. marcescens* and kanamycin, where bacterial growth was observed 15 hours after the start of the assay, indicating the presence of kanamycin resistance in the *S. marcescens* strain used.

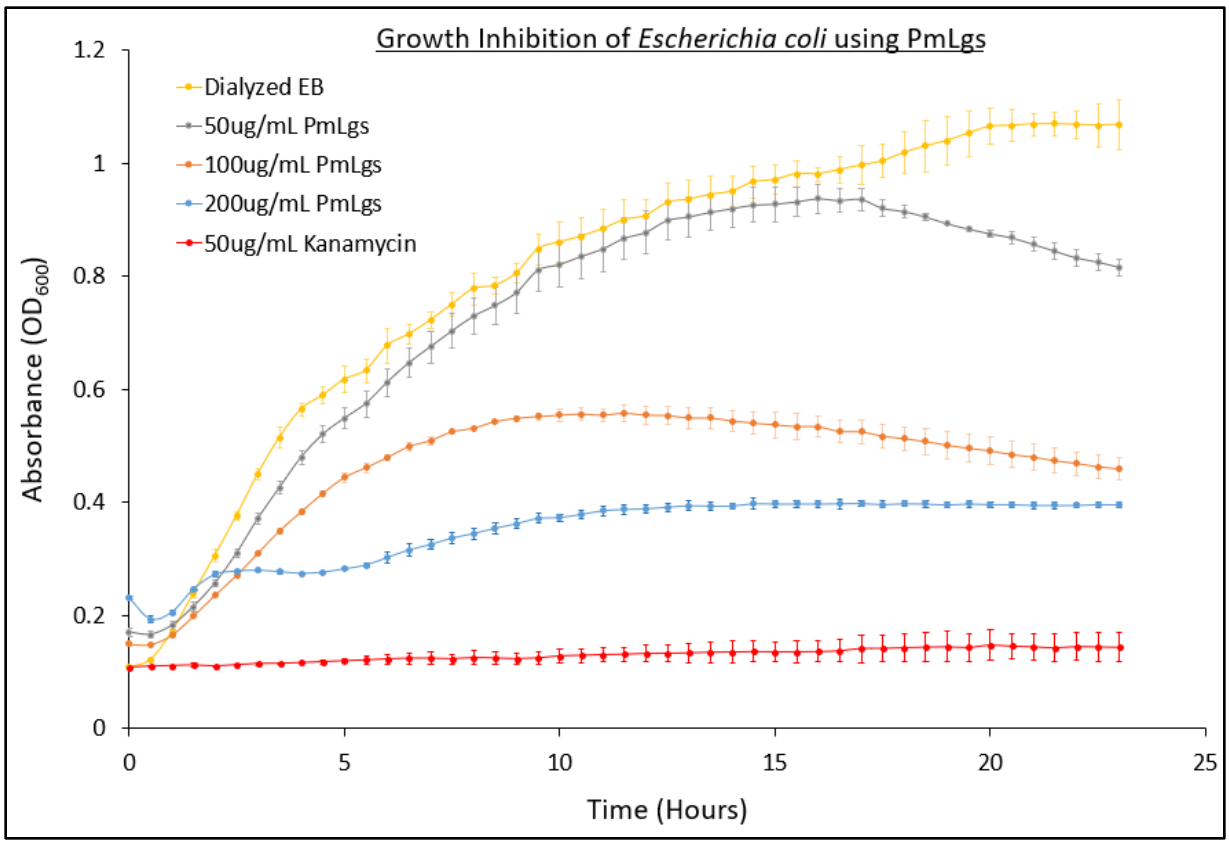

Figure 6.2: Growth curve of *Escherichia coli* incubated in purified *Peregrinus maidis* lugensin (PmLgs) in liquid culture, measured using the optical density of the culture at 600nm. Error bars represent standard deviation.

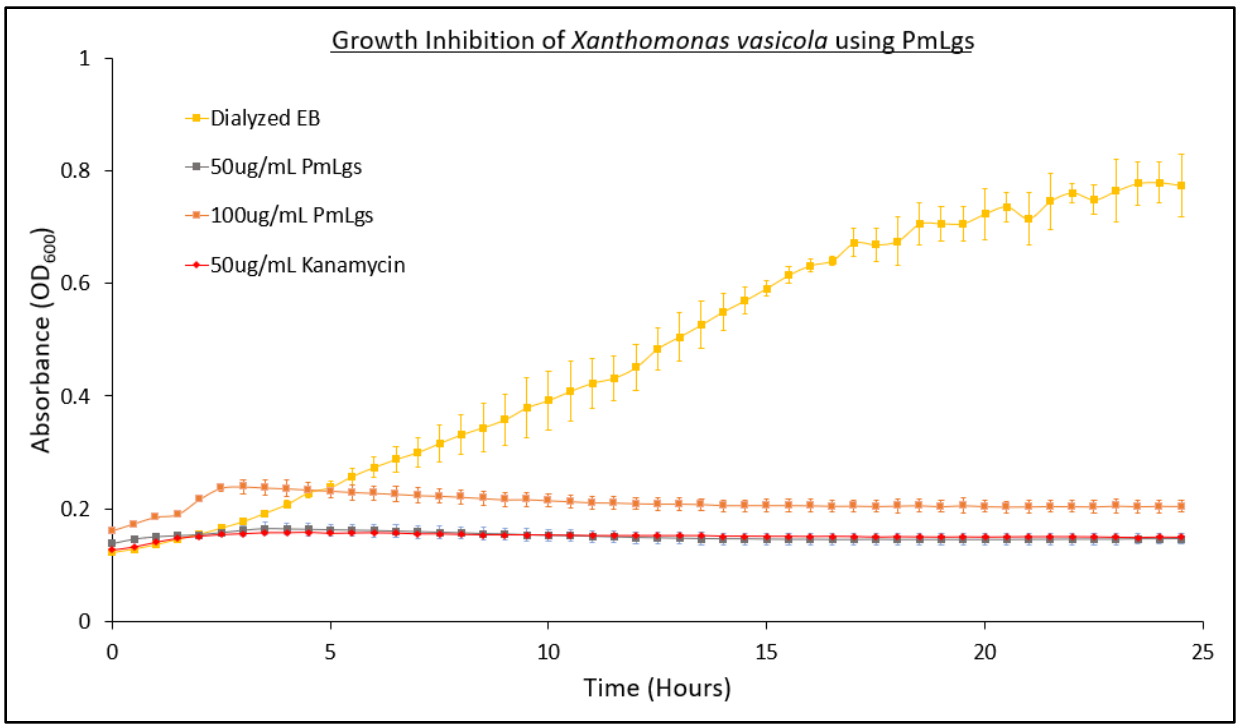

Figure 6.3: Growth curve of *Xanthomonas vasicola* incubated in purified *Peregrinus maidis* lugensin (PmLgs) in liquid culture, measured using the optical density of the culture at 600nm. Error bars represent standard deviation.

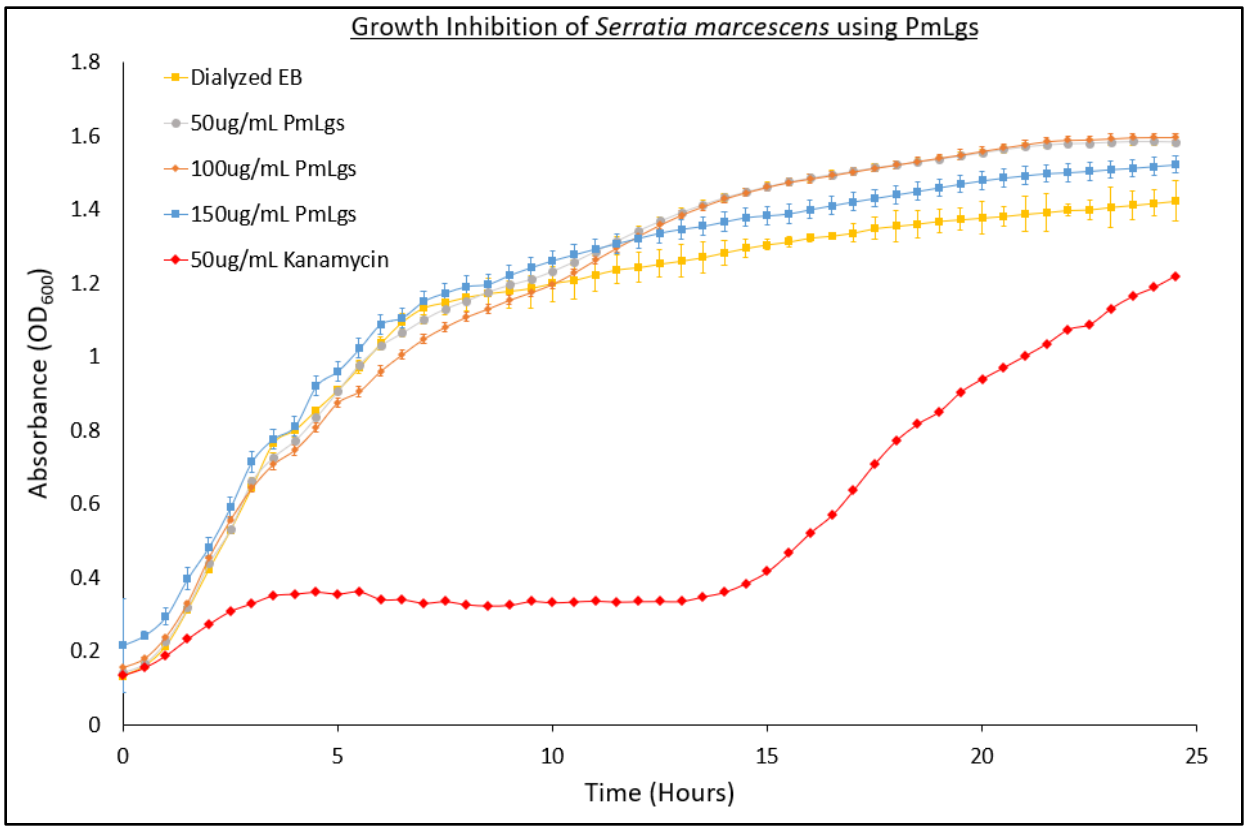

Figure 6.4: Growth curve of *Serratia marcescens* incubated in purified *Peregrinus maidis* lugensin (PmLgs) in liquid culture, measured using the optical density of the culture at 600nm. Error bars represent standard deviation.

Discussion

PmLgs shares high nucleotide sequence similarity with *N. lugens* lugensin B, an AMP with antibacterial activity (Zhou et al., 2019), and other uncharacterized hemipteran insect proteins from *N. lugens* and *L. striatellus*, with a lower degree of sequence similarity with uncharacterized dipteran proteins. Phylogenetic analysis also shows that *PmLgs* clusters together with other hemipteran AMPs, but not with the dipteran proteins, suggesting that it could be a delphacid-specific AMP. Significant structural homology was found between PmLgs and antibacterial peptides like *N. lugens* lugensin A and B, and a lower degree of homology was seen with insect antiviral peptides like gloverins. However, gloverins also share some other similarities with PmLgs, the cleaved, active form of both peptides are about 14 kDa in length, they possess an RXXR motif at the N-terminus, contain a high proportion of glycine residues and lack cysteine residues (Axén et al., 1997). Most importantly, like AMPs that function by disrupting cellular membranes, both PmLgs and gloverins interact with cell lipid membranes (Alviar et al., 2022).

The transcript and protein expression of PmLgs was shown to increase over the course of the insect life cycle, corroborating reports in the literature that AMP expression can be independent of pathogen presence and be affected by other factors such as age (Hanson and Lemaitre, 2023). In the present study, PmLgs was cloned and expressed in BL21 (DE3) *E. coli* without its signal peptide, then purified for use in antibody validation and antibacterial growth assays. PmLgs was able to inhibit the growth of *E. coli* and *Xanthomonas vasicola* (causal agent of bacterial leaf streak of corn) in a dose-dependent manner and had no effect on the growth of *Serratia marcescens*, showing that it has antibacterial properties, supporting the hypothesis that it is an AMP.

The authors of the original lugensin study found two *N. lugens lugensin* genes, *lugensin* A and *lugensin* B. The work here shows that there may be three or more *lugensin* genes within the *P.*

maidis genome which arose from gene duplication events, but more evidence in the form of genome sequence data from single insects is needed to determine if those genes are duplications or sequencing artefacts. Bioinformatic analyses which predict sequence and structural similarity between PmLgs and other insect AMPs can provide some insight into the function of PmLgs, and more empirical data would be valuable for further validation of protein function. The *N. lugens* study also performed antibacterial activity assays using Gram-negative and Gram-positive bacteria like *E. coli, B. subtilis,* and *Acidovorax avenae* subspecies *avenae,* and the assays performed in my study used only Gram-negative bacteria like *E. coli, Xanthomonas vasicola,* and *Serratia marcescens.* Additional experiments which test the ability of PmLgs to exert an antibacterial effect in a greater range of conditions which more closely mimic field settings that *P. maidis* encounters could be performed to verify that PmLgs is an AMP.

Further work could focus on investigating the response of *P. maidis* to viral challenge as some AMPs have antiviral properties and are induced in response to viral infection. Those AMPs typically function to eliminate or reduce viral titers to suppress deleterious symptoms associated with pathogenic viral infections. MMV infects *P. maidis* in a persistent-propagative manner, and this lifelong infection does not appear to have any negative effects on the overall fitness of the insect (Higashi et al., 2013). One possible hypothesis is that the insect regulates MMV titers with the help of PmLgs or other antiviral immune factors like the Toll, JAK-STAT, or antiviral RNAi pathways, maintaining it below a certain critical threshold where negative effects on insect health are not observed. PmLgs could have a dual antiviral and antibacterial function as enveloped viruses like MMV are encapsulated by lipid membranes. A study to investigate if PmLgs is involved in that regulatory role will provide more insight into the *P. maidis*-MMV interaction. Another study which could be undertaken is investigating the effect of PmLgs on the bacterial and fungal

communities within the insect, as hemipterans are known to harbor many bacterial and yeast endosymbionts (Vega and Dowd, 2005; Urban and Cryan, 2012). The antibacterial properties of PmLgs could allow for the insect host to exert some degree of microbial community regulation, and designing experiments to up or downregulate PmLgs followed by characterization of the insect microbiome could lead to the discovery of new roles played by PmLgs in insect immunity.

Assessing the effect of PmLgs on other bacterial species could lead to new biotechnologies being developed if this peptide exerts an inhibitory effect on economically relevant vector-borne bacterial pathogens like Candidatus *Liberibacter asiaticus* or *Xylella fastidiosa*, the causative agents of citrus greening disease and Pierce's disease respectively. The antifungal properties of PmLgs have yet to be characterized, and similar experiments could be conducted with the aim of investigating the effect of PmLgs on fungal community composition within *P. maidis* and on various plant or insect pathogenic fungi.

In this study, we have characterized PmLgs, a putative novel AMP from *P. maidis* which has antibacterial activity against some Gram-negative bacteria. That experimental data complemented with results from our computational analyses led us to hypothesize that PmLgs may be part of a family of previously undescribed, delphacid-specific AMPs.

References

Ahmed, A., Siman-Tov, G., Hall, G., Bhalla, N., & Narayanan, A. (2019). Human Antimicrobial Peptides as Therapeutics for Viral Infections. *Viruses*, *11*(8), 704.

Ammar, E.-D., & Nault, L. R. in B. R. (2002). *Virus transmission by leafhoppers, planthoppers and treehoppers (auchenorrhyncha, homoptera)* (Vol. 36, pp. 141–167). Academic Press.

Autrey, L. (1983). Maize mosaic virus and other maize virus diseases in the islands of the western Indian Ocean. In *Proceedings of the international maize virus diseases colloquium and workshop. The Ohio State University, Ohio Agricultural Research and Development Center, Wooster, Ohio* (Vol. 44691, pp. 167-181).

Axén, A., Carlsson, A., Engström, A., & Bennich, H. (1997). Gloverin, an antibacterial protein from the immune hemolymph of Hyalophora pupae. *European journal of biochemistry*, *247*(2), 614–619.

Barandoc-Alviar, K., Ramirez, G. M., Rotenberg, D., & Whitfield, A. E. (2016). Analysis of Acquisition and Titer of Maize Mosaic Rhabdovirus in Its Vector, *Peregrinus maidis* (Hemiptera: Delphacidae). *Journal of insect science (Online)*, *16*(1), 14.

Barandoc-Alviar, K., Rotenberg, D., Martin, K. M., & Whitfield, A. E. (2022). The physical interactome between *Peregrinus maidis* proteins and the maize mosaic virus glycoprotein provides insights into the cellular biology of a rhabdovirus in the insect vector. *Virology*, *577*, 163–173.

Brewbaker, J. L. 2003. Corn production in the tropics: the Hawaii experience. College of Tropical Agriculture and Human Resources, University of Hawaii Manoa, Honolulu, HI.

Bulet, P., & Stöcklin, R. (2005). Insect antimicrobial peptides: structures, properties and gene regulation. *Protein and peptide letters*, *12*(1), 3–11.

Cho, W. K., Lian, S., Kim, S. M., Park, S. H., & Kim, K. H. (2013). Current Insights into Research on Rice stripe virus. *The plant pathology journal*, *29*(3), 223–233.

Dissel, S., Seugnet, L., Thimgan, M. S., Silverman, N., Angadi, V., Thacher, P. V, Burnham, M. M., & Shaw, P. J. (2015). Differential activation of immune factors in neurons and glia contribute to individual differences in resilience/vulnerability to sleep disruption. *Brain, Behavior, and Immunity*, *47*, 75–85.

Engström Y. (1999). Induction and regulation of antimicrobial peptides in Drosophila. *Developmental and comparative immunology*, *23*(4-5), 345–358.

Falk B. W., Tsai J. H. 1985. Serological detection and evidence for multiplication of Maize mosaic virus in the planthopper vector, *Peregrinus maidis*. Phytopathology 75: 852–855.

Ganz T. (2003). Defensins: antimicrobial peptides of innate immunity. *Nature reviews. Immunology*, *3*(9), 710–720.

Gurr, G. M., Liu, J., Read, D. M. Y., Catindig, J. L. A., Cheng, J. A., Lan, L. P., & Heong, K. L. (2011). Parasitoids of Asian rice planthopper (Hemiptera: Delphacidae) pests and prospects for enhancing biological control by ecological engineering. *Annals of Applied Biology*, *158*(2), 149–176.

Hanson, M. A., & Lemaitre, B. (2023). Antimicrobial peptides do not directly contribute to aging in Drosophila, but improve lifespan by preventing dysbiosis. *Disease models & mechanisms*, *16*(4), dmm049965.

Heong, K. L., & Hardy, B. (2009). Planthoppers: New Threats to the Sustainability of Intensive Rice Production Systems in Asia (Issue 281811). *International Rice Research Institute (IRRI).*

Higashi, C. H. V, & Bressan, A. (2013). Influence of a propagative plant virus on the fitness and wing dimorphism of infected and exposed insect vectors. *Oecologia*, *172*(3), 847–856.

Hogenhout, S. A., Ammar, E.-D., Whitfield, A. E., & Redinbaugh, M. G. (2008). Insect Vector Interactions with Persistently Transmitted Viruses. *Annual Review of Phytopathology*, *46*(Volume 46, 2008), 327–359.

Jumper, J., Evans, R., Pritzel, A., Green, T., Figurnov, M., Ronneberger, O., Tunyasuvunakool, K., Bates, R., Žídek, A., Potapenko, A., Bridgland, A., Meyer, C., Kohl, S. A. A., Ballard, A. J., Cowie, A., Romera-Paredes, B., Nikolov, S., Jain, R., Adler, J., Back, T., Hassabis, D. (2021). Highly accurate protein structure prediction with AlphaFold. *Nature*, *596*(7873), 583–589.

Letunic, I., & Bork, P. (2021). Interactive Tree Of Life (iTOL) v5: an online tool for phylogenetic tree display and annotation. *Nucleic acids research*, *49*(W1), W293–W296.

Liu, W., Liu, J., Lu, Y., Gong, Y., Zhu, M., Chen, F., Liang, Z., Zhu, L., Kuang, S., Hu, X., Cao, G., Xue, R., & Gong, C. (2015). Immune signaling pathways activated in response to different pathogenic micro-organisms in Bombyx mori. *Molecular Immunology*, *65*(2), 391–397.

Livak, K. J., & Schmittgen, T. D. (2001). Analysis of relative gene expression data using real-time quantitative PCR and the 2(-Delta Delta C(T)) Method. *Methods (San Diego, Calif.)*, *25*(4), 402–408.

Madeira, F., Madhusoodanan, N., Lee, J., Eusebi, A., Niewielska, A., Tivey, A. R. N., Lopez, R., & Butcher, S. (2024). The EMBL-EBI Job Dispatcher sequence analysis tools framework in 2024. *Nucleic Acids Research*, *52*(W1), W521–W525.

Manniello, M. D., Moretta, A., Salvia, R., Scieuzo, C., Lucchetti, D., Vogel, H., Sgambato, A., & Falabella, P. (2021). Insect antimicrobial peptides: potential weapons to counteract the antibiotic resistance. *Cellular and molecular life sciences: CMLS*, *78*(9), 4259–4282.

Nault, L. R. (1997). Arthropod Transmission of Plant Viruses: a New Synthesis. *Annals of the Entomological Society of America*, *90*(5), 521–541.

Singh, B. U., & Seetharama, N. (2008). Host plant interactions of the corn planthopper, *Peregrinus maidis* Ashm. (Homoptera: Delphacidae) in maize and sorghum agroecosystems. *Arthropod-Plant Interactions*, *2*(3), 163–196.

Stączek S, Cytryńska M, Zdybicka-Barabas A. Unraveling the Role of Antimicrobial Peptides in Insects. *International Journal of Molecular Sciences*. 2023; 24(6):5753.

Stuart, B. A. R., Franitza, A. L., & E, L. (2022). Regulatory Roles of Antimicrobial Peptides in the Nervous System: Implications for Neuronal Aging. *Frontiers in Cellular Neuroscience*, *16*.

Tauszig, S., Jouanguy, E., Hoffmann, J. A., & Imler, J. L. (2000). Toll-related receptors and the control of antimicrobial peptide expression in Drosophila. *Proceedings of the National Academy of Sciences of the United States of America*, *97*(19), 10520–10525.

Urban, J. M., & Cryan, J. R. (2012). Two ancient bacterial endosymbionts have coevolved with the planthoppers (Insecta: Hemiptera: Fulgoroidea). *BMC evolutionary biology*, *12*, 87.

Vega, F. E., & Dowd, P. F. (2005). The Role of Yeasts as Insect Endosymbionts. In F. E. Vega & M. Blackwell (Eds.), *Insect-Fungal Associations Ecology and Evolution* (p. 0). Oxford University Press.

Whitfield, A. E., Rotenberg, D., Aritua, V., & Hogenhout, S. A. (2011). Analysis of expressed sequence tags from Maize mosaic rhabdovirus-infected gut tissues of Peregrinus maidis

reveals the presence of key components of insect innate immunity. *Insect molecular biology*, *20*(2), 225–242.

Xavier, C. A. D., Tyson, C., Kerner, L. M., & Whitfield, A. E. (2024). RNAi-mediated knockdown of exportin 1 negatively affected ovary development, survival and maize mosaic virus accumulation in its insect vector *Peregrinus maidis*. *Insect molecular biology*, *33*(4), 295–311.

Yi, H. Y., Chowdhury, M., Huang, Y. D., & Yu, X. Q. (2014). Insect antimicrobial peptides and their applications. *Applied microbiology and biotechnology*, *98*(13), 5807–5822.

Zhou, G., Xu, D., Xu, D., & Zhang, M. (2013). Southern rice black-streaked dwarf virus: a white-backed planthopper-transmitted fijivirus threatening rice production in Asia. *Frontiers in Microbiology*, *4*.

Zhou, X., Peng, L. Y., Wang, Z. C., Wang, W., Zhu, Z., Huang, X. H., Chen, L. B., Song, Q. S., & Bao, Y. Y. (2019). Identification of novel antimicrobial peptides from rice planthopper, Nilaparvata lugens. *Insect biochemistry and molecular biology*, *113*, 103215.

Supplementary Information

Supplementary Table 1: Primers used for pET vector modification, 5' RACE sequencing, qPCR analysis, and PmLgs cloning.

No.	Primer Name	Sequence (5' – 3')	Purpose
1	SumoLgs_F1	CAG ATT GGT GGT TCC AAG CGG TAC GAC TCC	pET vector modification.
2	mCherryLgs_R1	CCT TGC TCA CCA TAC GCC TTC CAA AAG GAA T	pET vector modification.
3	LgsmCherry_F2	ATT CCT TTT GGA AGG CGT ATG GTG AGC AAG G	pET vector modification.
4	LgsSumo_R2	GGA GTC GTA CCG CTT GGA ACC ACC AAT CTG	pET vector modification.
5	pET_vector_end_F	AGA CAA GCT TAG GTA TTT ATT CGG	pET vector modification.
6	PmLgs_R	CTT ACG CCT TCC AAA AGG AAT T	pET vector modification.
7	Sumo_removal_F	AAG CGG TAC GAC TCC CCT CCA CC	pET vector modification.
8	Sumo_removal_R	GCT AGC GCT GCC GCG CGG CAC	pET vector modification.
9	M13F	GTA AAA CGA CGG CCAG T	5'RACE sequencing.
10	InFusion GSP1R	GAT TAC GCC AAG CTT TGG AGG GGA GTC GTA CCG CTT AGC AAG GG	5'RACE sequencing.
11	caccPmLgs_F	CAC CAT GGA TGT GAG AGT GC	PmLgs cloning into pENTR vector.
12	pENTR_Lgs_R	CTT ACG CCT TCC AAA AGG AAT T	PmLgs cloning into pENTR vector.
13	qRPL10_F	CGA AGA AAT GGG GTT TCA	RPL10 qPCR forward primer.
14	qRPL10_R	CTC TGG CCT GTA CTT CAC	RPL10 qPCR reverse primer.
15	qPmLgs_F	TGT GAG AGT GCT GGT AGT	PmLgs qPCR forward primer.
16	qPmLgs_R	GAG GAG GTG GTC GAT TTA TG	PmLgs qPCR reverse primer.
17	qMMV-N_F	GAG CAT CTG GTA GAG GAG	MMV-N qPCR forward primer.
18	qMMV-N_R	CAT AGG TTC AGG AGC GTA	MMV-N qPCR reverse primer.

Supplementary Table 2: Amino acid sequences of insect-derived AMPs. Signal peptide regions are shown in blue, disordered regions are shown in red, and beta-sheet regions are shown in green.

Protein	Amino Acid Sequence
Peregrinus maidis Lugensin	MDVRVLVVLLVVAVVSSLAKRYDSPPPGYDNKLINRPPPPKTFADRTRMYRSAPD ETMHERLRRSPEEKRGTVVLSGTRTEQRGGPPQQSVRGEYNHNLWRGKNGATI DANTYYQRNWGGGPKQDYGGGIRGSIPFGRR
QCL07879.1 Lugensin A [*Nilaparvata lugens*]	MDLKVLVIVVVAVMSSTTFAKHHDDRPPPGYDRKLINRPPPPRNFLEGRRVYRSL PETIHERMRRSPQHGSVVVSGSRTEGRGGAPAQQSVRGDYNHNLWRGKNGAT VDANAYYQRNWGAGPRHDYGGGIRASIPFGRR
QCL07880.1 lugensin B [*Nilaparvata lugens*]	MDLKMLVVFLVVVASAYARLHQTPPPEFDGRLINRPPPPKFDYYPRGRVVRSAPE AEPMHERMRRSPQDGKHGSVVVSGSRTEGRGGAPAQQSVRGDYNHNLWRGK NGATVDANAYYQRNWGAGPRQDYGGGIRASIPFGRR
XP_026764963.2 gloverin [*Galleria mellonella*]	MQSLYIFAGILVAVAAQEYIQPYIMVDRYPDWYISRSQNEHLRLRRQLSVNKNGD VTLAHGSPNDKVFGTLGSRGESAFGKLGYQHNFINDNRGKLTGTAYGSRVLSPYG NSNHLGGRVDWASKHTSASLDVSKQMHGPTAIQAAAGGRWPVGRNGEISAQG TYDRIGRMQDYGGRLGYTYRF
AAG44367.1 gloverin precursor [*Trichoplusia ni*]	MQSSILLIFAAFVACTYAQVSLPPGYAQKYPQYKYSKVARHPRDTTWEHNVGRGK IFGTLGSNDDSVFGRGGYKQDIFNDHRGRLSGQAYGSRVINDYGGSSILGGKLDW SNDNARAALDVHKEIGRGSGMKLSGDGVWKLDHNTRFSAGGNLQKNFGHNRP EFGIQGKIEHDF
ABV68856.1 gloverin [*Trichoplusia ni*]	MQLSTIFCFAVLIACARAQVFVKPGHKDEDLAWMRSMGKGHVFGTLGSTDGSLI GKLGYKQNIYNDQRGNLGGTAYGSRVINEYGGTSSFGGKLDWKNANDNARASL DVHKQVGGSSGMTLTGDGVWKLDSKTRLVAGGNLDKTFGYSKPELGIQAKIEHD FK

Supplementary Table 3: Summary table of number of adult male and female *P. maidis* tissues imaged for immunofluorescence staining experiments.

	Salivary Glands	Guts	Fat Bodies	Male Reproductive Organs	Female Reproductive Organs
Positive Stained Samples	3	27	8	11	7
Negative Control Samples	3	11	6	6	11

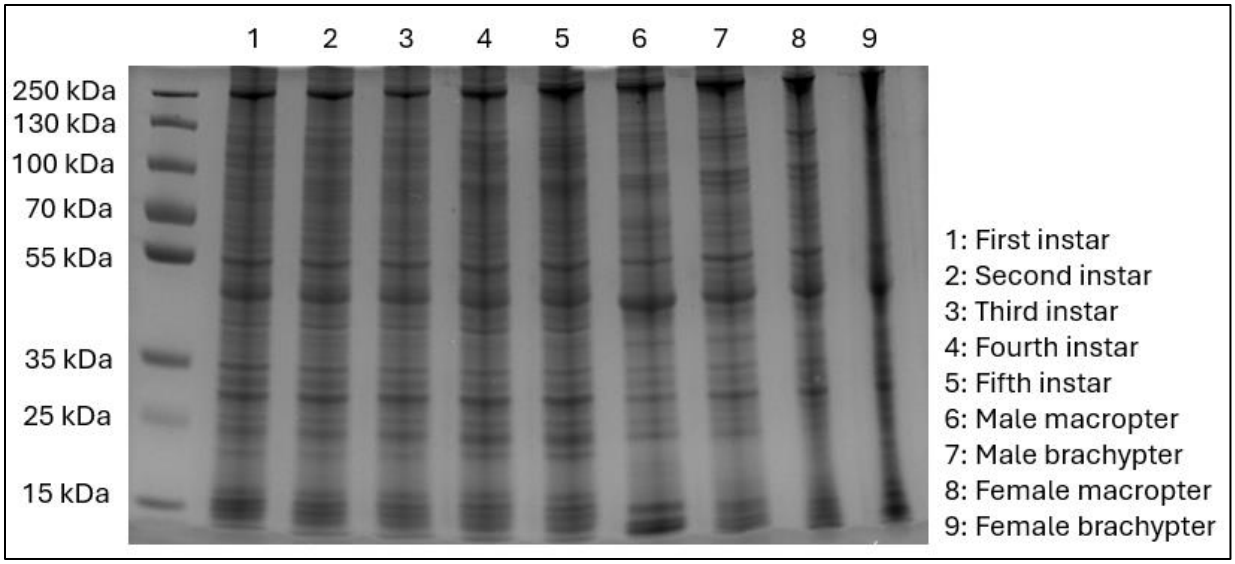

Supplementary Figure 1: Coomassie blue-stained gel showing an approximately equal quantity of crude insect protein extract loaded into each lane of a 10% polyacrylamide gel.

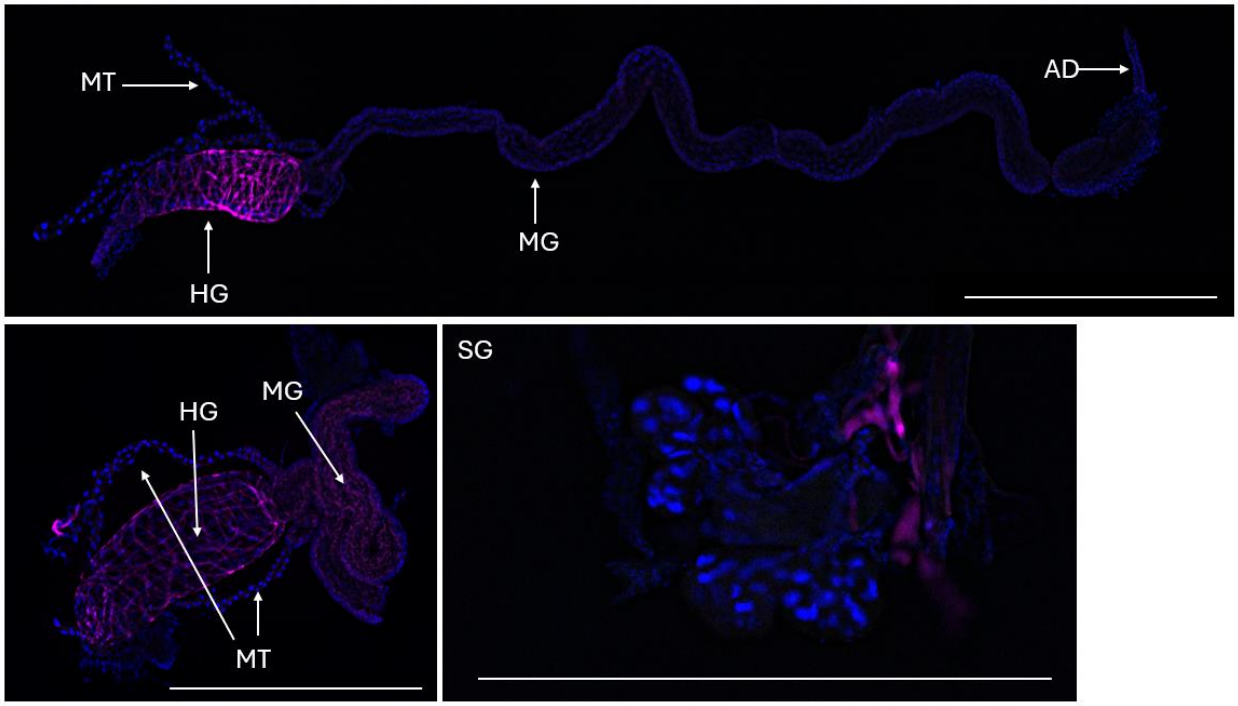

Supplementary Figure 2: Immunofluorescence staining negative controls for *Peregrinus maidis* guts and salivary glands. Actin fibers were stained using AF 594-conjugated phalloidin (magenta), cell nuclei were stained using DAPI (blue), and anti-PmLgs primary antibodies were omitted from samples that were stained using AF 488-conjugated rabbit antibodies (green). No signals from AF488 were observed in the negative controls. MG: midgut; AD: anterior diverticulum; SG: salivary glands; HG: hindgut; MT: Malpighian tubule. These images are representative of multiple imaged tissues from adult male and female *P. maidis* insects. The scale bar represents 1 mm.

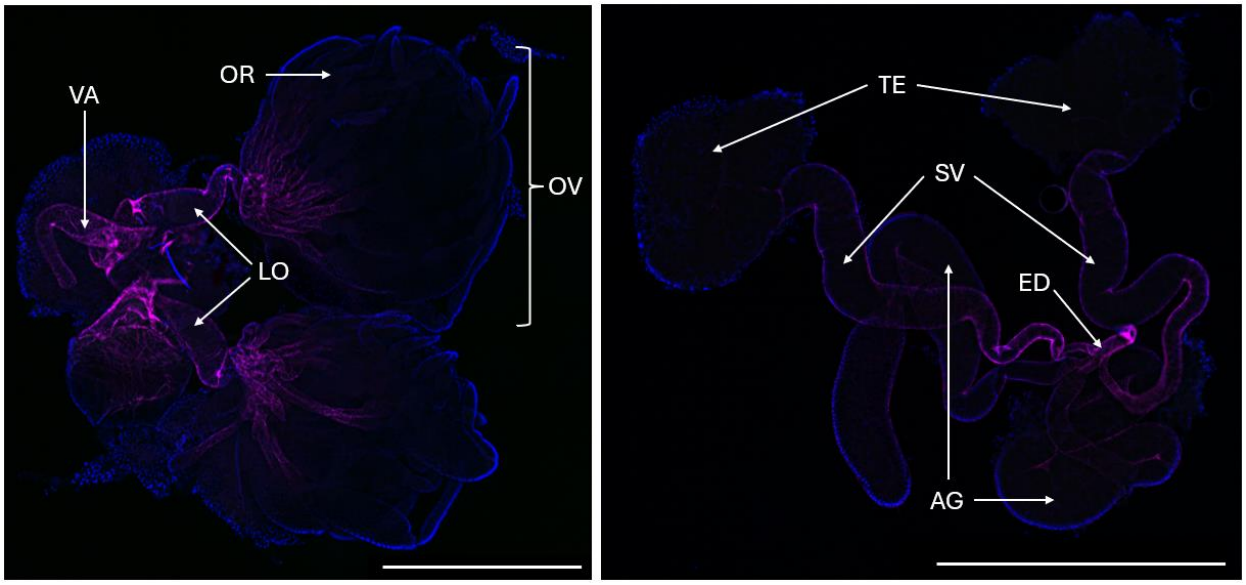

Supplementary Figure 3: Immunofluorescence staining negative controls for *Peregrinus maidis* female (left) and male (right) reproductive organs. Actin fibers were stained using AF 594-conjugated phalloidin (magenta), cell nuclei were stained using DAPI (blue), and anti-PmLgs primary antibodies were omitted from samples that were stained using AF 488-conjugated rabbit antibodies (green). No signals from AF488 were observed in the negative controls. OV: ovary; OR: ovarioles; LO: lateral oviduct; VA: vagina; TE: testes; AG: accessory gland; SV: seminal vesicle; ED: ejaculatory duct. These images are representative of multiple imaged tissues from adult male and female *P. maidis* insects. The scale bar represents 1 mm.

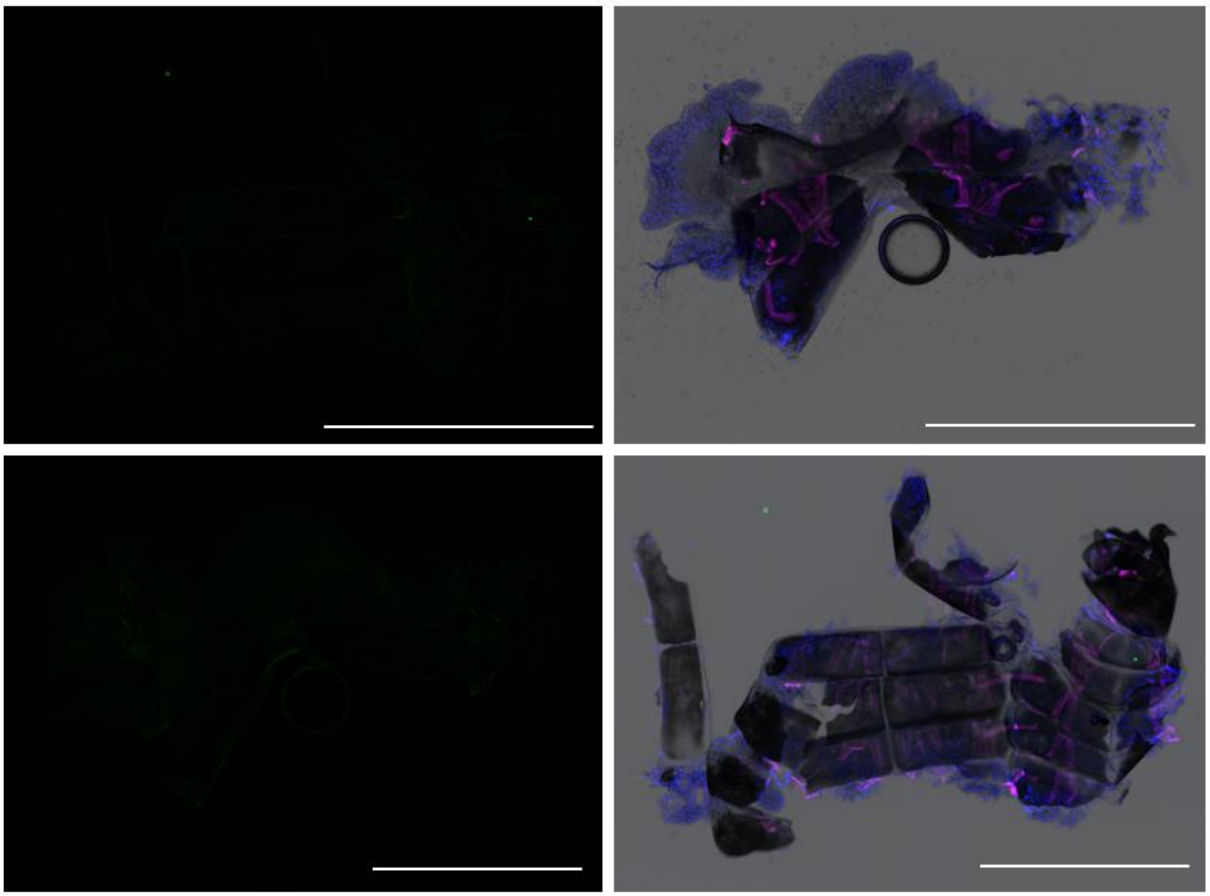

Supplementary Figure 4: Immunofluorescence staining negative controls for fat bodies of adult *Peregrinus maidis*. Actin fibers were stained using AF 594-conjugated phalloidin (magenta), cell nuclei were stained using DAPI (blue), and anti-PmLgs primary antibodies were omitted from samples that were stained using AF 488-conjugated rabbit antibodies (green). The images in the left column show that no AF488 signals are detected from fat bodies on the inner surface of *P. maidis* abdomens, and the images in the right column show an overlay of the brightfield channel on the fluorescence microscopy images for clearer visualization of the dissected insect abdomens. These images are representative of multiple imaged tissues from adult male and female P. maidis insects. The scale bar represents 1 mm.

CHAPTER 4

Investigating the Antiviral Properties of MMV-G-Interacting *Peregrinus maidis* Proteins

Abstract

Peregrinus maidis, the corn planthopper, is a hemipteran insect pest found in tropical and subtropical regions of the world. It feeds on maize and sorghum and is the sole vector of maize mosaic virus (MMV), a plant- and insect-infecting rhabdovirus. The insect host factors involved in the immune response to MMV are currently unknown, and previous studies have shown that proper function and interaction of rhabdovirus glycoproteins with host proteins is critical for viral infection. A membrane-based yeast-two-hybrid library screen was previously used to identify 107 insect proteins which interacted with the MMV glycoprotein, and from that study, three insect protein interactor candidates were shortlisted for further study, apolipophorin III, cyclophilin A, and lugensin, and we hypothesize that those interactors play antiviral roles in the *P. maidis*-MMV interaction. We attempted to revalidate the protein-protein interaction between the MMV glycoprotein and the three *P. maidis* proteins using a membrane-based yeast-two-hybrid assay. The transcript expression levels of *apolipohorin III* and *cyclophilin A* over insect development and transcript expression levels of the three *P. maidis* proteins over the course of MMV infection were quantified using RT-qPCR. Co-injection of MMV virions and double-stranded RNA targeting those three insect genes were also performed to investigate if those proteins were involved in the viral life cycle. The interactions between the viral glycoprotein and apolipophorin III, and the glycoprotein and lugensin were strong, and the interaction between the glycoprotein and cyclophilin A was relatively weaker. *Apolipophorin III* transcript expression levels generally increased as insects developed, and no significant difference was observed in *cyclophilin A* transcript expression over development, but very high variability was present in the *cyclophilin A* data. There was no significant difference in transcript expression levels of the three proteins between MMV-injected and buffer-injected insects. dsRNA-mediated RNAi was

efficient for all dsRNA constructs, and no significant differences in viral titers between the knockdown and control groups were observed in any group. These negative observations could be caused by several confounding factors, such as the possible uncoupling of transcript abundance levels from protein abundance, or the unnatural route of viral entry with direct hemocoel microinjections, bypassing the gut barrier entirely. Further experimentation addressing those possibilities will yield greater insight into the *P. maidis*-MMV interaction.

Introduction

Peregrinus maidis, the corn planthopper, is a tropical insect pest on maize and sorghum (Namba and Higa, 1971). It causes extensive crop damage when feeding, impacting yields and causing significant economic damage. *P. maidis* also serves as the sole vector of maize mosaic virus (MMV), transmitting it in a persistent-propagative manner (Ammar and Hogenhout, 2008). MMV is a rhabdovirus capable of infecting both plants and insects, and infected plants exhibit symptoms like stunting and chlorosis, negatively impacting crop health and yield. The mechanism of virus entry into insect cells is currently unknown, and research focused on identifying and characterizing the insect factors involved will deepen our understanding of the vector-virus interaction, potentially leading to the development of tools and strategies to reduce or eliminate the transmission of this plant virus to crops, ensuring continued food security.

Insects lack an acquired immune system, so they can only respond to pathogen challenges with their innate immune system, which consists of a humoral and a cellular component (Strand, 2008; Hillyer, 2016; Mahanta, 2023). The humoral components include responses like the induction of effector molecules which include antimicrobial peptides, complement-like proteins, and melanization enzymes, and the cellular components involve phagocytosis and hemocyte

encapsulation of foreign bodies (Arbouzova and Zeidler, 2006; Eleftherianos et al., 2006; Valanne et al., 2011; Iatsenko et al., 2016).

Insects respond to viral infections by activating the RNAi pathway, triggering the production of double-stranded RNA (dsRNA) that eventually becomes small, interfering RNA (siRNA) that targets viral RNA molecules for degradation and inhibits further viral replication (Galiana-Arnoux et al., 2006; Zambon et al., 2006). Signal transduction pathways like Jak-STAT, Imd, and Toll are also activated during viral infection, and in some instances result in the production of antiviral AMPs (Costa et al., 2009; Kingsolver et al., 2013; Marques and Imler, 2016). AMPs are a class of immune-related peptides which are found in virtually all organisms as part of their innate immune systems (Ahmed et al., 2019). They are typically short, cationic, oligopeptides with a wide range of structures, and they can have antibacterial, antiviral, or antifungal properties. Most AMPs identified and characterized to date have been isolated from insects (Yi et al., 2014).

Previously, a split-ubiquitin membrane-based yeast-two-hybrid assay was used to identify *P. maidis* proteins which interacted with the MMV glycoprotein (Barandoc-Alviar et al., 2022). A total of 107 insect protein interactors were identified in that study, and three *P. maidis* protein candidates among them were shortlisted for further investigation: apolipophorin III, cyclophilin A, and *P. maidis* lugensin. I hypothesize that these proteins could be antiviral or proviral towards MMV, serving to modulate the speed and severity of viral infection within the insect.

Nilaparvata lugens lugensin is a protein which was experimentally shown to possess antibacterial properties (Zhou et al., 2019). Previous bioinformatic analyses of *P. maidis* lugensin (PmLgs) showed that it bears significant sequence and structural similarities to *N. lugens* lugensin, and in vitro experiments using bacterial growth inhibition assays shows an inhibitory effect on bacterial growth, suggesting that it could potentially be a new class of delphacid-specific AMPs. These

pieces of data led us to hypothesize that PmLgs is an AMP with antiviral properties which allow the insect to modulate virus infection. A possible mechanism of action for PmLgs could be surface lipid membrane permeabilization, like that of other AMPs.

Insects rely on a single functional lipoprotein for lipid transport, comprised primarily of apolipophorin I, apolipophorin II, and lipids, and some insect orders like Orthoptera and Lepidoptera also have a third apolipophorin, apolipophorin III (Apo3) (Weers, 1993). In addition to their roles in lipid transport, insect Apo3, which is homologous to mammalian apolipoprotein E, has been shown to play a role in immune response towards pathogens. *Galleria mellonella* Apo3 was shown to bind to bacterial cell wall components of Gram-positive bacteria and inhibited microbial pathogenic activity (Halwani et al., 2000). *Hyphantria cunea* Apo3 induces antimicrobial peptide (AMP) expression and binds to *E. coli* membranes (Kim et al., 2004). Additionally, *Manduca sexta* Apo3 is involved in programmed cell death of skeletal muscles and neurons (Sun et al., 1995). Apolipophorins could play a role in viral infection as well, as seen in a study where apolipoprotein A1 serum levels were elevated in rabies virus-infected mice that had high levels of viral replication (Yamada et al., 2021). Additionally, silencing *Apo3* transcripts in *Ae. aegypti* resulted in lower Zika virus RNA copy numbers in midguts (Chen et al., 2024).

P. maidis Apo3 (PmApo3) interacted with the MMV glycoprotein in a MbY2H assay, and this interaction indicates that it could be involved in virus recognition upon virion entry. PmApo3 could also serve an antiviral role by binding to and disrupting the virion outer lipid membrane to reduce virion infectivity, or it could serve as a proviral protein by assisting with virion transport.

Cyclophilins are a class of proteins belonging to the immunophilins, and they have been found in almost all organisms to date (Handschumacher et al., 1984; Wang and Heitman, 2005; de Wilde et al., 2018). All cyclophilins have peptidyl-prolyl *cis-trans* isomerase activity, but their structures

are diverse. Some cyclophilins also have additional functions beyond protein folding, like protein trafficking, cell signaling, and immune signaling. In the context of viruses, cyclophilins have been shown to play proviral and antiviral roles. Human immunodeficiency virus type-1 virions rely on cyclophilin A for nuclear trafficking and viral replication, inhibition of cyclophilin A using cyclosporine A in Dengue virus-infected mosquito cell lines resulted in reduced NS1 viral protein secretion, and silencing cyclophilin B expression in *Bemisia tabaci* resulted in reduced transmission of tomato yellow leaf curl virus (Schaller et al., 2011; Kanakala et al., 2019; Rosales Ramirez and Ludert, 2019). Cyclophilin A was shown to inhibit early viral replication of Influenza A virus by binding to the M1 viral protein, and cyclophilin A could also inhibit virus replication by enhancing RIG-I-mediated antiviral immune responses (Liu et al., 2009; Liu et al., 2012; Liu et al., 2017). The results from these studies involving cyclophilins, and the fact that *P. maidis* cyclophilin A (PmCypA) interacted with the MMV glycoprotein suggests that PmCypA could be proviral and play roles in MMV movement and trafficking within host cells.

In this chapter, the protein-protein interaction between the MMV glycoprotein and the three *P. maidis* proteins PmApo3, PmCypA, and PmLgs detected in a previous MbY2H library screen were validated with additional replicates of MbY2H assays, and a strong interaction between MMV-G and PmLgs and MMV-G and PmApo3 was detected, while a weaker interaction was potentially present between MMV-G and PmCypA. These insect proteins were further characterized by quantifying their transcript expression levels at different life stages, and at different stages of MMV infection. No significant difference between expression levels of the three protein transcripts was observed between virus-infected or uninfected insects. dsRNA-mediated RNAi of those three transcripts with simultaneous injection of MMV virions was also performed to evaluate the effect of transcript knockdown on viral titers, and no significant difference in titers was

observed between the treatment group and control group which was injected with dsRNA targeting green fluorescent protein (GFP). These results indicate that protein abundance levels could remain unaffected by transcript levels, resulting in no observable differences between groups.

Materials and Methods

Bait and Prey Plasmid Cloning

The plasmids pBT3_SUC_EV (empty vector bait plasmid) pPR3-N_EV (empty vector prey plasmid) pOst-NubI (positive control prey plasmid), and NMY51 yeast reporter strain were obtained from the DUALmembrane starter kit (Dualsystems Biotech). The bait plasmid pBT3_SUC_MMV-G containing the full-length MMV-G open reading frame was obtained from Karen Barandoc-Alviar (Barandoc-Alviar et al., 2022). PmApo3, PmCypA, and PmLgs were cloned into pPR3-N using Primers 1 through 6 and restriction digests with SfiI enzyme to produce the prey vectors pPR3-N_Apo3, pPR3-N_CypA, and pPR3-N_Lgs, respectively (Supplementary Table 1). The plasmids were used for yeast transformations after Sanger sequencing verification.

Split-ubiquitin Membrane-based Yeast-two-hybrid Screen

NMY51 yeast was transformed by first streaking and selecting single colonies of yeast from a yeast extract peptone dextrose (YPD) plate. The colonies were inoculated into YPD media and grown at 30°C, 225 RPM until the liquid culture reached an OD_{600} value of 0.7, then the yeast was made competent using a standard lithium acetate transformation protocol with single-stranded DNA. The transformed yeast cultures were then grown on dropout media plates at 30°C for 72 hours to screen for successful plasmid transformation (DDO: -Leu/-Trp) and for protein-protein interaction between the bait and prey proteins (QDO: -Leu/-Trp/-His/-Ade). The addition of 40mM

3-AT to media was required to reduce the number of background colonies, so all media plates used for further MbY2H screening also contained 40mM 3-AT.

For further screening of the interaction strength between the bait and prey proteins, transformed yeasts which grew on QDO plates were also grown on QDO plates containing 20µg/mL X-gal for β-galactosidase activity screening as NMY51 contains the color reporter lacZ. The plates containing X-gal were grown for 96 hours at 30°C. All MbY2H screens were repeated at least three times to ensure reproducibility.

Insect Microinjection

Adult *P. maidis* insects (1 week after final molt) were microinjected using a Nanoject III™ (Drummond Scientific Company). The injection solution was prepared by diluting 2.5µL of purified MMV virions with various dsRNA constructs (final concentration of 500ng/µL of dsRNA) and water to a final volume of 10 µL. Eighty nanoliters of that solution were then injected (60nL/second) into the hemocoel of each insect after they were anesthetized on ice. The injected insects were then kept on three-week-old corn plants and collected at time points of zero, six, twelve, and eighteen days after injection for RNA extraction.

RNA Extraction, cDNA Synthesis, and RT-qPCR

Varying numbers of *Peregrinus maidis* insects were pooled to form individual biological replicates for different life stages; first instar (40), second instar (20), third instar (4), fourth instar (3), fifth instar (3), and adult (3). The insects were homogenized in TRIzol reagent (ThermoFisher) using micropestles in 1.7mL microcentrifuge tubes, and RNA was extracted following the manufacturer's protocols. The RNA samples were then treated with DNase I using the TURBO

DNA-free kit (ThermoFisher) to remove residual contaminating DNA before RNA quantification was performed with the NanoDrop One spectrophotometer (Thermo Fisher Scientific).

For the MMV virions and dsRNA co-injection experiments, three biological replicates each consisting of three adult male or female insects were collected for each treatment at each time point. The insects were homogenized using a TissueLyser II (Qiagen) and RNA extraction and DNAse treatment using Trizol reagent proceeded following the protocol above.

The Verso cDNA Synthesis kit (ThermoFisher) was used to synthesize cDNA using 500ng of total RNA, then the synthesized cDNA was diluted 5-fold using nuclease-free water for use as template material in subsequent RT-qPCR analysis assays to quantify gene expression in various *P. maidis* life stages. For RT-qPCR analysis of gene expression and viral transcript quantification in the co-injection experiments, 750ng of total RNA was used as template material for cDNA synthesis, and the final cDNA reaction was diluted 10-fold afterwards using nuclease-free water. The RT-qPCR reaction mixes were set up using iTaq Universal SYBR Green Supermix (Bio-Rad) and run on a CFX Connect Real-Time System (Bio-Rad) and the cycling conditions are as follows: an initial denaturation step at 95°C for 1 min, then 40 cycles of amplification involving a step at 95°C for 15s followed by a step at 60°C for 1 min. Melt curve analyses showed that amplicons produced a single peak and all wells were run in duplicate to serve as technical replicates. The comparative cycle threshold method ($2^{-\Delta\Delta Ct}$) or normalized RNA abundance method ($2^{-\Delta Ct}$) was used to quantify gene expression levels and virus abundance. Following previous publications investigating *P. maidis* target gene expression, the internal reference gene chosen for these RT-qPCR experiments was *RPL10* (Barandoc-Alviar et al., 2016; Xavier et al., 2024). All primers used for RT-qPCR had efficiencies between 90% to 110% and primer sequences are available in Supplementary Table 1. All primers used for RT-qPCR analysis are available in Supplementary Table 1.

Statistical analysis of life stage gene expression analysis of *PmApo3* and *PmCypA* was performed using the Kruskal-Wallis test with post-hoc Dunn's and Bonferroni correction. Statistical analysis of gene expression over MMV infection was performed using the Student's T-test.

Results

Membrane-based Yeast-two-hybrid Assays

The MbY2H assay detected a strong interaction between the MMV glycoprotein (MMV-G) and PmLgs, and between MMV-G and PmApo3, and a weaker interaction was detected between MMV-G and PmCypA (Figure 1.1). The plates containing X-gal in the media were left to grow for an additional day, possibly resulting in the growth of colonies observed in the empty vector negative controls. The MMV-G and NubI pair was used as a positive interaction control for the assay. The assay was repeated at least 3 times and the images shown are a representative sample of the results.

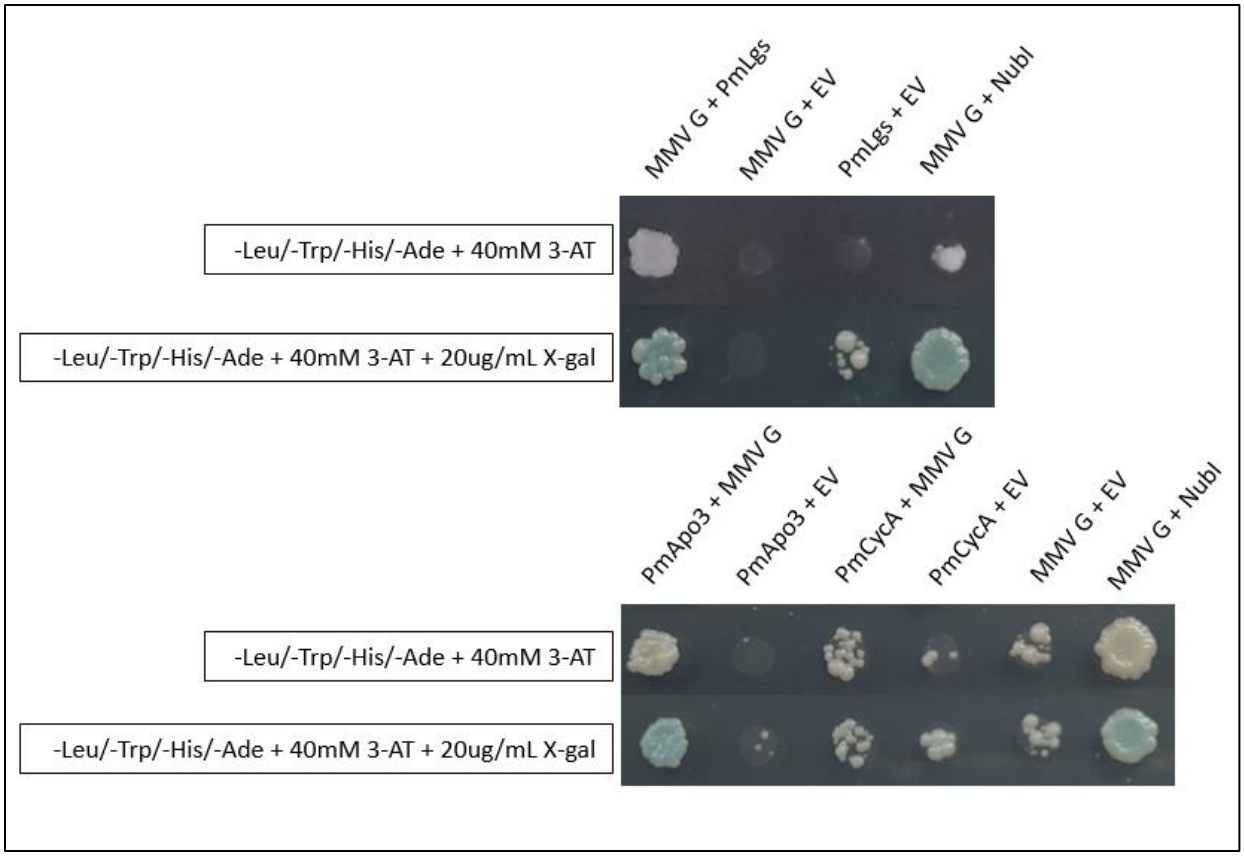

Figure 1.1: A split-ubiquitin membrane-based yeast-two-hybrid assay was used to detect a strong protein-protein interaction between the MMV glycoprotein (MMV-G) and PmLgs, MMV-G and PmApo3, and a weaker interaction between MMV-G and PmCypA. EV represents the empty vector negative controls, and NubI is a positive interaction control for the assay. The plates containing X-gal were incubated for an additional day, possibly resulting in the growth of colonies on some negative controls.

Expression Analysis Across Life Stage Development

PmApo3 and *PmCypA* transcript expression levels were normalized to that of *RPL10*. *PmApo3* expression was significantly lower in first instars compared to fifth instars, female brachypters, female macropters, and male brachypters, and there was also a significant difference observed in *PmApo3* expression levels of third instars compared to that of female brachypters (Figure 2.1) No significant difference in *PmCypA* transcript expression levels was observed across life stages (Figure 2.2). Higher levels of variation were also observed in *PmCypA* expression levels in all life stages compared to *PmApo3* expression.

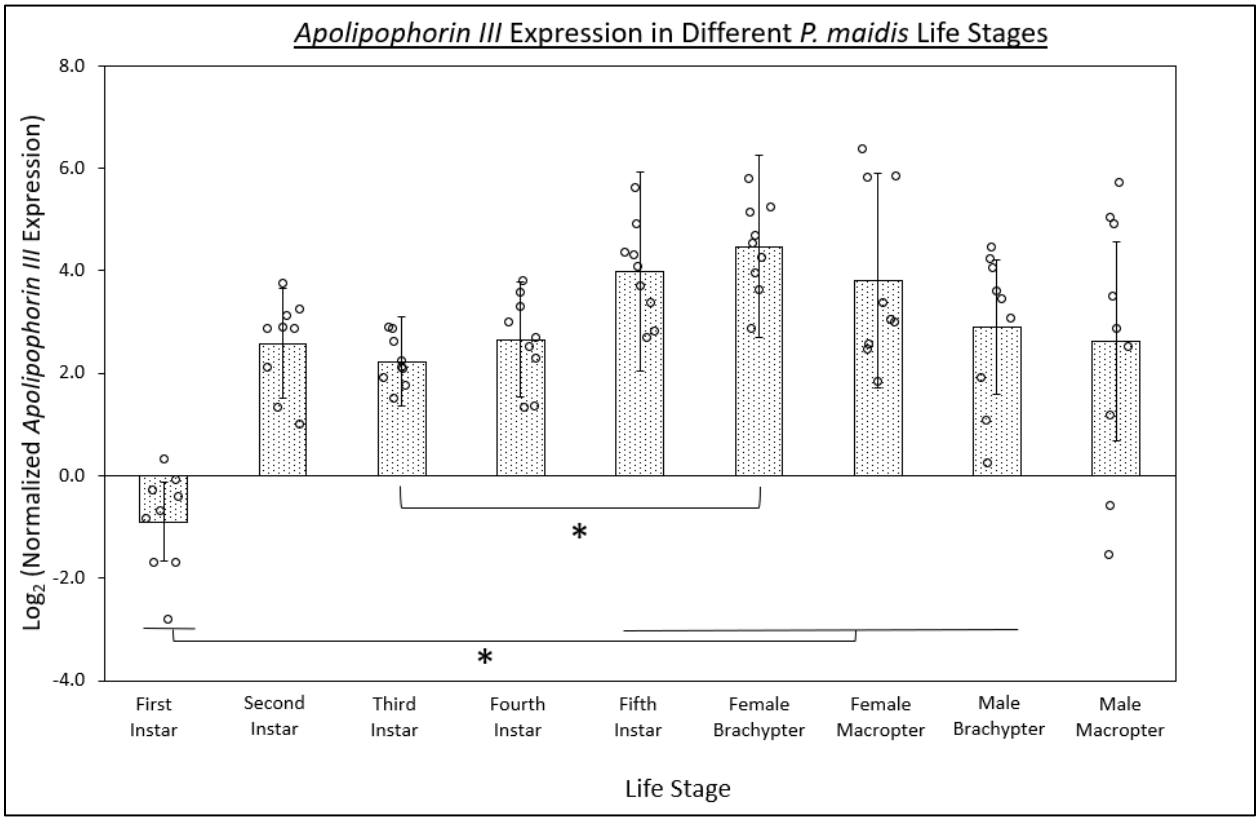

Figure 2.1: *Peregrinus maidis apolipophorin III* (*PmApo3*) transcript expression levels in different insect life stages. Each life stage is represented by at least nine biological replicates, with each biological replicate consisting of three insects. Error bars represent standard deviation.

Significant differences were observed between first instars and fifth instars, female brachypters, female macropters, and male brachypters. An asterisk denotes $p < 0.001389$ (after Bonferroni correction with an initial $p < 0.05$).

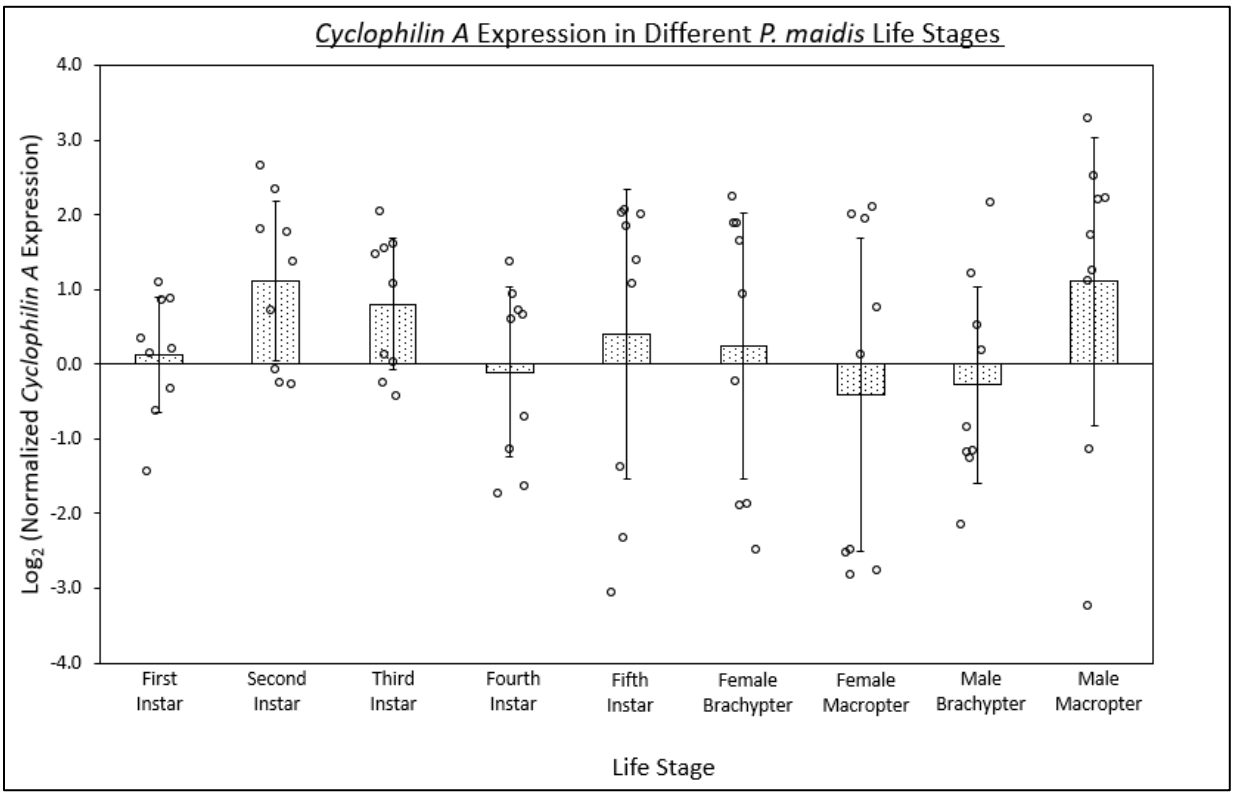

Figure 2.2: *Peregrinus maidis cyclophilin A* (*PmCypA*) transcript expression levels in different insect life stages. Each life stage is represented by at least nine biological replicates, with each biological replicate consisting of three insects. Error bars represent standard deviation. No significant difference in transcript expression levels was observed between groups.

Transcript Expression Response to MMV Infection

Adult *P. maidis* insects were injected with MMV virions or a buffer solution of TBS 7.4, then the insects were collected for RNA extraction, cDNA synthesis, and qRT-PCR. Transcript levels of MMV nucleoprotein increased over time, showing that the injected virions were viable and

replicated within the insects, and no amplification of nucleoprotein transcripts was observed in samples from buffer-injected insects. (Figure 5.1). Transcript expression levels of *PmApo3*, *PmCypA*, and *PmLgs* were quantified at various time points, and no significant differences in gene expression were observed between the virion-injected and buffer-injected groups (Figure 3.2, 3.3, and 3.4).

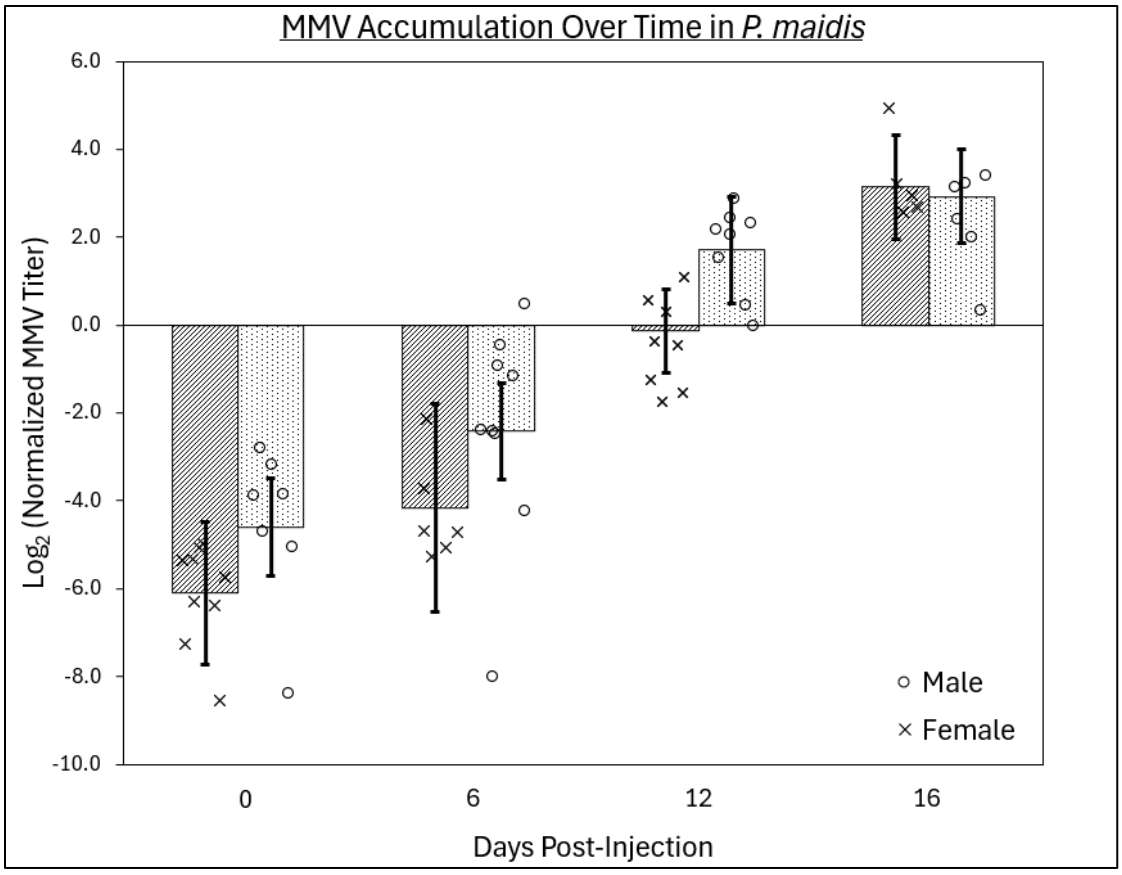

Figure 3.1: Quantification of MMV nucleoprotein transcripts shows that the initial virions were viable and replicated within insects. Viral titers are significantly higher in male insects compared to female insects at 12 DPI (p=0.005). Error bars represent standard deviation.

Figure 3.2: Quantification of *P. maidis apolipophorin III* (*PmApo3*) transcripts shows no significant difference in *PmApo3* expression present between virus or buffer-injected groups for male and female insects. Error bars represent standard deviation.

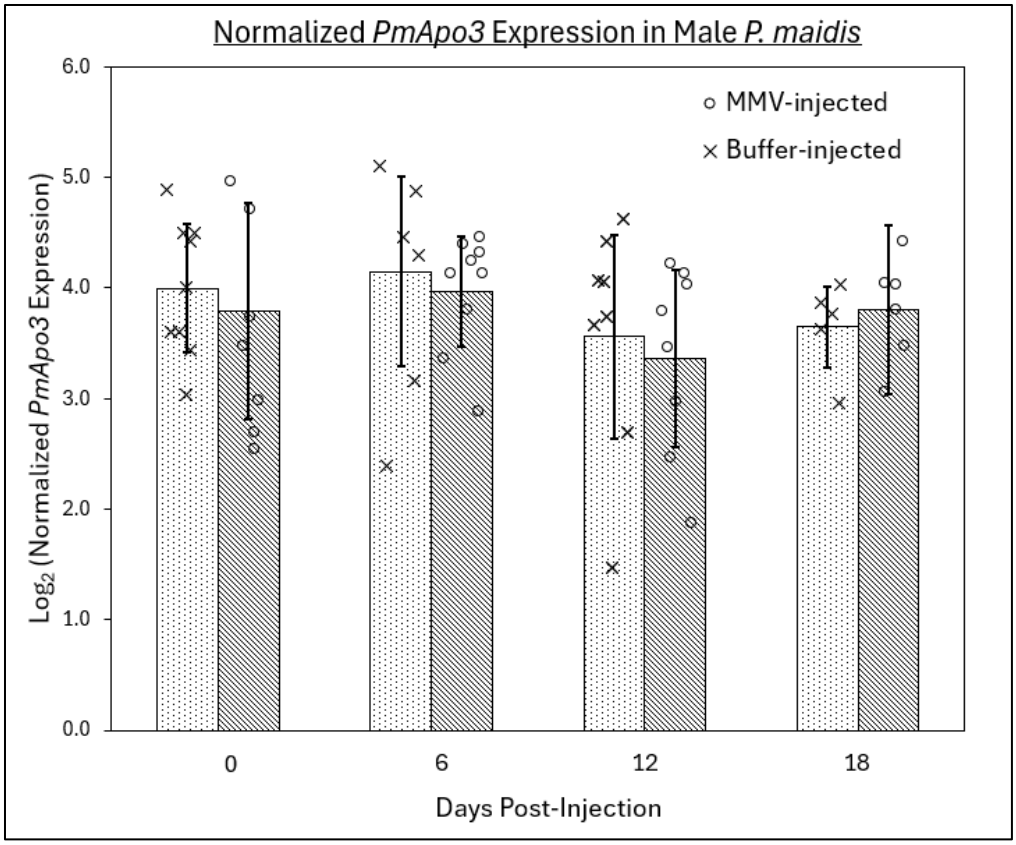
Normalized *PmApo3* Expression in Male *P. maidis*
MMV-injected
Buffer-injected
Log_2 (Normalized *PmApo3* Expression)
6.0
5.0
4.0
3.0
2.0
1.0
0.0
0
6
12
18
Days Post-Injection

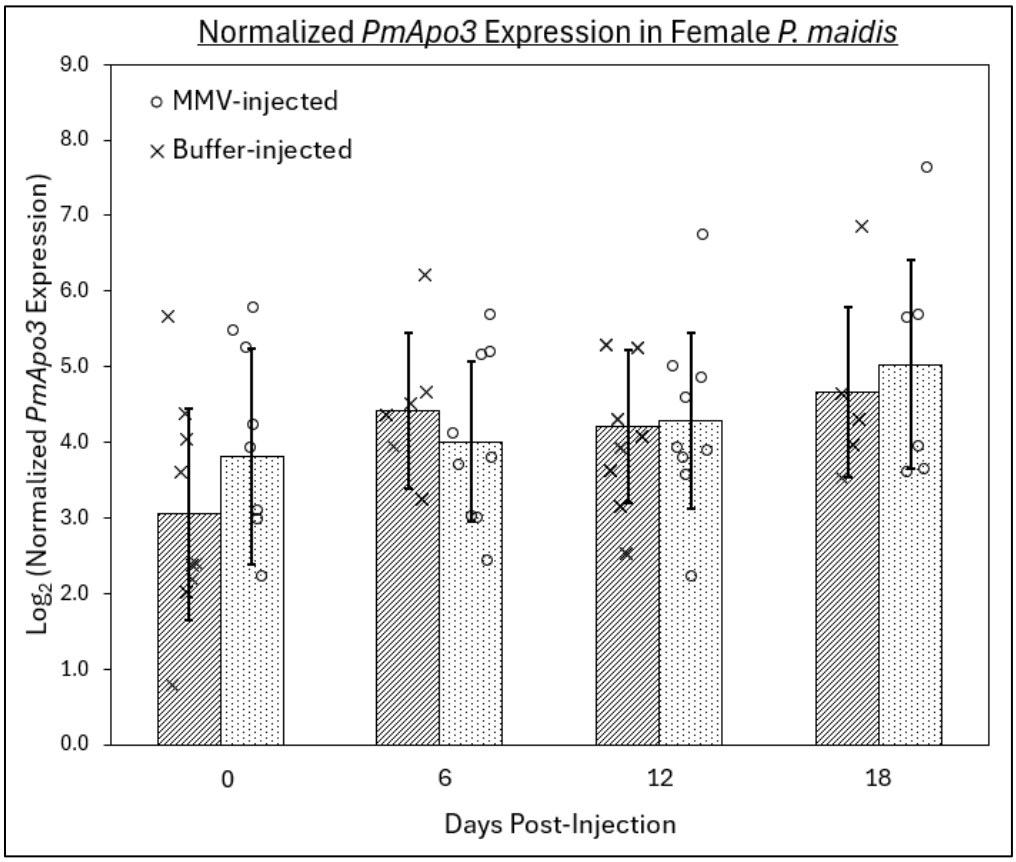
Normalized *PmApo3* Expression in Female *P. maidis*
MMV-injected
Buffer-injected
Log_2 (Normalized *PmApo3* Expression)
9.0
8.0
7.0
6.0
5.0
4.0
3.0
2.0
1.0
0.0
0
6
12
18
Days Post-Injection

Figure 3.3: Quantification of *P. maidis cyclophilin A* (*PmCypA*) transcripts shows no significant difference in *PmCypA* expression between virus or buffer-injected groups for male and female insects. Error bars represent standard deviation.

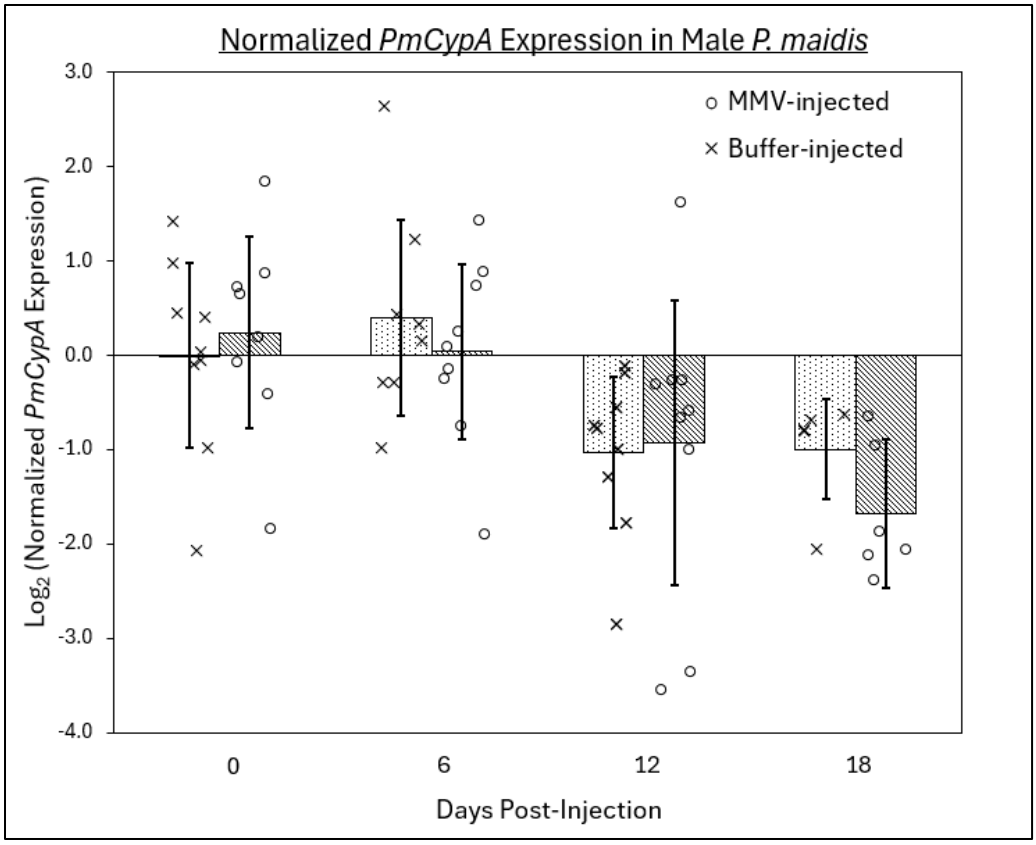
Normalized PmCypA Expression in Male P. maidis
MMV-injected
Buffer-injected
Log2 (Normalized PmCypA Expression)
3.0
2.0
1.0
0.0
-1.0
-2.0
-3.0
-4.0
0
6
12
18
Days Post-Injection

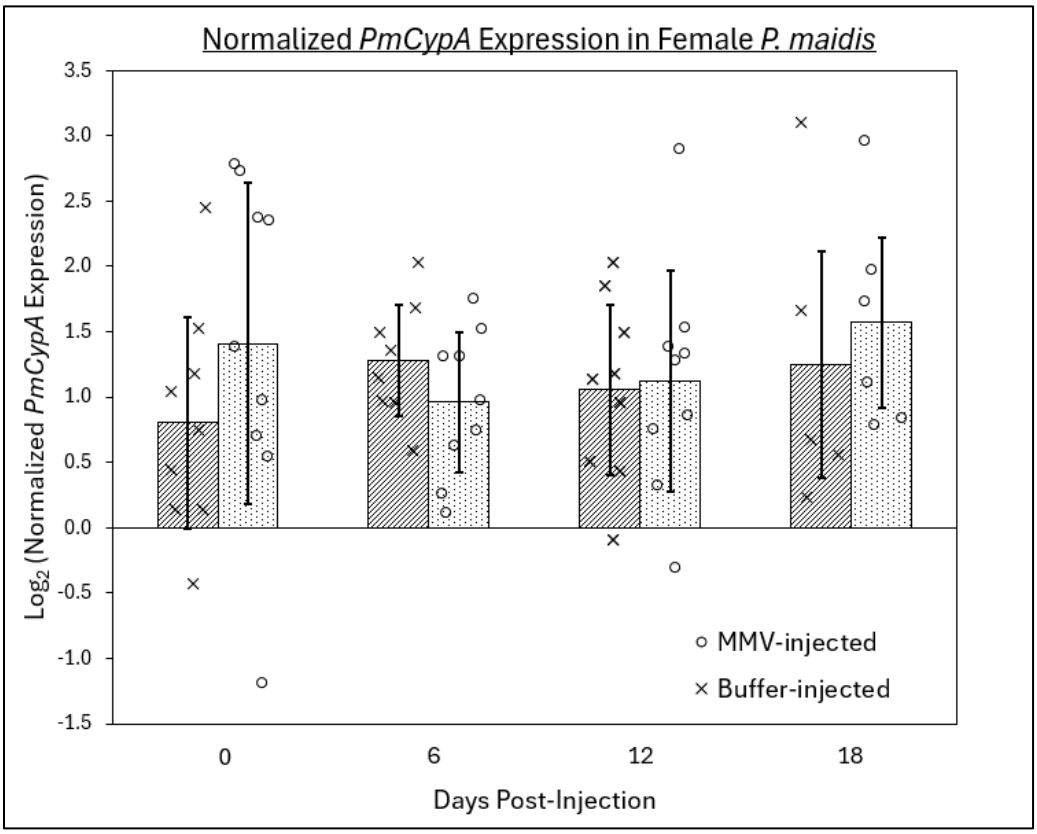
Normalized PmCypA Expression in Female P. maidis
Log2 (Normalized PmCypA Expression)
3.5
3.0
2.5
2.0
1.5
1.0
0.5
0.0
-0.5
-1.0
-1.5
MMV-injected
Buffer-injected
0
6
12
18
Days Post-Injection

Figure 3.4: Quantification of *P. maidis* lugensin (*PmLgs*) transcripts shows no significant difference in *PmLgs* expression is present between virus or buffer-injected groups for male and female insects. Error bars represent standard deviation.

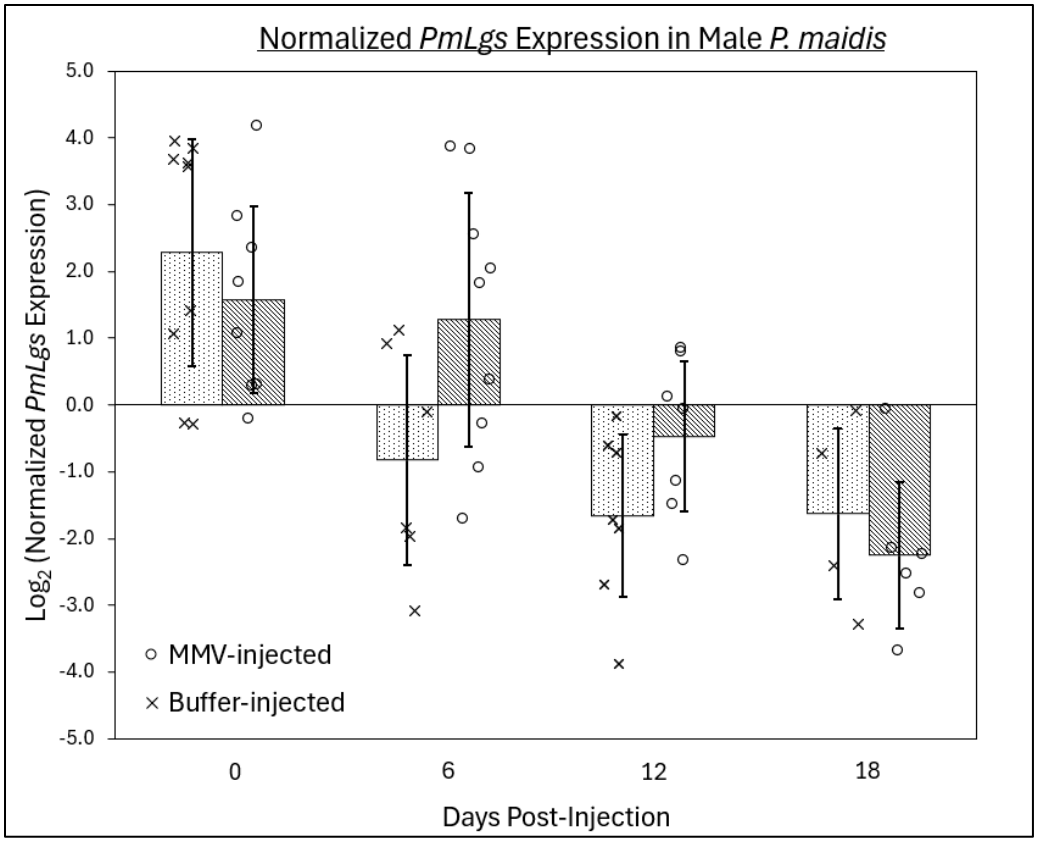
Normalized *PmLgs* Expression in Male *P. maidis*
5.0
4.0
3.0
2.0
1.0
0.0
-1.0
-2.0
-3.0
-4.0
-5.0
Log2 (Normalized *PmLgs* Expression)
MMV-injected
Buffer-injected
0
6
12
18
Days Post-Injection

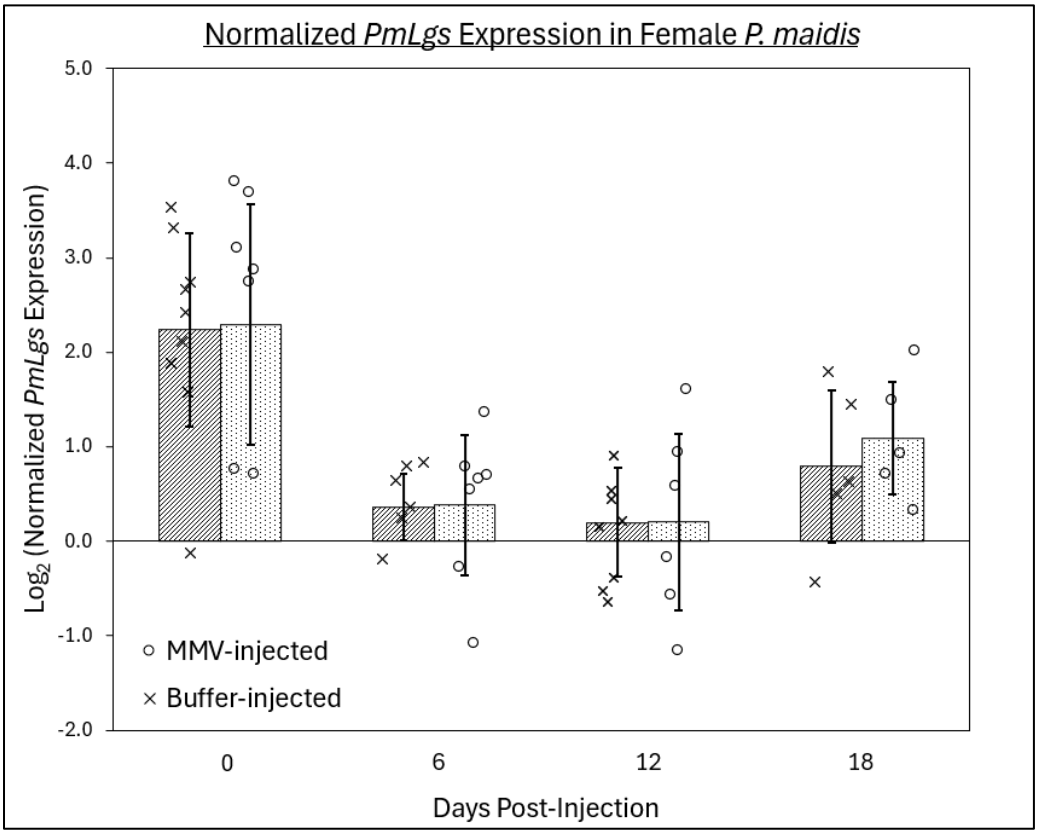
Normalized *PmLgs* Expression in Female *P. maidis*
5.0
4.0
3.0
2.0
1.0
0.0
-1.0
-2.0
Log2 (Normalized *PmLgs* Expression)
MMV-injected
Buffer-injected
0
6
12
18
Days Post-Injection

Co-injection of MMV and dsRNA

MMV virions and dsRNA targeting *PmApo3, PmCypA, PmLgs,* or *GFP* transcripts were co-injected into *P. maidis* adults, then the insects were kept on healthy corn plants and collected at various time points post-injection for RNA extraction, cDNA synthesis, and transcript quantification using qRT-PCR. Expression levels of *PmApo3* were significantly lower in dsApo3-injected male and female insects compared to dsGFP-injected male and female insects at time points of 6, 12, and 18 DPI (Figure 4.1). MMV viral titer accumulation was not significantly different between dsApo3 or dsGFP-injected insects for both the male and female groups (Figure 4.2). Expression levels of *PmCypA* were significantly lower in dsCypA-injected male and female insects compared to dsGFP-injected male and female insects at time points of 6, 12, and 18 DPI (Figure 4.3). MMV viral titer accumulation was not significantly different between dsCypA or dsGFP-injected insects for both the male and female groups (Figure 4.4). Expression levels of *PmLgs* were significantly lower in dsLgs-injected male and female insects compared to dsGFP-injected male and female insects at all time points of 0, 6, 12, and 18 DPI (Figure 4.5). MMV viral titer accumulation was not significantly different between dsLgs or dsGFP-injected male and female insects, except at 0 DPI for both groups (Figure 4.6).

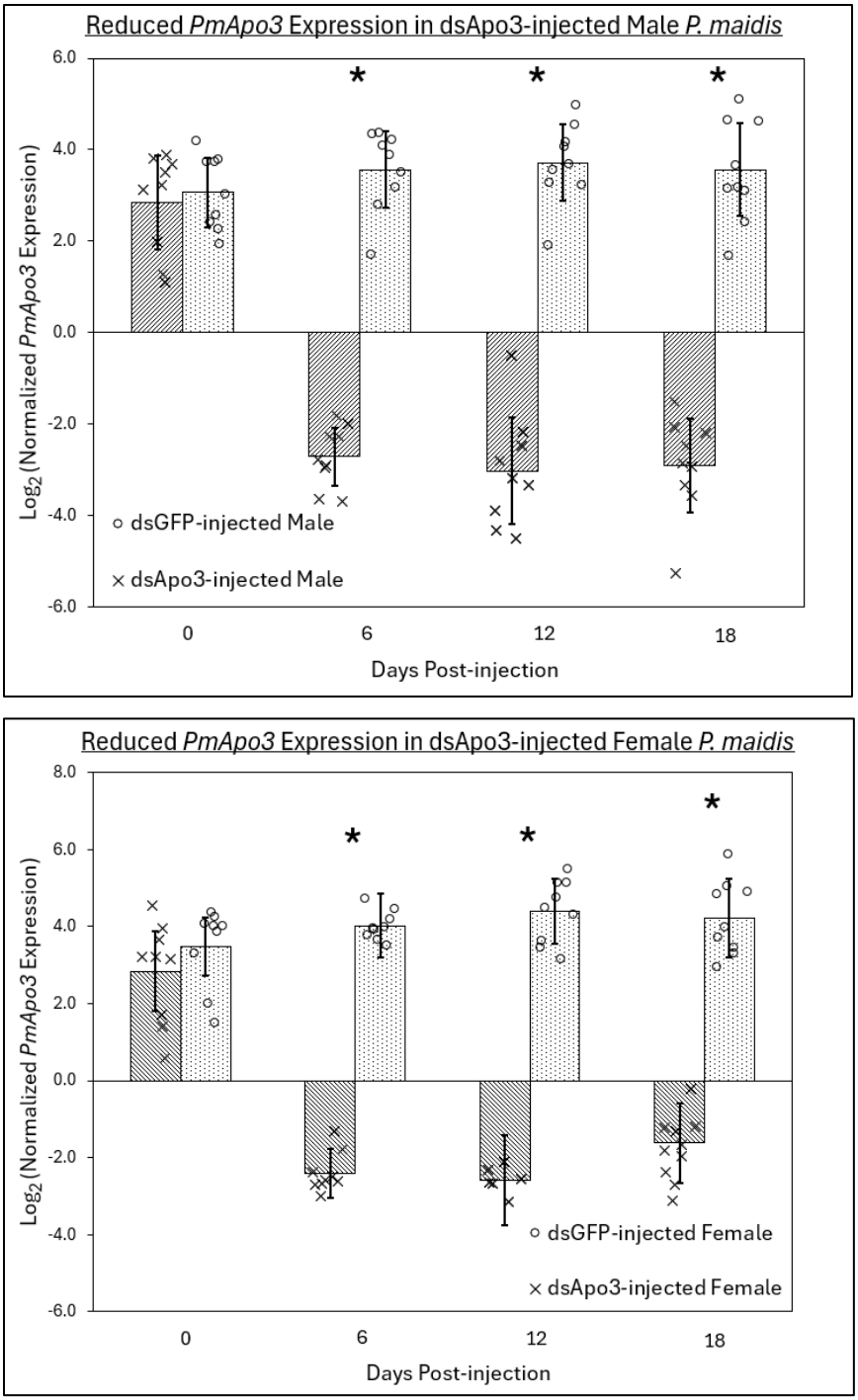

Figure 4.1: Quantification of *P. maidis apolipophorin III* (*PmApo3*) transcripts shows that *PmApo3* expression is significantly lower in male and female insects which were injected with dsApo3 compared to those which were injected with dsGFP at time points of 6, 12, and 18 DPI. Each point represents the average of 3 insects, error bars represent standard deviation.

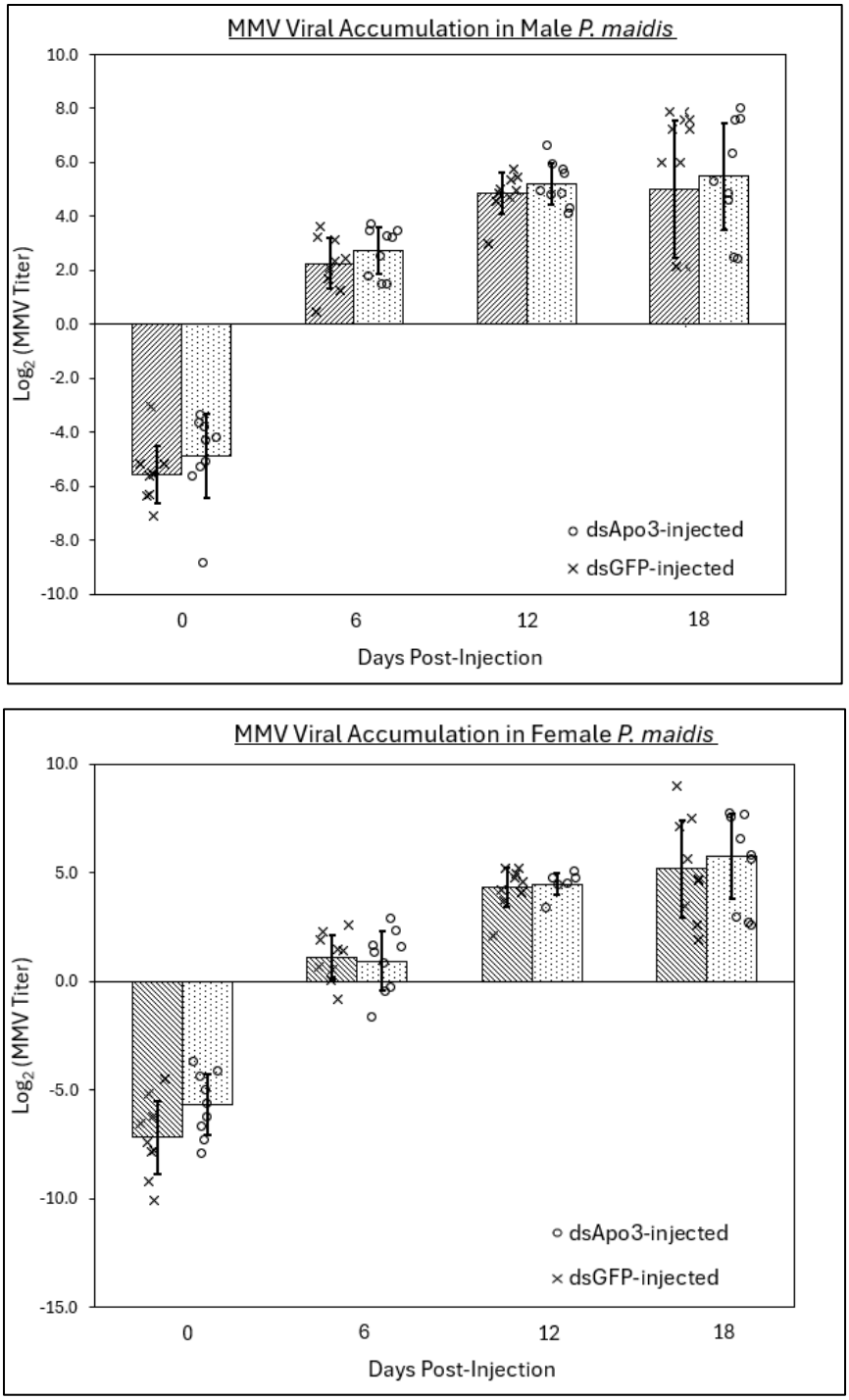

Figure 4.2: Quantification of MMV nucleoprotein transcripts shows that there is no significant difference in viral accumulation at any time point between insects injected with dsApo3 or dsGFP for both male and female insects. Each point represents the average of 3 insects, error bars represent standard deviation.

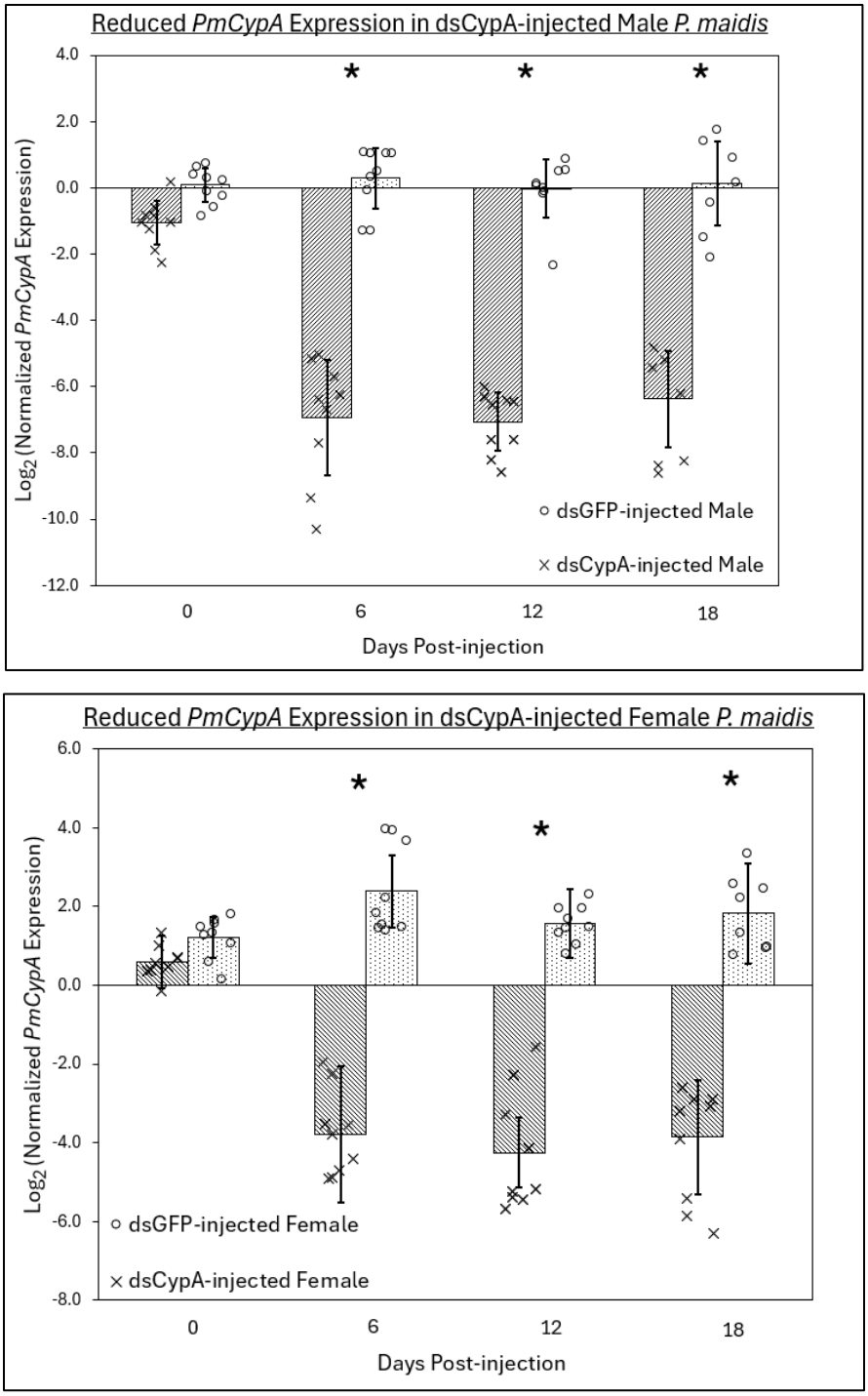

Figure 4.3: Quantification of *P. maidis* cyclophilin A (*PmCypA*) transcripts shows that *PmCypA* expression is significantly lower in male and female insects which were injected with dsCypA compared to those which were injected with dsGFP at time points of 6, 12, and 18 DPI. Each point represents the average of 3 insects, error bars represent standard deviation.

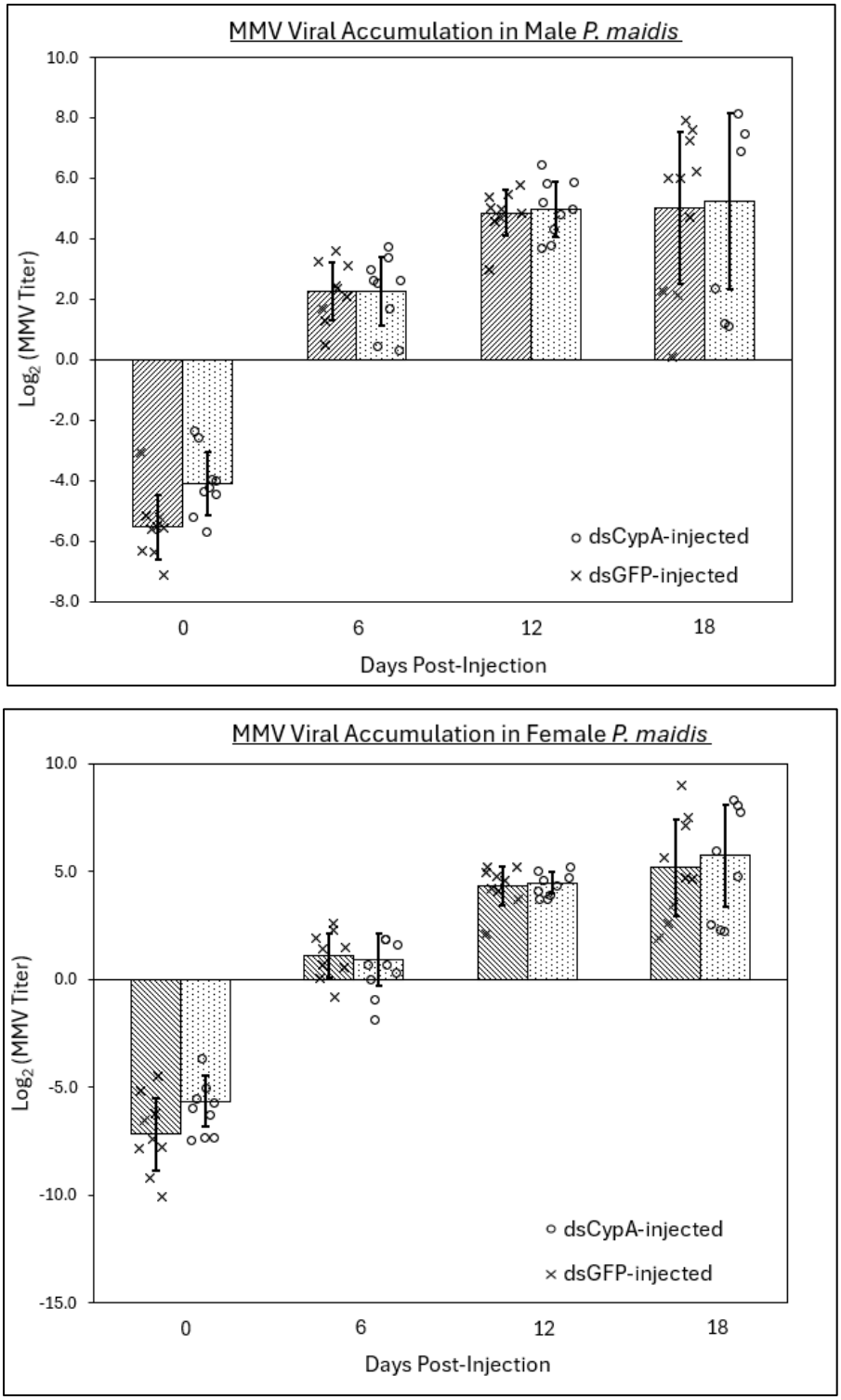

Figure 4.4: Quantification of MMV nucleoprotein transcripts shows that there is no significant difference in viral accumulation at any time point between insects injected with dsCypA or dsGFP for both male and female insects. Error bars represent standard deviation.

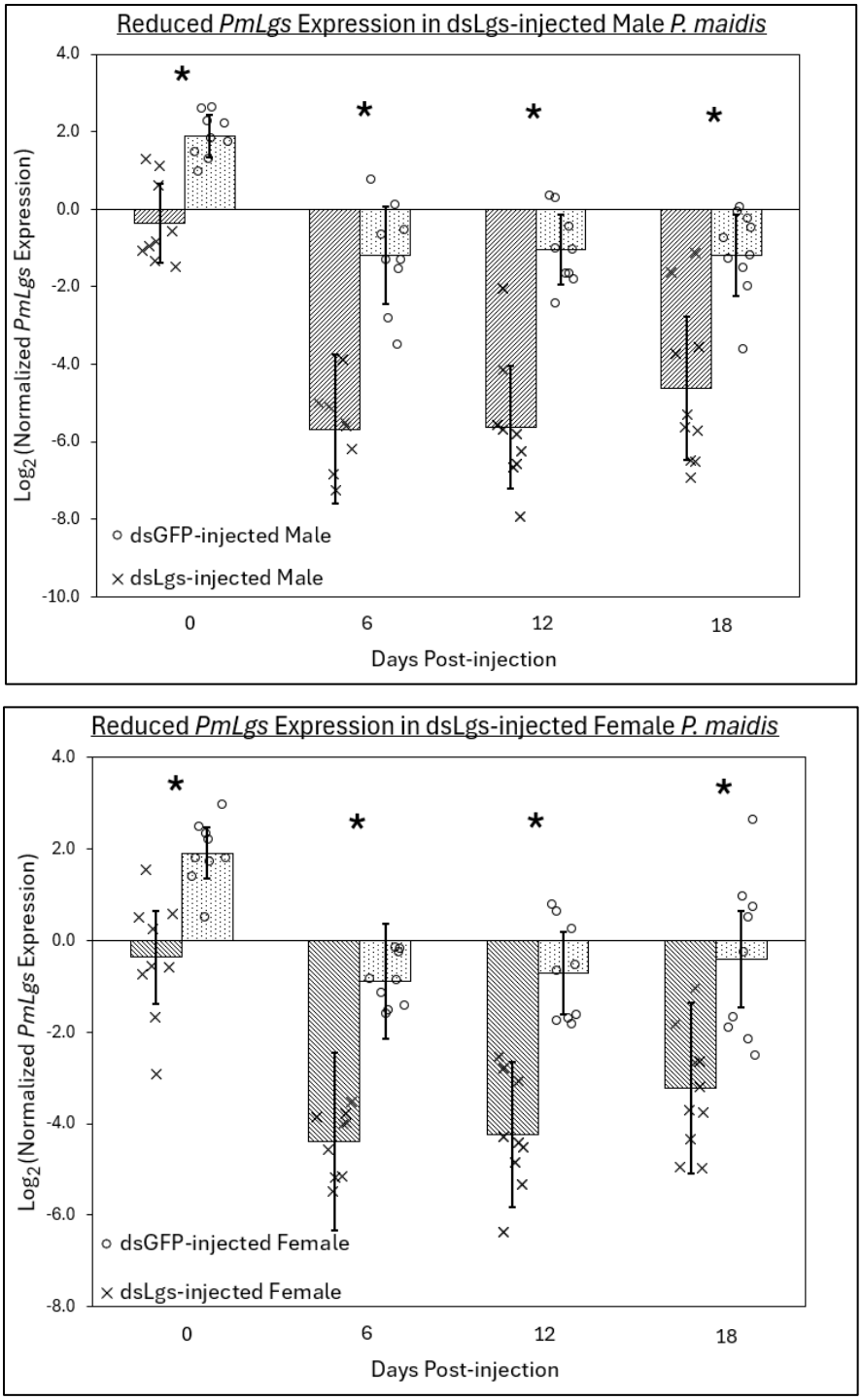

Figure 4.5: Quantification of *P. maidis lugensin* (*PmLgs*) transcripts shows that *PmLgs* expression is significantly lower in male and female insects which were injected with dsLgs compared to those which were injected with dsGFP at all tested time points of 0, 6, 12, and 18 DPI. Error bars represent standard deviation.

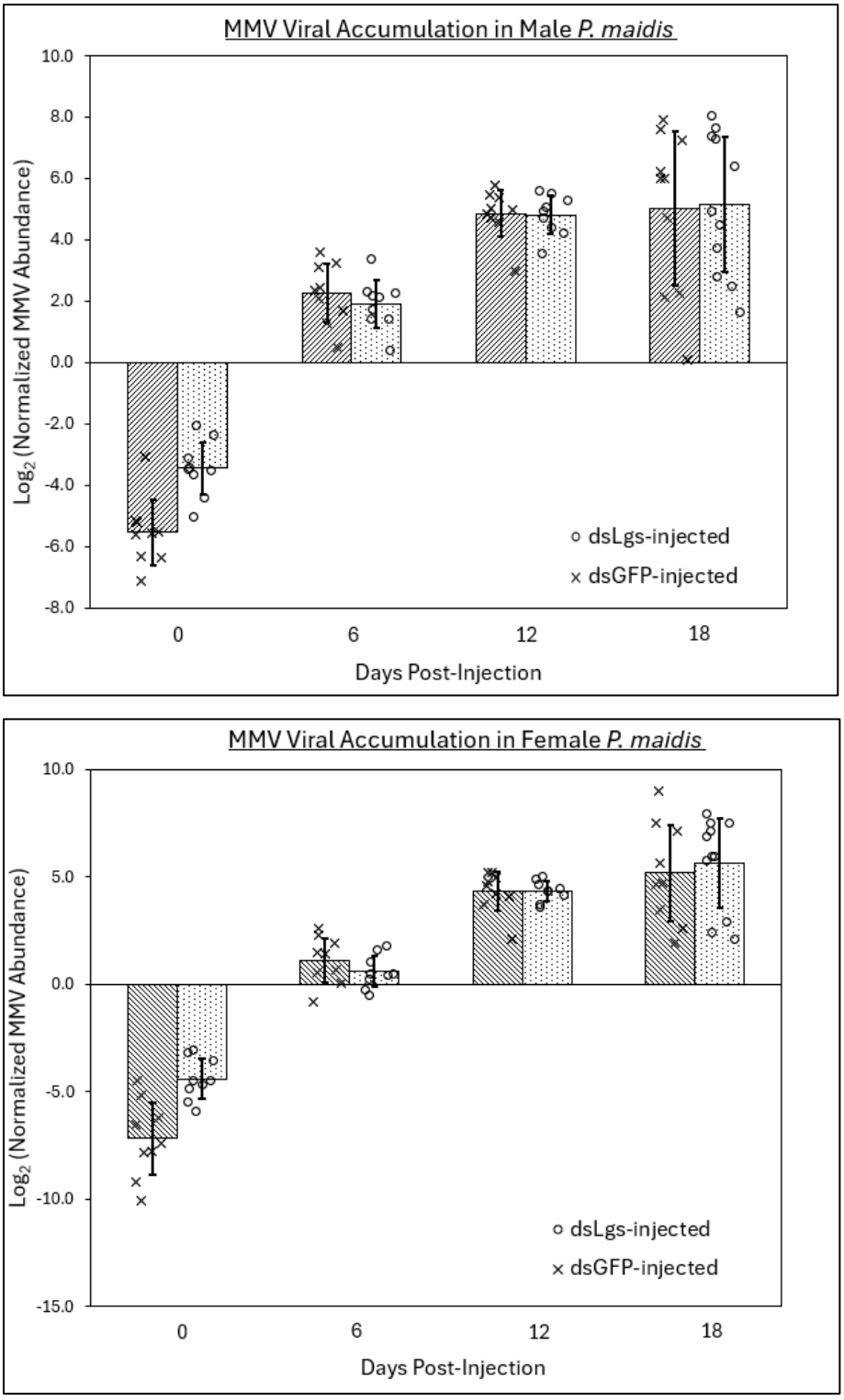

Figure 4.6: Quantification of MMV nucleoprotein transcripts shows that there is no significant difference in viral accumulation at any time point between insects injected with dsLgs or dsGFP for both male and female insects, except at 0 DPI. Error bars represent standard deviation.

Discussion

In this study, we sought to validate the interaction detected in an MbY2H assay between *P. maidis* apolipophorin III, cyclophilin A, and lugensin with the MMV glycoprotein. The MbY2H assay was repeated using MMV-G as bait and the different *P. maidis* proteins as prey. A strong G-PmLgs and G-PmApo3 interaction was observed, and a weak G-PmCypA interaction was also observed. The expression levels of those insect proteins in different life stages and various stages of MMV infection were also quantified using quantitative real-time PCR. *PmApo3* transcript expression was lower in first instars compared to older life stages, and *PmCypA* transcript expression was similar throughout all life stages, but high variability was present in the PmCypA transcript expression levels. Functional analysis experiments involving co-injection of MMV virions and dsRNA targeting those protein transcripts were also performed, and RNAi was highly efficient for all dsRNA constructs. There were no significant differences observed in viral titers between the experimental and control groups at any time point tested, except in the MMV and dsLgs-injected male and female insects at 0 days post-injection.

The MbY2H results showed that this assay may not be optimal for detecting an interaction between MMV-G and PmCypA as there was relatively high levels of nonspecific interaction between PmCypA and the empty bait vector, even though the interaction was validated in a prior study (Barandoc-Alviar et al., 2022). Further validation of the MbY2H results can be performed by using other biological assays like cell culture-based expression localization assays or protein-protein interaction assays like bimolecular fluorescence complementation to investigate the strength of the interaction between MMV-G and the three *P. maidis* proteins, PmApo3, PmCypA, and PmLgs.

The unnatural route of viral entry into the insect using hemocoel injections instead of a natural route of entry via the midgut epithelium could have resulted in the lack of a significant difference

in transcript expression observed for the three genes between MMV-injected and buffer-injected insect groups. Further work using insects which acquired MMV naturally through feeding on infected plants could produce different results, and that work could be aided with the use of transgenic MMV-GFP virus to identify infected individuals without the need for destructive sampling (Kanakala et al., 2023).

The initial quantity of virions injected into the dsLgs-injected male and female insects was significantly different compared to that injected into the MMV and dsGFP-injected group, and previous reports show that there is a dose-response curve present in the insect response to MMV infection. However, it is unclear if the difference in initial virion quantity observed here is large enough to result in an observable effect on viral accumulation throughout the course of the experiment, performing additional experiments that vary the initial quantities of virions injected into insects and producing a dose-response curve would provide that data.

Three insect proteins, PmApo3, PmCypA, and PmLgs, which interacted with the MMV glycoprotein in an MbY2H library screen were tested and validated using a separate MbY2H assay. The insect proteins were also characterized using vivo experiments, and transcript expression levels of the three proteins did not differ between MMV-infected and uninfected insects and knocking down transcript expression of those three proteins individually had no effect on viral titer accumulation. This observation could be due to transcript expression levels being uncoupled from protein abundance levels, so future experiments could look to investigate protein abundance and transcript abundance simultaneously, allowing us to elucidate the relationship between MMV and those insect proteins in greater detail.

References

Ahmed, A., Siman-Tov, G., Hall, G., Bhalla, N., & Narayanan, A. (2019). Human Antimicrobial Peptides as Therapeutics for Viral Infections. *Viruses*, *11*(8), 704.

Ammar, E.-D., & Hogenhout, S. A. (2008). A neurotropic route for Maize mosaic virus (Rhabdoviridae) in its planthopper vector *Peregrinus maidis*. *Virus research*, *131*(1), 77–85.

Arbouzova, N. I., & Zeidler, M. P. (2006). JAK/STAT signalling in *Drosophila*: insights into conserved regulatory and cellular functions. *Development (Cambridge, England)*, *133*(14), 2605–2616.

Barandoc-Alviar, K., Ramirez, G. M., Rotenberg, D., & Whitfield, A. E. (2016). Analysis of Acquisition and Titer of Maize Mosaic Rhabdovirus in Its Vector, *Peregrinus maidis* (Hemiptera: Delphacidae). *Journal of insect science (Online)*, *16*(1), 14.

Barandoc-Alviar, K., Rotenberg, D., Martin, K. M., & Whitfield, A. E. (2022). The physical interactome between *Peregrinus maidis* proteins and the maize mosaic virus glycoprotein provides insights into the cellular biology of a rhabdovirus in the insect vector. *Virology*, *577*, 163–173.

Costa, A., Jan, E., Sarnow, P., & Schneider, D. (2009). The Imd Pathway Is Involved in Antiviral Immune Responses in Drosophila. *PLOS ONE*, *4*(10), e7436.

Chen, T.-Y., Raduwan, H., Marín-López, A., Cui, Y., & Fikrig, E. (2024). Zika virus exists in enterocytes and enteroendocrine cells of the Aedes aegypti midgut. *IScience*, *27*(7).

de Wilde, A. H., Pham, U., Posthuma, C. C., & Snijder, E. J. (2018). Cyclophilins and cyclophilin inhibitors in nidovirus replication. *Virology*, *522*, 46–55.

Eleftherianos, I., Marokhazi, J., Millichap, P. J., Hodgkinson, A. J., Sriboonlert, A., ffrench-Constant, R. H., & Reynolds, S. E. (2006). Prior infection of Manduca sexta with non-pathogenic Escherichia coli elicits immunity to pathogenic *Photorhabdus luminescens*: Roles of immune-related proteins shown by RNA interference. *Insect Biochemistry and Molecular Biology*, *36*(6), 517–525.

Galiana-Arnoux, D., Dostert, C., Schneemann, A., Hoffmann, J. A., & Imler, J. L. (2006). Essential function in vivo for Dicer-2 in host defense against RNA viruses in drosophila. *Nature immunology*, *7*(6), 590–597.

Halwani, A. E., & Dunphy, G. B. (1999). Apolipophorin-III in *Galleria mellonella* potentiates hemolymph lytic activity. *Developmental and comparative immunology*, *23*(7-8), 563–570.

Handschumacher, R. E., Harding, M. W., Rice, J., Drugge, R. J., & Speicher, D. W. (1984). Cyclophilin: A Specific Cytosolic Binding Protein for Cyclosporin A. *Science*, *226*(4674), 544–547.

Hillyer J. F. (2016). Insect immunology and hematopoiesis. *Developmental and comparative immunology*, *58*, 102–118.

Iatsenko, I., Kondo, S., Mengin-Lecreulx, D., & Lemaitre, B. (2016). PGRP-SD, an Extracellular Pattern-Recognition Receptor, Enhances Peptidoglycan-Mediated Activation of the Drosophila Imd Pathway. *Immunity*, *45*(5), 1013–1023.

Kanakala, S., Kontsedalov, S., Lebedev, G., & Ghanim, M. (2019). Plant-Mediated Silencing of the Whitefly *Bemisia tabaci* Cyclophilin B and Heat Shock Protein 70 Impairs Insect Development and Virus Transmission. *Frontiers in Physiology*, *10*, 557.

Kim, H. J., Je, H. J., Park, S. Y., Lee, I. H., Jin, B. R., Yun, H. K., Yun, C. Y., Han, Y. S., Kang, Y. J., & Seo, S. J. (2004). Immune activation of apolipophorin-III and its distribution in hemocyte from *Hyphantria cunea*. *Insect biochemistry and molecular biology*, *34*(10), 1011–1023.

Kingsolver, M. B., Huang, Z., & Hardy, R. W. (2013). Insect antiviral innate immunity: pathways, effectors, and connections. *Journal of molecular biology*, *425*(24), 4921–4936.

Liu, W., Li, J., Zheng, W., Shang, Y., Zhao, Z., Wang, S., Bi, Y., Zhang, S., Xu, C., Duan, Z., Zhang, L., Wang, Y. L., Jiang, Z., Liu, W., & Sun, L. (2017). Cyclophilin A-regulated ubiquitination is critical for RIG-I-mediated antiviral immune responses. *eLife*, *6*, e24425.

Liu, X., Sun, L., Yu, M., Wang, Z., Xu, C., Xue, Q., Zhang, K., Ye, X., Kitamura, Y., Liu, W. (2009). Cyclophilin A interacts with influenza A virus M1 protein and impairs the early stage of the viral replication. *Cell Microbiology 11*(5):730-41.

Liu, X., Zhao, Z., Xu, C., Sun, L., Chen, J., Zhang, L., & Liu, W. (2012). Cyclophilin A restricts influenza A virus replication through degradation of the M1 protein. *PloS one*, *7*(2), e31063.

Livak, K. J., & Schmittgen, T. D. (2001). Analysis of relative gene expression data using real-time quantitative PCR and the 2(-Delta Delta C(T)) Method. *Methods (San Diego, Calif.)*, *25*(4), 402–408.

Mahanta, D. K., Bhoi, T. K., Komal, J., Samal, I., Nikhil, R. M., Paschapur, A. U., Singh, G., Kumar, P. V. D., Desai, H. R., Ahmad, M. A., Singh, P. P., Majhi, P. K., Mukherjee, U., Singh, P., Saini, V., Shahanaz, Srinivasa, N., & Yele, Y. (2023). Insect-pathogen crosstalk and the cellular-molecular mechanisms of insect immunity: uncovering the underlying

signaling pathways and immune regulatory function of non-coding RNAs. *Frontiers in Immunology*, *14*.

Marques, J. T., & Imler, J. L. (2016). The diversity of insect antiviral immunity: insights from viruses. *Current opinion in microbiology*, *32*, 71–76.

Namba, R. & Higa, S. (1971). Host plant studies of the corn planthopper, *Peregrinus maidis* (Ashmead), in Hawaii. *Hawaiian Entomological Society*, *21*, 105–108.

Rosales Ramirez, R., & Ludert, J. E. (2019). The Dengue Virus Nonstructural Protein 1 (NS1) Is Secreted from Mosquito Cells in Association with the Intracellular Cholesterol Transporter Chaperone Caveolin Complex. *Journal of virology*, *93*(4), e01985-18.

Schaller, T., Ocwieja, K. E., Rasaiyaah, J., Price, A. J., Brady, T. L., Roth, S. L., Hué, S., Fletcher, A. J., Lee, K., KewalRamani, V. N., Noursadeghi, M., Jenner, R. G., James, L. C., Bushman, F. D., & Towers, G. J. (2011). HIV-1 capsid-cyclophilin interactions determine nuclear import pathway, integration targeting and replication efficiency. *PLoS pathogens*, *7*(12), e1002439.

Strand, M. R. (2008). The insect cellular immune response. *Insect Science*, *15*(1), 1–14.

Sun, D., Ziegler, R., Milligan, C. E., Fahrbach, S., & Schwartz, L. M. (1995). Apolipophorin III is dramatically up-regulated during the programmed death of insect skeletal muscle and neurons. *Journal of neurobiology*, *26*(1), 119–129.

Valanne, S., Wang, J. H., & Rämet, M. (2011). The Drosophila Toll signaling pathway. *Journal of immunology (Baltimore, Md.: 1950)*, *186*(2), 649–656.

Wang, P., & Heitman, J. (2005). The cyclophilins. *Genome biology*, *6*(7), 226.

Weers, P. M., Van Marrewijk, W. J., Beenakkers, A. M., & Van der Horst, D. J. (1993). Biosynthesis of locust lipophorin. Apolipophorins I and II originate from a common precursor. *Journal of Biological Chemistry*, *268*(6), 4300–4303.

Xavier, C. A. D., Tyson, C., Kerner, L. M., & Whitfield, A. E. (2024). RNAi-mediated knockdown of exportin 1 negatively affected ovary development, survival and maize mosaic virus accumulation in its insect vector Peregrinus maidis. *Insect molecular biology*, *33*(4), 295–311.

Yamada, K., Kuribayashi, K., Inomata, N., Noguchi, K., Kimitsuki, K., Demetria, C. S., Saito, N., Inoue, S., Park, C. H., Kaimori, R., Suzuki, M., Saito-Obata, M., Kamiya, Y., Manalo, D. L., Quiambao, B. P., & Nishizono, A. (2021). Validation of serum apolipoprotein A1 in rabies virus-infected mice as a biomarker for the preclinical diagnosis of rabies. *Microbiology and immunology*, *65*(10), 438–448.

Yi, H. Y., Chowdhury, M., Huang, Y. D., & Yu, X. Q. (2014). Insect antimicrobial peptides and their applications. *Applied microbiology and biotechnology*, *98*(13), 5807–5822.

Zambon, R. A., Vakharia, V. N., & Wu, L. P. (2006). RNAi is an antiviral immune response against a dsRNA virus in Drosophila melanogaster. *Cellular microbiology*, *8*(5), 880–889.

Zhou, X., Peng, L. Y., Wang, Z. C., Wang, W., Zhu, Z., Huang, X. H., Chen, L. B., Song, Q. S., & Bao, Y. Y. (2019). Identification of novel antimicrobial peptides from rice planthopper, Nilaparvata lugens. *Insect biochemistry and molecular biology*, *113*, 103215.

Supplementary Information

Supplementary Table 1: Primers used for MbY2H vector cloning and qRT-PCR analysis.

No.	Primer Name	Sequence (5’ – 3’)	Purpose
1	SfiI_Apo3_F	ATT AAC AAG GCC ATT ACG GCC ATG GCA AAC TAT TGT ACT GT	Primer to clone PmApo3 ORF into prey vector.
2	SfiI_Apo3_R	AAC TGA TTG GCC GAG GCG GCC CTA GTG TTG ATG ACC TTC ATG	Primer to clone PmApo3 ORF into prey vector.
3	SfiI_CycA_F	ATT AAC AAG GCC ATT ACG GCC ATG GCA CGT TCA AAG GTA TAC T	Primer to clone PmCypA ORF into prey vector.
4	SfiI_CycA_R	AAC TGA TTG GCC GAG GCG GCC CTA GAG CTG ACC GCA GTC	Primer to clone PmCypA ORF into prey vector.
5	SfiI_LgsNSP_F	ATT AAC AAG GCC ATT ACG GCC AAG CGG TAC GAC TCC CCT	Primer to clone PmLgs ORF into prey vector.
6	SfiI_LgsNSP_R	AAC TGA TTG GCC GAG GCG GCC CTA ACG CCT TCC AAA AGG AA	Primer to clone PmLgs ORF into prey vector.
7	qRPL10_F	CGA AGA AAT GGG GTT TCA	RPL10 forward primer for qPCR.
8	qRPL10_R	CTC TGG CCT GTA CTT CAC	RPL10 reverse primer for qPCR.
9	qMMV-N_F	GAG CAT CTG GTA GAG GAG	MMV-N qPCR forward primer.
10	qMMV-N_R	CAT AGG TTC AGG AGC GTA	MMV-N qPCR reverse primer.
11	qPmLgs_F	TGT GAG AGT GCT GGT AGT	PmLgs qPCR forward primer.
12	qPmLgs_R	GAG GAG GTG GTC GAT TTA TG	PmLgs qPCR reverse primer.
13	qApo3_F	AGC ACT TGG GTG AGA CAA TC	PmApo3 qPCR forward primer.
14	qApo3_R	GAA TCG GGT TGA GCT TCC TT	PmApo3 qPCR reverse primer.
15	qCypA_F	CCA GAT GTT GTG CCG AAG A	PmCypA qPCR forward primer.
16	qCypA_R	GCC GTT GTG TTT GGT GAA AT	PmCypA qPCR reverse primer.